

**ECO2M: A TOUGH2 Fluid Property Module for Mixtures of  
Water, NaCl, and CO<sub>2</sub>, Including Super- and Sub-Critical Conditions, and  
Phase Change Between Liquid and Gaseous CO<sub>2</sub>**

*Karsten Pruess*

Earth Sciences Division, Lawrence Berkeley National Laboratory  
University of California, Berkeley, CA 94720

April 2011

This work was supported by the U.S. Department of Energy under Contract No. DE-AC02-05CH11231 with the  
Lawrence Berkeley National Laboratory.



## Abstract

ECO2M is a fluid property module for the TOUGH2 simulator (Version 2.0) that was designed for applications to geologic storage of CO<sub>2</sub> in saline aquifers. It includes a comprehensive description of the thermodynamics and thermophysical properties of H<sub>2</sub>O - NaCl - CO<sub>2</sub> mixtures, that reproduces fluid properties largely within experimental error for temperature, pressure and salinity conditions in the range of  $10\text{ }^{\circ}\text{C} \leq T \leq 110\text{ }^{\circ}\text{C}$ ,  $P \leq 600\text{ bar}$ , and salinity from zero up to full halite saturation. The fluid property correlations used in ECO2M are identical to the earlier ECO2N fluid property package, but whereas ECO2N could represent only a single CO<sub>2</sub>-rich phase, ECO2M can describe all possible phase conditions for brine-CO<sub>2</sub> mixtures, including transitions between super- and sub-critical conditions, and phase change between liquid and gaseous CO<sub>2</sub>. This allows for seamless modeling of CO<sub>2</sub> storage and leakage. Flow processes can be modeled isothermally or non-isothermally, and phase conditions represented may include a single (aqueous or CO<sub>2</sub>-rich) phase, as well as two- and three-phase mixtures of aqueous, liquid CO<sub>2</sub> and gaseous CO<sub>2</sub> phases. Fluid phases may appear or disappear in the course of a simulation, and solid salt may precipitate or dissolve. TOUGH2/ECO2M is upwardly compatible with ECO2N and accepts ECO2N-style inputs. This report gives technical specifications of ECO2M and includes instructions for preparing input data. Code applications are illustrated by means of several sample problems, including problems that had been previously solved with TOUGH2/ECO2N.



## TABLE OF CONTENTS

LIST OF FIGURES .....	vii
LIST OF TABLES .....	ix
PREFACE .....	1
1. INTRODUCTION .....	1
2. COMPONENTS, PHASES, AND THERMODYNAMIC VARIABLES	
IN THE SYSTEM Water-NaCl-CO <sub>2</sub> .....	3
2.1 Treatment of Dissolved and Solid Salt .....	7
2.2 Partitioning of Fluid Components among Phases .....	8
2.3 Phase Change .....	13
2.4 “Hairtrigger” vs. “Finite Window” for Phase Change .....	15
2.5 Conversion of Units .....	16
3. THERMOPHYSICAL PROPERTIES OF Water-NaCl-CO <sub>2</sub> MIXTURES .....	18
3.1 Density .....	20
3.2 Viscosity .....	21
3.3 Specific Enthalpy .....	21
4. HEAT EXCHANGE WITH IMPERMEABLE REGIONS .....	25
5. PREPARATION OF INPUT DATA .....	28
5.1 Initialization Choices with ECO2N-style Primary Variables .....	28
5.2 Permeability Change from Precipitation and Dissolution of Salt .....	32
5.3 Choice of Program Options .....	34
6. SAMPLE PROBLEMS .....	40
6.1 Problem No. 1 (*rtab*) - Demonstration of Initialization Options .....	40
6.2 Problem No. 2 (*rcc3*) - Radial Flow from a CO <sub>2</sub> Injection Well .....	44
6.3 Problem No. 3 (*r1d*) - CO <sub>2</sub> Leakage from a Deep Fault Zone .....	49
6.4 Problem No. 4 (*rwaf*) - Migration of a CO <sub>2</sub> Plume in a Sloping Aquifer, Intersected by a Fault .....	61
7. CONCLUDING REMARKS .....	71
ACKNOWLEDGEMENT .....	72
REFERENCES .....	73

APPENDIX A. Three-Phase Relative Permeabilities .....	77
APPENDIX B. Three-Phase Capillary Pressures .....	81
APPENDIX C. Notation for Mass Fractions .....	83

## LIST OF FIGURES

Figure 1.	Possible phase combinations in the system water-CO <sub>2</sub> .....	4
Figure 2.	Phase states of CO <sub>2</sub> .....	4
Figure 3.	Dissolved CO <sub>2</sub> mass fractions at T = 30 °C for pure water (0m) and 4-molar NaCl brine .....	9
Figure 4.	H <sub>2</sub> O mass fractions in gas at T = 30 °C for pure water (0m) and 4-molar NaCl brine .....	10
Figure 5.	Concentration of water in gas and CO <sub>2</sub> in the liquid (aqueous) phase for salinities ranging from zero to fully saturated .....	10
Figure 6.	CO <sub>2</sub> phase partitioning in the system H <sub>2</sub> O - NaCl - CO <sub>2</sub> .....	11
Figure 7.	Schematic of the temperature-pressure tabulation of CO <sub>2</sub> properties .....	19
Figure 8.	Model for converging-diverging pore channels .....	33
Figure 9.	Porosity-permeability relationship for tubes-in-series model .....	34
Figure 10.	TOUGH2/ECO2M input file for sample problem 1 .....	41
Figure 11.	Primary variables internally used in ECO2M for the INCON data given in Fig. 10 .....	43
Figure 12.	Output data for sample problem 1 .....	43
Figure 13.	Schematic of sample problem 2 - radial flow from a CO <sub>2</sub> injection well .....	44
Figure 14.	TOUGH2 input file for grid generation for radial injection problem .....	45
Figure 15.	Modified MESH file for radial injection problem .....	45
Figure 16.	TOUGH2/ECO2M input file for radial injection problem .....	46
Figure 17.	Part of printed output for radial flow problem .....	47
Figure 18.	Part of printed output for radial flow problem with permeability reduction from solids precipitation .....	48
Figure 19.	T,P-diagram of a typical geothermal-hydrostatic profile .....	49
Figure 20.	TOUGH2 input file for generating a 1-D vertical grid for a fault zone .....	50
Figure 21.	Modified MESH file for 1-D vertical fault leakage problem .....	51

Figure 22.	Input file for generating a static geothermal-hydrostatic profile .....	52
Figure 23.	Part of printed output for obtaining a geothermal-hydrostatic profile .....	53
Figure 24.	Input file for CO <sub>2</sub> migration along a fault zone .....	54
Figure 25.	Part of printed output for fault leakage problem .....	56
Figure 26.	Part of printed output for continuation run of fault leakage problem .....	57
Figure 27.	Saturation and temperature profiles at different times .....	59
Figure 28.	Time dependence of water and CO <sub>2</sub> outflow at the landsurface, and temperatures at two different depths .....	59
Figure 29.	Water and CO <sub>2</sub> fluxes as shown in Fig. 28, with the heavy superposed lines indicating the top and bottom of three-phase conditions, respectively .....	60
Figure 30.	Temperature-pressure profiles at different times .....	60
Figure 31.	Geometric dimensions of the 2-D rectangular domain modeled .....	61
Figure 32.	Computational grid showing the entire aquifer (top) and a zoom into the region with refined gridding (bottom) .....	62
Figure 33.	TOUGH2/ECO2M input file for a problem of CO <sub>2</sub> plume migration in a sloping aquifer that is intersected by a vertical fault .....	65
Figure 34.	Part of printout of primary variables at beginning of run .....	66
Figure 35.	Part of printed output for CO <sub>2</sub> plume migration and leakage problem .....	67
Figure 36.	Water fluxes at the top and bottom of the fault .....	68
Figure 37.	CO <sub>2</sub> fluxes at the top and bottom of the fault .....	69
Figure 38.	Advancement of the plume over time .....	69
Figure 39.	CO <sub>2</sub> plume at t = 178.6 yr, for a case without a leaky fault present, simulated with TOUGH2/ECO2N .....	70



## LIST OF TABLES

Table 1.	Fluid components in ECO2M .....	3
Table 2.	Primary thermodynamic variables used for multiphase mixtures of brine and CO <sub>2</sub> .....	7
Table 3.	Molecular weights in the system H <sub>2</sub> O–NaCl–CO <sub>2</sub> .....	17
Table 4.	Parameters for molar volume of dissolved CO <sub>2</sub> .....	20
Table 5.	Dissolved aqueous CO <sub>2</sub> mass fractions along the CO <sub>2</sub> saturation line .....	24
Table 6.	ECO2N-style primary variables .....	29



## **Preface**

This report describes technical specifications and use of ECO2M, a fluid property module for modeling the flow of (NaCl) brine-CO<sub>2</sub> mixtures with the TOUGH2 reservoir simulator (Pruess, 2004). ECO2M is an enhanced version of the ECO2N fluid property module (Pruess, 2005; Pruess and Spycher, 2007). It can describe conditions in which both a liquid and a gaseous CO<sub>2</sub>-rich phase are present, while ECO2N was limited to just a single CO<sub>2</sub>-rich phase. ECO2M uses the same correlations as ECO2N to describe thermodynamic and thermophysical properties of H<sub>2</sub>O–NaCl–CO<sub>2</sub> mixtures largely within experimental errors for 10 °C ≤ T ≤ 110 °C, P ≤ 600 bar. This includes density, viscosity, and specific enthalpy of fluid phases as function of temperature, pressure, and composition, as well as partitioning of mass components H<sub>2</sub>O, NaCl and CO<sub>2</sub> among the different phases. The aqueous phase includes salinity from zero up to full halite saturation, a mixture we refer to as brine with no specific NaCl content (or range) implied by the term. By covering all possible phase compositions in brine-CO<sub>2</sub> systems, ECO2M can seamlessly model scenarios of CO<sub>2</sub> storage and leakage all the way to the land surface, including transitions between super- and sub-critical conditions, and phase change between liquid and gaseous CO<sub>2</sub>.

In order to make this report self-contained, we include much of the material that was covered in the earlier ECO2N user's guide (Pruess, 2005). Users will want to have the TOUGH2 User's Guide (Pruess et al., 1999) available, as its contents are not included here.

## **1. Introduction**

Injection of CO<sub>2</sub> into saline formations has been proposed as a means whereby emissions of heat-trapping greenhouse gases into the atmosphere may be reduced. Such injection would induce coupled processes of multiphase fluid flow, heat transfer, chemical reactions, and mechanical deformation. The present report describes a fluid property module "ECO2M" for the general-purpose reservoir simulator TOUGH2 (Pruess et al., 1999; Pruess, 2004), that can be used to model non-isothermal multiphase flow in the system H<sub>2</sub>O - NaCl - CO<sub>2</sub>. TOUGH2/ECO2M represents fluids as consisting of one, two, or three phases, that may include a water-rich aqueous phase, and one or two CO<sub>2</sub>-rich phases referred to as "liquid" or "gas." In addition, solid salt may also be present. For supercritical temperatures  $T \geq T_{\text{crit}} = 31.04$  °C, we

arbitrarily assign the single CO<sub>2</sub>-rich phase as “liquid” when  $P \geq P_{\text{crit}} = 73.82$  bar, and as “gas” when  $P < P_{\text{crit}}$ . The only chemical reactions modeled by ECO2M include equilibrium phase partitioning of water and carbon dioxide between the different fluid phases, and precipitation and dissolution of solid salt. The partitioning of H<sub>2</sub>O and CO<sub>2</sub> between the phases is modeled as a function of temperature, pressure, and salinity, using the correlations of Spycher and Pruess (2005). Dissolution and precipitation of salt is treated by means of local equilibrium solubility. Associated changes in fluid porosity and permeability may also be modeled. All phases - aqueous, gas, liquid, solid - may appear or disappear in any grid block during the course of a simulation. Thermodynamic conditions covered include a temperature range from ambient to 110 °C (approximately), pressures up to 600 bar, and salinity from zero to fully saturated. These parameter ranges should be adequate for most conditions encountered during storage of CO<sub>2</sub> into and leakage of CO<sub>2</sub> from deep saline aquifers.

ECO2M is written in Fortran 77 and is "plug-compatible" with TOUGH2, Version 2.0. The code is intrinsically single-precision, but requires 64-bit arithmetic, which on 32-bit processors (PCs and workstations) may be realized by using compiler options for generating 64-bit arithmetic. For example, on an IBM RS/6000 computer, this may be accomplished with the compiler option “-qautodbl=dblpad”. ECO2M may be linked with standard TOUGH2 modules like any of the other fluid property modules included in the TOUGH2 V 2.0 package. As an example, we list the linking instruction that would be used on an IBM RS/6000 workstation.

```
f77 -o xco2m t2fm.o t2cg22.o eco2m.o meshm.o t2f.o t2solv.o ma28.o
```

Execution of an input file \*rcc3\* would be made with the command

```
xco2m <rcc3 >rcc3.out
```

The present report is a user's guide for the TOUGH2/ECO2M simulator. Information provided in the TOUGH2 users' guide (Pruess et al., 1999) is relevant but is not duplicated here. We begin with a discussion of phase conditions and thermodynamic variables in the system H<sub>2</sub>O - NaCl - CO<sub>2</sub>, for conditions of interest in geologic sequestration of CO<sub>2</sub>. This is followed by a

discussion of our thermophysical property model, and guidance for preparing input data. Several sample problems are provided which document code performance and serve as a tutorial and template for applications.

## 2. Components, Phases, and Thermodynamic Variables in the System Water-NaCl-CO<sub>2</sub>

The fluid components modeled by ECO2M are the same as in ECO2N, and are labeled in the same manner; see Table 1.

Table 1. Fluid components in ECO2M

# 1: water
# 2: NaCl
# 3: CO <sub>2</sub>

In the two-component system water-CO<sub>2</sub>, at temperatures above the freezing point of water and not considering hydrate phases, three different fluid phases may be present: an aqueous phase that is mostly water but may contain some dissolved CO<sub>2</sub>, a liquid CO<sub>2</sub>-rich phase that may contain some dissolved water, and a gaseous CO<sub>2</sub>-rich phase that also may contain some water. Altogether there may be seven different phase combinations (Fig. 1). If NaCl (“salt”) is added as a third fluid component, the number of possible phase combinations doubles, because in each of the seven phase combinations depicted in Fig. 1 there may or may not be an additional phase consisting of solid salt. Liquid and gaseous CO<sub>2</sub> may coexist along the saturated vapor pressure curve of CO<sub>2</sub>, which ends at the critical point ( $T_{\text{crit}}$ ,  $P_{\text{crit}}$ ) = (31.04 °C, 73.82 bar; Vargaftik, 1975), see Fig. 2. At supercritical temperatures or pressures there is just a single CO<sub>2</sub>-rich phase.

ECO2M can represent all of the phase conditions and transitions depicted in Fig. 1. TOUGH2/ECO2M may therefore be applied to flow systems that involve both sub- and super-critical temperature and pressure conditions, as well as transitions between them.

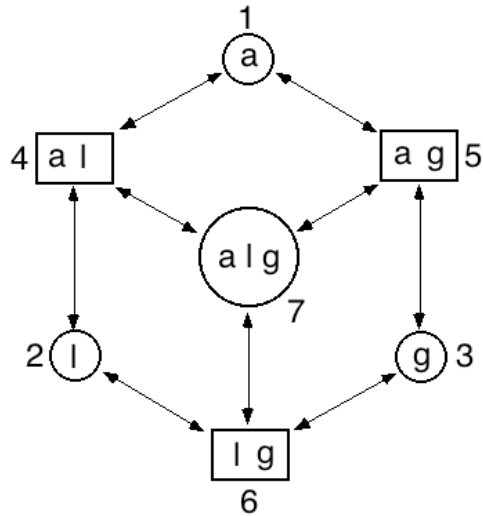


Figure 1. Possible fluid phase combinations in the system water-CO<sub>2</sub>, and transitions between them in the P-T range of ECO2M. The phase designations are a - aqueous, l - liquid CO<sub>2</sub>, g - gaseous CO<sub>2</sub>. Separate liquid and gas phases of CO<sub>2</sub> exist only at subcritical conditions. Phase combinations are identified by a numerical index that ranges from 1 to 7.

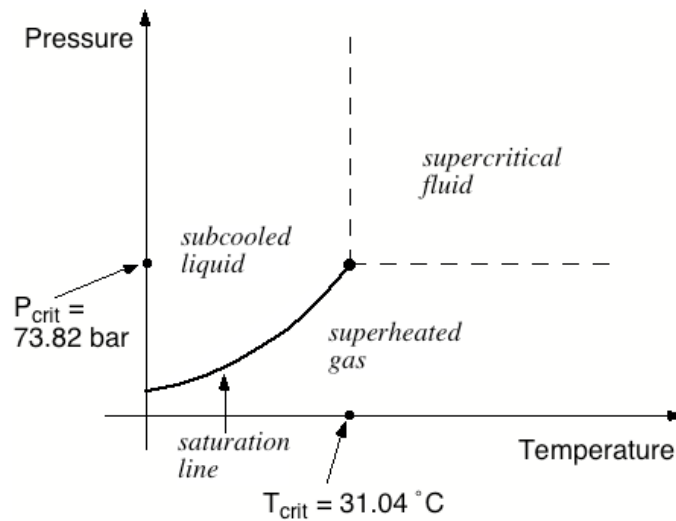


Figure 2. Phase states of CO<sub>2</sub>.

In the numerical simulation of brine-CO<sub>2</sub> flows, we are concerned with the fundamental thermodynamic variables that characterize the brine-CO<sub>2</sub> system, and their change with time in different subdomains (grid blocks) of the flow system. Four “primary variables” are required to define the state of water-NaCl-CO<sub>2</sub> mixtures, which according to conventional TOUGH2 usage

are denoted by X1, X2, X3, and X4. Depending upon the phase combination present, not all thermodynamic parameters are independent, and different sets of primary thermodynamic variables must be used for different phase combinations. In most fluid property modules for TOUGH2, the meaning of primary variables and the corresponding phase compositions are identified by employing different numerical ranges. For example, in ECO2N the third primary variable X3 can either be in the range [0, 1] or [10, 11]. Specification of X3 in the range  $0 \leq X3 \leq 1$  is used to indicate that only a single (aqueous or CO<sub>2</sub>-rich) phase is present, and X3 denotes mass fraction X of CO<sub>2</sub> in that phase. When X3 is in the range  $10 \leq X3 < 11$ , this indicates two-phase conditions (aqueous plus a CO<sub>2</sub>-rich phase), and X3 denotes  $S_c + 10$ , where  $S_c$  is the saturation of the CO<sub>2</sub>-rich phase. This approach works well when only a few different phase compositions need to be distinguished, but would become awkward for the seven different phase compositions considered in ECO2M. Accordingly, ECO2M uses a different approach, in which different phase compositions, and the meaning of primary thermodynamic variables, are identified and distinguished by means of a separate numerical index, that ranges from 1 to 7 as shown in Fig. 1. This is the same treatment as previously used in TMVOC, a version of TOUGH2 for three-phase flow of water, soil gas, and a non-aqueous phase liquid (NAPL; Pruess and Battistelli, 2002).

In addition to facilitating the identification of phase compositions and recognition of primary thermodynamic variables, using an index to identify phase conditions offers the possibility to “decouple” the assignment of phase conditions from the numerical values of primary variables. This provides flexibility in the handling of phase transitions (appearance and disappearance of phases), which can be exploited to greatly improve the stability and robustness of simulator behavior; see Sec. 2.4, below.

Because of the necessity to specify a phase composition index as part of the initial conditions, input formats for TOUGH2/ECO2M are different from other fluid property modules that do not use a phase composition index. Differences arise in (1) default initial conditions in data block PARAM, (2) domain-specific initial conditions in block INDOM, and (3) element-specific initial conditions in block INCON. A data block INDEX consisting of a single record

without parameters is required to engage reading of phase indices; see the detailed explanation of input formats in Sec. 5.

A summary of the fluid components and phases modeled by ECO2M, and the choice of primary thermodynamic variables, appears in Table 2. Different variables are used for different phase conditions, but the first two primary variables are the same, regardless of the number and nature of phases present. For storing “secondary parameters” into the PAR-array of TOUGH2, phases are ordered in the sequence 1 - aqueous, 2 - liquid CO<sub>2</sub>, 3 - gaseous CO<sub>2</sub>, 4 - solid salt. Default parameter choices for ECO2M in data block MULTI are (NK, NEQ, NPH, NB) = (3, 4, 4, 6); specifying NB=8 will turn on molecular diffusion. Regardless of phase compositions that may actually occur in a given flow system, the number-of-phases parameter NPH must always be specified as NPH=4 in ECO2M, for three possible fluid phases plus a possible solid phase. For flow problems in which no liquid-gas or three-phase conditions arise, TOUGH2/ECO2M may optionally be run in isothermal mode by specifying NEQ = NK (= 3). However, when liquid-gas or three-phase conditions may evolve, it is necessary to allow non-isothermal conditions by specifying NEQ = 4.

Note from Table 2 that for liquid-gas and three-phase conditions, temperature is not among the primary variables. This is because for these conditions, the system is on the saturation line (see Fig. 2) and temperature is a unique function of pressure when both a liquid and a gaseous CO<sub>2</sub> phase are present,  $T = T_{\text{sat,CO}_2}(P)$ . Phase conditions for which temperature is not among the primary variables (Index = 6 or 7 in Table 2) may optionally be initialized using temperature instead of pressure as first primary variable. Such conditions are limited to  $T \leq T_{\text{crit}} = 31.04$  °C, and ECO2M recognizes this type of initialization simply from the small numerical value of the first primary variable which would otherwise be pressure in units of Pa. The code then proceeds to replace this variable with  $X1 = P_{\text{sat,CO}_2}(T)$  in the initialization phase.

Note that, as in ECO2N, we neglect the pressure effects that may arise from the presence of dissolved water in the CO<sub>2</sub>-rich phases. This is a reasonable approximation, as water concentrations in the CO<sub>2</sub>-rich phases remain small for the modest temperatures  $T < 110$  (°C) considered here.



Table 2. Primary thermodynamic variables used for multiphase mixtures of brine and CO<sub>2</sub>.

Phases	Phase Conditions	Phase Index	Primary Variables			
			X1	X2	X3	X4
# 1: aqueous # 2: liquid CO <sub>2</sub> # 3: gaseous CO <sub>2</sub> # 4: solid salt	aqueous only	1	P	X <sub>sm</sub>	X	T
	liquid only	2	P	X <sub>sm</sub>	X	T
	gas only	3	P	X <sub>sm</sub>	X	T
	aqueous and liquid	4	P	X <sub>sm</sub>	S <sub>a</sub>	T
Components # 1: water # 2: NaCl # 3: CO <sub>2</sub>	aqueous and gas	5	P	X <sub>sm</sub>	S <sub>a</sub>	T
	liquid and gas	6	P	X <sub>sm</sub>	S <sub>g</sub>	Y
	three phase	7	P	X <sub>sm</sub>	S <sub>a</sub>	S <sub>g</sub>

Primary Variables

- P - pressure (Pa); when several phases are present, P is pressure of the (most) non-wetting phase (liquid or gaseous CO<sub>2</sub>)
- X<sub>sm</sub> - salt mass fraction X<sub>s</sub> in two-component water-salt system, or solid saturation S<sub>s</sub>+10; when X<sub>sm</sub> < 0, it specifies NaCl molality as m = -X<sub>sm</sub>
- X - CO<sub>2</sub> mass fraction
- T - temperature (°C)
- S<sub>a</sub> - aqueous phase saturation
- S<sub>g</sub> - gas phase saturation
- Y - water mass fraction

**2.1 Treatment of Dissolved and Solid Salt**

The second primary variable is denoted X<sub>sm</sub> and pertains to the NaCl component. This is the only variable for which we maintain the customary TOUGH2 approach of using different numerical ranges to identify different phase conditions. When no solid salt is present, X<sub>sm</sub> denotes X<sub>s</sub>, the salt mass fraction referred to the two-component system water-salt. When solid salt is present, X<sub>s</sub> is no longer an independent variable, as it is determined by the equilibrium

solubility of NaCl, which is a function of temperature. In the presence of solid salt, we use as second primary variable the parameter “solid saturation plus ten,”  $X_{sm} = S_s + 10$ . Here,  $S_s$  is defined in analogy to fluid saturations and denotes the fraction of void space occupied by solid salt. The reason for defining the salt concentration variable  $X_s$  with respect to the two-component system  $H_2O - NaCl$  is that this choice makes the salt concentration variable independent of  $CO_2$  concentration, which simplifies the calculation of the partitioning of the  $H_2O$  and  $CO_2$  components between the aqueous and  $CO_2$ -rich phases (see below). In the three-component system  $H_2O - NaCl - CO_2$ , the total salt mass fraction in the aqueous phase will for given  $X_s$  of course depend on  $CO_2$  concentration. Salt mass fraction in the two-component system  $H_2O - NaCl$  can be expressed in terms of salt molality (moles  $m$  of salt per kg of water) as follows.

$$X_s = \frac{mM_{NaCl}}{1000 + mM_{NaCl}} \quad (1)$$

Here  $M_{NaCl} = 58.448$  is the molecular weight of NaCl, and the number 1000 appears in the denominator because molality is defined as moles per 1000 g of water. For convenience we also list the inverse of Eq. (1).

$$m = \frac{1000X_s/M_{NaCl}}{1 - X_s} \quad (2)$$

## 2.2 Partitioning of Fluid Components among Phases

The partitioning of  $H_2O$  and  $CO_2$  among co-existing aqueous and  $CO_2$ -rich phases is calculated from a slightly modified version of the correlations developed in (Spycher and Pruess, 2005). These correlations, derived from the requirement that chemical potentials of all components must be equal in different phases, allow prediction of the equilibrium composition of aqueous and  $CO_2$ -rich phases as functions of temperature, pressure, and salinity in the temperature range  $12\text{ }^\circ\text{C} \leq T \leq 110\text{ }^\circ\text{C}$ , for pressures up to 600 bar, and salinity up to saturated NaCl brines. In the indicated parameter range, mutual solubilities of  $H_2O$  and  $CO_2$  are calculated with an accuracy typically within experimental uncertainties. The modification made in ECO2M

is that CO<sub>2</sub> molar volumes are calculated using a tabular EOS based on Altunin's correlation (1975), instead of the Redlich-Kwong equation of state used in (Spycher and Pruess, 2005). This was done to maintain consistency with the temperature and pressure conditions for phase change between liquid and gaseous conditions used elsewhere in ECO2M. Altunin's correlations yield slightly different molar volumes than the Redlich-Kwong EOS whose parameters were fitted by Spycher and Pruess (2005) to obtain the best overall match between observed and predicted CO<sub>2</sub> concentrations in the aqueous phase. The (small) differences in Altunin's molar volumes cause predictions for the mutual solubility of water and CO<sub>2</sub> to be somewhat different also. However, the differences are generally small, see Figs. 3-5.

For conditions of interest in geologic storage of CO<sub>2</sub>, equilibrium between aqueous and CO<sub>2</sub>-rich phases corresponds to a dissolved CO<sub>2</sub> mass fraction  $X_{aq}$  in the aqueous phase on the order of a few percent, while the mass fraction of water in the CO<sub>2</sub>-rich phases,  $Y_{l,eq}$  and  $Y_{g,eq}$ , typically is a fraction of a percent, so that the CO<sub>2</sub> mass fraction in the CO<sub>2</sub>-rich phases is

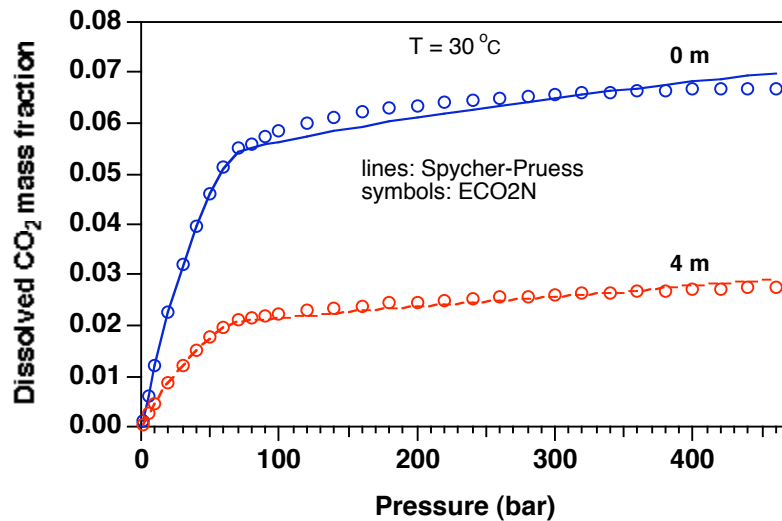


Figure 3. Dissolved CO<sub>2</sub> mass fractions in two-phase system at T = 30 °C for pure water (0-molal) and 4-molal NaCl brine. Lines represent the original correlation of Spycher and Pruess (2005) that uses a Redlich-Kwong EOS for molar volume of CO<sub>2</sub>. Symbols represent data calculated by ECO2M in which the molar volume of CO<sub>2</sub> is obtained from the correlations of Altunin (1975).

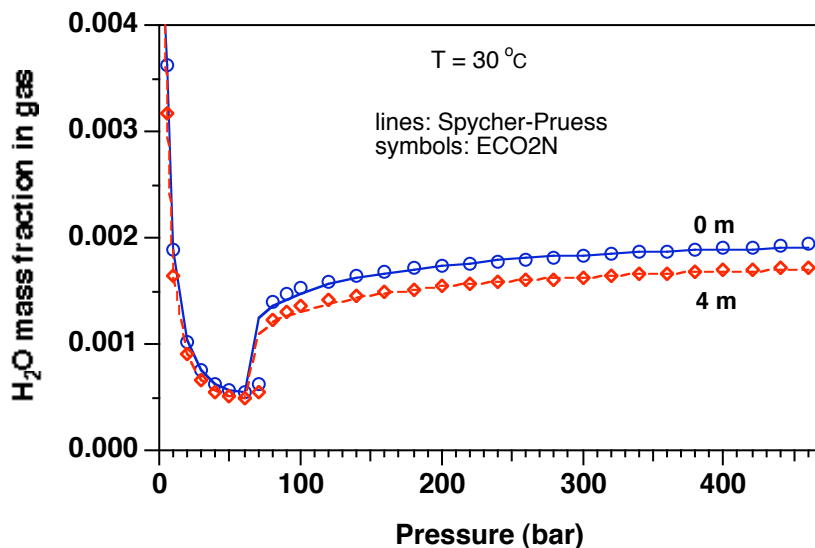


Figure 4.  $H_2O$  mass fractions in  $CO_2$ -rich phase in two-phase system at  $T = 30\text{ }^\circ\text{C}$  for pure water (0-molal) and 4-molal NaCl brine. Lines represent the correlation of Spycher and Pruess (2005) that uses a Redlich-Kwong EOS for molar volume of  $CO_2$ . Symbols represent data calculated by ECO2M in which the molar volume of  $CO_2$  is obtained from the correlations of Altunin (1975).

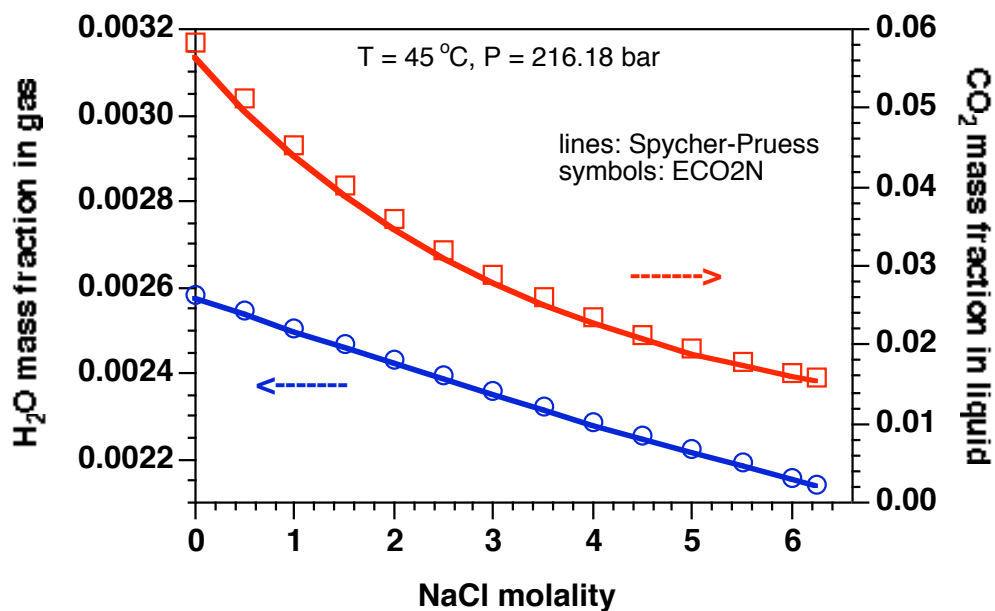


Figure 5. Concentration of water in the  $CO_2$ -rich phase and  $CO_2$  in the aqueous phase at  $(T, P) = (45\text{ }^\circ\text{C}, 216.18\text{ bar})$ , for salinities ranging from zero to fully saturated. Lines were calculated from the correlation of Spycher and Pruess (2005) that uses a Redlich-Kwong EOS for molar volume of  $CO_2$ . Symbols represent data calculated by ECO2M from a modified correlation in which the molar volume of  $CO_2$  is obtained from the correlations of Altunin (1975).

larger than 0.99. Fig. 6 depicts the relationship between total CO<sub>2</sub> mass fraction  $X_{\text{tot}}$  and phase composition of the fluid mixture for conditions in which a single CO<sub>2</sub>-rich phase may be present, which for specificity of notation we here assume to be liquid. The conditions are as follows (see Appendix C for notation).

- $X_{\text{tot}} < X_{\text{aq},l}$  corresponds to single-phase aqueous conditions;
- $X_{\text{tot}} > X_{l,\text{eq}}$  corresponds to a single liquid CO<sub>2</sub>-rich phase;
- intermediate values ( $X_{\text{aq},l} \leq X_{\text{tot}} \leq X_{l,\text{eq}}$ ) correspond to two-phase conditions with different proportions of aqueous and liquid phases.

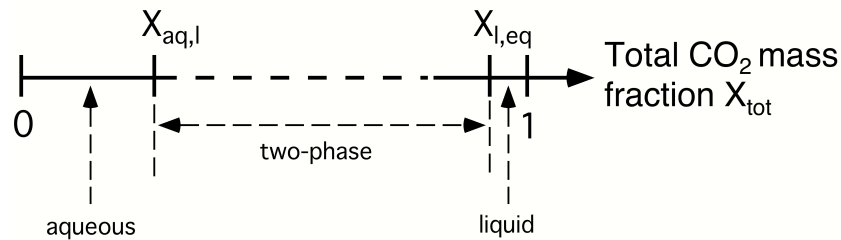


Figure 6. CO<sub>2</sub> phase partitioning in the system H<sub>2</sub>O - NaCl - CO<sub>2</sub>. The CO<sub>2</sub> mass fraction in brine-CO<sub>2</sub> mixtures can vary in the range from 0 (no CO<sub>2</sub>) to 1 (no brine).  $X_{\text{aq},l}$  and  $X_{l,\text{eq}}$  denote, respectively, the CO<sub>2</sub> mass fractions in aqueous and CO<sub>2</sub>-rich phases corresponding to equilibrium phase partitioning in two-phase conditions. Mass fractions less than  $X_{\text{aq},l}$  correspond to conditions in which only an aqueous phase is present, while mass fractions larger than  $X_{l,\text{eq}}$  correspond to single-phase liquid CO<sub>2</sub> conditions. Mass fractions intermediate between  $X_{\text{aq},l}$  and  $X_{l,\text{eq}}$  correspond to two-phase conditions with different proportions of aqueous and liquid phases.

Some further comments are in order about water dissolution in the CO<sub>2</sub>-rich phases. In the presence of an aqueous phase, the CO<sub>2</sub> mass fractions  $X_{l,\text{eq}}$  and  $X_{g,\text{eq}}$  in co-existing liquid and/or gaseous CO<sub>2</sub>-rich phases are obtained from the Spycher and Pruess (2005) phase partitioning relationships. Special considerations apply for two-phase liquid-gas conditions with no aqueous phase present. In this case, water mass fractions in liquid and gaseous phases,  $Y_l$  and  $Y_g$ , are smaller than the equilibrium values,  $Y_l < Y_{l,\text{eq}}$  and  $Y_g < Y_{g,\text{eq}}$ . Total water mass fraction  $Y$  in two-phase liquid-gas conditions is the ratio of effective water density to total fluid density, and is given by

$$Y = \frac{S_l \rho_l Y_l + S_g \rho_g Y_g}{S_l \rho_l + S_g \rho_g} \quad (3)$$

where  $S_l$  and  $S_g = 1 - S_l - S_s$  are the saturations and  $\rho_l$  and  $\rho_g$  are the densities of liquid and gaseous phases, respectively. The maximum possible total water mass fraction  $Y_{\max}$  in two-phase liquid-gas conditions is the ratio of water density in equilibrium with an aqueous phase to total fluid density,

$$Y_{\max} = \frac{S_l \rho_l Y_{l,\text{eq}} + S_g \rho_g Y_{g,\text{eq}}}{S_l \rho_l + S_g \rho_g} \quad (4)$$

In two-phase liquid-gas conditions, we use the total water mass fraction as a primary variable, and it is then necessary to calculate water mass fractions  $Y_l$  and  $Y_g$  of the individual phases from  $Y$ . We postulate that the ratio of water mass fractions in liquid and gaseous phases,  $Y_l/Y_g$ , is the same for two-phase liquid-gas conditions as it is for the three-phase system aqueous-liquid-gas, i.e.,

$$\frac{Y_l}{Y_g} = \frac{Y_{l,\text{eq}}}{Y_{g,\text{eq}}} \quad (5)$$

Eqs. (3) and (5) provide two relationships from which both  $Y_l$  and  $Y_g$  can be calculated. Substituting Eq. (5) into (3), we obtain

$$Y_g = Y \frac{S_l \rho_l + S_g \rho_g}{S_l \rho_l (Y_{l,\text{eq}}/Y_{g,\text{eq}}) + S_g \rho_g} \quad (6)$$

$Y_l$  is then obtained by substituting Eq. (6) into (5).

In two-phase liquid-gas conditions, as well as in three-phase conditions of aqueous-liquid-gas, temperature is a unique function of fluid pressure and is obtained by inverting the expression  $P_{s,\text{CO}_2} = P_{s,\text{CO}_2}(T)$  for the  $\text{CO}_2$  saturation line.

Dissolved NaCl concentrations may for typical sequestration conditions range as high as 6.25 molal. This corresponds to mass fractions of up to  $X_{sm} = 26.7\%$  in the two-component system water-salt. Phase conditions as a function of  $X_{sm}$  are as follows:

- $X_{sm} \leq XEQ$  corresponds to dissolved salt only;
- $X_{sm} > XEQ$  corresponds to conditions of a saturated NaCl brine and solid salt.

Here XEQ denotes the equilibrium solubility of NaCl, which in ECO2M is evaluated as in EWASG (Battistelli et al., 1997) as a function of temperature, using an equation by Potter cited in Chou (1987). No dependence of XEQ on aqueous  $CO_2$  concentration is taken into account.

### 2.3 Phase Change

Generally speaking, a change of phase composition (appearance or disappearance of a phase) will occur when certain parameters such as mass fractions or fluid pressures move past certain threshold values. For example, if a grid block is single-phase aqueous (INDEX = 1; see Table 2), a transition to two-phase aqueous-liquid conditions (INDEX = 4) should occur when dissolved  $CO_2$  mass fraction exceeds the equilibrium value,  $X > X_{aq,l}$ . (Our notation here assumes that fluid pressures correspond to liquid  $CO_2$ ; for lower pressures, the transition would occur to aqueous-gas.) Similarly, when only a liquid  $CO_2$  phase is present (INDEX = 2), a transition to two-phase liquid-gas conditions (INDEX = 6) should occur when in the course of a simulation the fluid pressure drops below the  $CO_2$  saturation pressure at prevailing temperature,  $P < P_{sat,CO_2}(T)$ . In our experience, using such a “hairtrigger” threshold criterion may cause unstable behavior, with repeated back-and-forth phase changes that limit convergence rates and attainable time steps. In the present section, we review the criteria applied in ECO2M to determine the appearance and disappearance of phases without concerning ourselves with issues of numerical stability. The subsequent Sec. 2.4 will generalize some of the concepts developed here by introducing the concept of a “finite window” for phase change.

In single-phase conditions (indices 1-3 in Table 2), the third primary variable X3 is the  $CO_2$  mass fraction  $X$  in that phase. In single-phase aqueous conditions, we must have  $X \leq X_{aq,l}$ , while in single-phase liquid or gas conditions, we must have  $X \geq X_{l,eq}$  or  $X \geq X_{g,eq}$ . The possibility of phase change is evaluated during a simulation by monitoring  $X$  in each grid block.

The criteria for phase change from single-phase to two-phase conditions may be written as follows.

- single-phase aqueous conditions: a transition to two-phase conditions (evolution of a CO<sub>2</sub>-rich phase) will occur when  $X > X_{\text{aq,l}}$  (or  $X > X_{\text{aq,g}}$ ; whether the evolving CO<sub>2</sub>-rich phase is liquid or gas depends on the P,T-conditions; recall that for supercritical temperatures, we arbitrarily assign the single CO<sub>2</sub>-rich phase as “liquid” when  $P \geq P_{\text{crit}}$ , and as “gas” when  $P < P_{\text{crit}}$ );
- single-phase liquid or single-phase gas conditions: a transition to two-phase conditions with an aqueous phase will occur when  $X < X_{\text{l,eq}}$  (or  $X < X_{\text{g,eq}}$  in the case of a gaseous CO<sub>2</sub>-rich phase);

When two-phase conditions evolve in a previously single-phase grid block, primary variables are switched as shown in Table 2. The starting value of the saturation of the newly evolving phase is chosen as  $10^{-6}$ .

In two-phase conditions, (indices 4-6 in Table 2) the third primary variable X3 denotes saturation of one of the two phases. For two-phase conditions to persist, this phase saturation must remain in the range (0, 1). Transitions to single-phase conditions are recognized as follows.

- for aqueous-liquid and aqueous-gas conditions,  $X3 = S_{\text{a}}$ , the saturation of the aqueous phase;  $X3 < 0$  indicates that the aqueous phase disappears, and we make a transition to single-phase liquid or single-phase gas conditions;  $X3 > 1 - S_{\text{s}}$  indicates that the non-aqueous phase disappears, and we make a transition to single-phase aqueous conditions;
- for liquid-gas conditions,  $X3 = S_{\text{g}}$ , the saturation of the gas phase;  $X3 < 0$  indicates that the gas phase disappears, and we make a transition to single-phase liquid;  $X3 > 1 - S_{\text{s}}$  indicates that the liquid phase disappears, and we make a transition to single-phase gas.

In two-phase conditions, we also need to test for evolution of the third phase. In aqueous-liquid conditions, a gas phase will evolve if  $P < P_{\text{sat,CO}_2}(T)$ . Similarly, in aqueous-gas conditions a liquid phase will evolve when  $P > P_{\text{sat,CO}_2}(T)$ . Finally, in two-phase liquid-gas conditions, we check whether an aqueous phase evolves by comparing total water mass fraction Y, the fourth



primary variable, with the maximum possible water mass fraction  $Y_{\max}$  (Eq. 4, above); as long as  $Y \leq Y_{\max}$  no aqueous phase evolves, while for  $Y > Y_{\max}$  we make a transition to three-phase aqueous-liquid-gas conditions. The newly evolving aqueous phase is then initialized with a small saturation of  $S_a = 10^{-6}$ .

In three-phase conditions, disappearance of a phase is recognized by saturations dropping below 0. If  $S_a < 0$ , aqueous phase disappears; if  $S_g < 0$ , gas phase disappears, and if  $S_l = 1 - S_a - S_g - S_s < 0$ , liquid phase disappears.

Phase change involving (dis-)appearance of solid salt is recognized as follows. When no solid salt is present, the second primary variable  $X_{sm}$  is the concentration (mass fraction referred to total water plus salt) of dissolved salt in the aqueous phase. The possibility of precipitation starting is evaluated by comparing  $X_{sm}$  with XEQ, the equilibrium solubility of NaCl at prevailing temperature. If  $X_{sm} \leq XEQ$  no precipitation occurs, whereas for  $X_{sm} > XEQ$  precipitation starts. In the latter case, variable  $X_{sm}$  is switched to  $S_s+10$ , where solid saturation  $S_s$  is initialized with a small non-zero value ( $10^{-6}$ ). If a solid phase is present, the variable  $X_{sm} = S_s+10$  is monitored. Solid phase disappears if  $X_{sm} < 10$ , in which case primary variable  $X_{sm}$  is switched to salt concentration, and is initialized as slightly below saturation,  $X_{sm} = XEQ - 10^{-6}$ .

#### **2.4 “Hairtrigger” vs. “Finite Window” for Phase Change**

The phase change criteria discussed in the previous section may give rise to unstable behavior, with repeated back-and-forth phase changes that limit convergence rates and time step sizes. Unstable behavior related to phase change is especially likely for flow processes in which thermodynamic conditions are close to the  $CO_2$  saturation line for extended regions and time periods, as is often the case in problems that involve  $CO_2$  leakage to shallow horizons, or all the way to the land surface. We found that a much more stable behavior and improved simulation progress can be achieved by employing a “finite window” for phase change, in which parameters have to exceed or drop below threshold values by a finite amount before phase composition is changed. Thus, ECO2M offers the possibility of specifying a finite window  $\delta$ , so that the transition from a single liquid phase to two-phase liquid-gas conditions will not be made when

the “hairtrigger criterion”  $P < P_{\text{sat,CO}_2}(T)$  is satisfied, but will only be made when  $P < (1 - \delta)P_{\text{sat,CO}_2}(T)$ . Here,  $\delta$  is a parameter that may be specified by the user as part of the TOUGH2/ECO2M input file and may typically be chosen of order  $\delta \approx 10^{-3} - 10^{-5}$ . As a further refinement, the user may choose to adopt a hairtrigger criterion only for the first few ( $\text{ITER} < \text{IHAIR}$ ) Newtonian iterations during a time step, and switch to the finite window criterion for the subsequent Newtonian iterations  $\text{ITER} \geq \text{IHAIR}$ . This combines the flexibility of being able to make phase transitions during the early part of the iteration with the stability to achieve convergence in the later part. Similar considerations apply for phase changes that are triggered by changes in dissolved mass fractions, such as emergence of a  $\text{CO}_2$ -rich phase from single-phase aqueous conditions, or emergence of an aqueous phase when only a single  $\text{CO}_2$ -rich phase is present; in these case the finite window for phase change may be applied to mass fractions rather than pressures. An optional user-selectable switch between hairtrigger and finite phase change windows is available for the transitions aqueous  $\implies$  aqueous-liquid (1  $\implies$  4), aqueous  $\implies$  aqueous-gas (1  $\implies$  3), liquid  $\implies$  aqueous-liquid (2  $\implies$  4), liquid  $\implies$  liquid-gas (2  $\implies$  6), aqueous-liquid  $\implies$  aqueous-liquid-gas (4  $\implies$  7); and aqueous-gas  $\implies$  aqueous-liquid-gas (5  $\implies$  7). The data input for selecting a finite window for phase change is explained in Sec. 5.3, below.

## 2.5 Conversion of Units

The Spycher and Pruess (2005) model for phase partitioning in the system  $\text{H}_2\text{O}$ – $\text{NaCl}$ – $\text{CO}_2$  is formulated in molar quantities (mole fractions and molalities), while TOUGH2/ECO2M describes phase compositions in terms of mass fractions. This section presents the equations and parameters needed for conversion between the two sets of units. The conversion between various concentration variables (mole fractions, molalities, mass fractions) does not depend upon whether or not concentrations correspond to equilibrium between liquid and gas phases; accordingly, the relations given below are valid regardless of the magnitude of concentrations.

Let us consider an aqueous phase with dissolved  $\text{NaCl}$  and  $\text{CO}_2$ . For a solution that is  $m$ -molal in  $\text{NaCl}$  and  $n$ -molal in  $\text{CO}_2$ , total mass per kg of water is

$$M = 1000 \text{ (g H}_2\text{O)} + m M_{\text{NaCl}} \text{ (g NaCl)} + n M_{\text{CO}_2} \text{ (g CO}_2\text{)} \quad (7)$$

where  $M_{\text{NaCl}}$  and  $M_{\text{CO}_2}$  are the molecular weights of NaCl and  $\text{CO}_2$ , respectively (see Table 3).

Table 3. Molecular weights in the system  $\text{H}_2\text{O}$ –NaCl– $\text{CO}_2$  (Evans, 1982).

species	mol. weight
$\text{H}_2\text{O}$	18.016
Na	22.991
Cl	35.457
NaCl	58.448
$\text{CO}_2$	44.0

Assuming NaCl to be completely dissociated, the total moles per kg of water are

$$m_T = 1000/M_{\text{H}_2\text{O}} + 2m + n \quad (8)$$

The Spycher and Pruess (2005) correlations provide  $\text{CO}_2$  mole fraction  $x_2$  in the aqueous phase and  $\text{H}_2\text{O}$  mole fraction  $y_1$  in the gas phase as functions of temperature, pressure, and salt concentration (molality). For a  $\text{CO}_2$  mole fraction  $x_2$  we have  $n = x_2 m_T$  from which, using Eq. (8), we obtain

$$n = \frac{x_2(2m + 1000/M_{\text{H}_2\text{O}})}{1 - x_2} \quad (9)$$

$\text{CO}_2$  mass fraction  $X$  in the aqueous phase is obtained by dividing the  $\text{CO}_2$  mass in  $n$  moles by the total mass,

$$X = \frac{nM_{\text{CO}_2}}{1000 + mM_{\text{NaCl}} + nM_{\text{CO}_2}} \quad (10)$$

Assuming a single co-existing  $\text{CO}_2$ -rich phase, water mass fraction  $Y_C$  in that phase is simply

$$Y_C = \frac{y_1 \cdot M_{H_2O}}{y_1 \cdot M_{H_2O} + (1 - y_1) M_{CO_2}} \quad (11)$$

### 3. Thermophysical Properties of Water-NaCl-CO<sub>2</sub> Mixtures

Thermophysical properties needed to model the flow of water-salt-CO<sub>2</sub> mixtures in porous media include density, viscosity, and specific enthalpy of the fluid phases as functions of temperature, pressure, and composition, and partitioning of components among the fluid phases. Many of the needed parameters are obtained from the same correlations as were used in the EWASG property module of TOUGH2 (Battistelli et al., 1997). EWASG was developed for geothermal applications, and consequently considered conditions of elevated temperatures > 100 °C, and modest CO<sub>2</sub> partial pressures of order 1-10 bar. The present ECO2M module targets the opposite end of the temperature and pressure range, namely, modest temperatures below 110 °C, and high CO<sub>2</sub> pressures up to several hundred bar. ECO2M uses the exact same thermophysical property correlations as the earlier ECO2N module (Pruess, 2005; Pruess and Spycher, 2007).

Water properties in TOUGH2/ECO2M are calculated, as in other members of the TOUGH family of codes, from the steam table equations as given by the International Formulation Committee (1967). Properties of pure CO<sub>2</sub> are obtained from correlations developed by Altunin et al. (1975). We began using Altunin's correlations in 1999 when a computer program implementing them was kindly made available to us by Victor Malkovsky of the Institute of Geology of Ore Deposits, Petrography, Mineralogy and Geochemistry (IGEM) of the Russian Academy of Sciences, Moscow. Altunin's correlations were subsequently extensively cross-checked against experimental data and alternative PVT formulations, such as Span and Wagner (1996). They were found to be very accurate (García, 2003), so there is no need to change to a different formulation.

Altunin's correlations are not used directly in the code, but are used to tabulate density, viscosity, and specific enthalpy of pure CO<sub>2</sub> on a regular grid of (T, P)-values. These tabular data are provided in a file called "CO2TAB," and property values are obtained during a TOUGH2/ECO2M simulation by means of bivariate interpolation. Fig. 7 shows the manner in which CO<sub>2</sub> properties are tabulated, intentionally showing a coarse (T, P)-grid so that pertinent

features of the tabulation may be better seen. (For actual calculations, we use finer grid spacings; the CO2TAB data file distributed with ECO2M covers the range  $3.04\text{ }^{\circ}\text{C} \leq T \leq 103.04\text{ }^{\circ}\text{C}$  with  $\Delta T = 2\text{ }^{\circ}\text{C}$  and  $1\text{ bar} \leq P \leq 600\text{ bar}$  with  $\Delta P \leq 4\text{ bar}$  in most cases. The ECO2M distribution includes a utility program for generating CO2TAB files if users desire a different T,P-range or

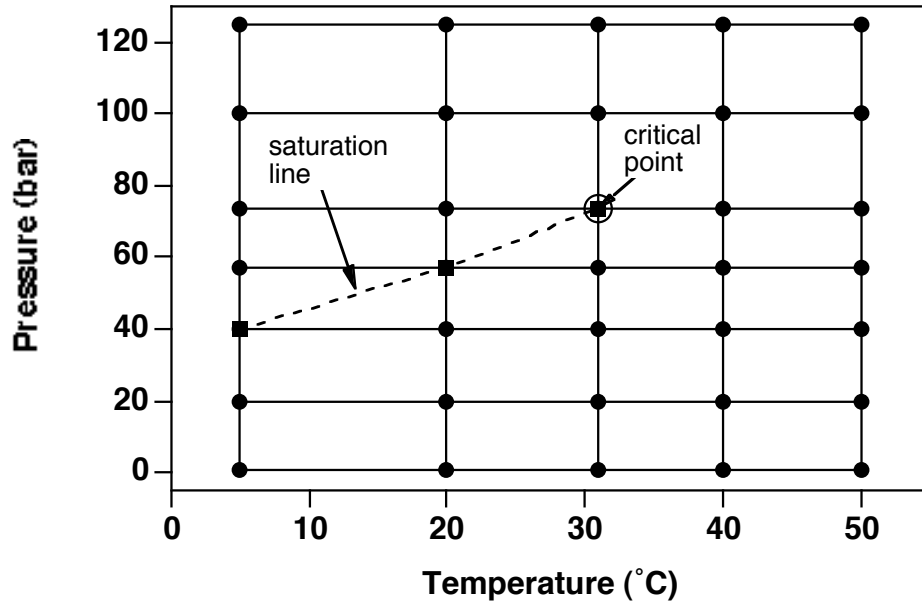


Figure 7. Schematic of the temperature-pressure tabulation of CO<sub>2</sub> properties. The saturation line (dashed) is given by the diagonals of interpolation rectangles.

different increments.) As shown in Fig. 7, the tabulation is made in such a way that for sub-critical conditions the saturation line is given by diagonals of the interpolation quadrangles. On the saturation line, two sets of data are provided, for liquid and gaseous CO<sub>2</sub>, respectively, and in quadrangles that include points on both sides of the saturation line, points on the "wrong" side are excluded from the interpolation. This scheme provides for an efficient and accurate determination of thermophysical properties of CO<sub>2</sub>.

ECO2M is applicable to water-salt-CO<sub>2</sub> mixtures at moderate temperatures,  $T < 110\text{ }^{\circ}\text{C}$ , where water concentrations in the CO<sub>2</sub>-rich phases are small. Accordingly, we neglect effects of dissolved water on the density and viscosity of the CO<sub>2</sub>-rich phases. However, due to the very large specific enthalpy of water vapor, caloric effects of water dissolution in the CO<sub>2</sub>-rich phases may be significant, even though water mass fractions are small. We approximate the specific enthalpy of water that is dissolved in the CO<sub>2</sub>-rich phases as being identical to the enthalpy of

saturated water vapor at the same temperature, neglecting heat-of-dissolution effects. Specific enthalpy of the CO<sub>2</sub>-rich phases is then calculated by adding the specific enthalpies of the CO<sub>2</sub> and water components, see below.

### 3.1 Density

Brine density  $\rho_b$  for the binary system water-salt is calculated as in Battistelli et al. (1997) from the correlations of Haas (1976) and Andersen et al. (1992). The calculation starts from aqueous phase density without salinity at vapor-saturated conditions, which is obtained from the correlations given by the International Formulation Committee (1967). Corrections are then applied to account for effects of salinity and pressure. The density of aqueous phase with a dissolved CO<sub>2</sub> mass fraction  $X$  is calculated assuming additivity of the volumes of brine and dissolved CO<sub>2</sub>.

$$\frac{1}{\rho_{\text{aq}}} = \frac{1-X}{\rho_b} + \frac{X}{\rho_{\text{CO}_2}} \quad (12)$$

where  $X$  is the mass fraction of CO<sub>2</sub> in the aqueous phase. Partial density of dissolved CO<sub>2</sub>,  $\rho_{\text{CO}_2}$ , is calculated as a function of temperature from the correlation for molar volume of dissolved CO<sub>2</sub> at infinite dilution developed by García (2001).

$$V_\phi = a + bT + cT^2 + dT^3 \quad (13)$$

In Eq. (13), molar volume of CO<sub>2</sub> is in units of cm<sup>3</sup> per gram-mole, temperature  $T$  is in °C, and  $a$ – $d$  are fit parameters given in Table 4.

Table 4. Parameters for molar volume of dissolved CO<sub>2</sub> (Eq. 13)

a	37.51
b	-9.585e-2
c	8.740e-4
d	-5.044e-7

Partial density of dissolved CO<sub>2</sub> in units of kg/m<sup>3</sup> is then

$$\rho_{\text{CO}_2} = \frac{M_{\text{CO}_2}}{V_\phi} * 10^3 \quad (14)$$

where  $M_{\text{CO}_2} = 44.0$  is the molecular weight of CO<sub>2</sub>.

Dissolved CO<sub>2</sub> amounts at most to a few percent of total aqueous density. Accordingly, dissolved CO<sub>2</sub> is always dilute, regardless of total fluid pressure. It is then permissible to neglect the pressure dependence of partial density of dissolved CO<sub>2</sub>, and to use the density corresponding to infinite dilution.

As had been mentioned above, the density of the CO<sub>2</sub>-rich phase(s) is obtained by neglecting effects of water, and approximating the density by that of pure CO<sub>2</sub> at the same temperature and pressure conditions. Density is obtained through bivariate interpolation from a tabulation of CO<sub>2</sub> densities as function of temperature and pressure, that is based on the correlations developed by Altunin (1975).

### 3.2 Viscosity

Brine viscosity is obtained as in EWASG from a correlation presented by Phillips et al. (1981), that reproduces experimental data in the temperature range from 10–350 °C for salinities up to 5 molal and pressures up to 500 bar within 2 %. No allowance is made for dependence of brine viscosity on the concentration of dissolved CO<sub>2</sub>. Viscosity of the CO<sub>2</sub>-rich phases is approximated as being equal to pure CO<sub>2</sub>, and is obtained through tabular interpolation from the correlations of Altunin (1975).

### 3.3 Specific Enthalpy

Specific enthalpy of brine is calculated from the correlations developed by Lorenz et al. (2000), which are valid for all salt concentrations in the temperature range from 25 °C ≤ T ≤ 300 °C. The enthalpy of aqueous phase with dissolved CO<sub>2</sub> is obtained by adding the enthalpies of the CO<sub>2</sub> and brine (pseudo-) components, and accounting for the enthalpy of dissolution of CO<sub>2</sub>.

$$h_{\text{aq}} = (1 - X)h_b + Xh_{\text{CO}_2,\text{aq}} \quad (15)$$

$h_{\text{CO}_2,\text{aq}} = h_{\text{CO}_2} + h_{\text{dis}}$  is the specific enthalpy of aqueous (dissolved)  $\text{CO}_2$ , which includes heat of dissolution effects that are a function of temperature and salinity. For gas-like (low pressure)  $\text{CO}_2$ , the specific enthalpy of dissolved  $\text{CO}_2$  is

$$h_{\text{CO}_2,\text{aq}}(T, P, X_s) = h_{\text{CO}_2,\text{g}}(T, P) + h_{\text{dis,g}}(T, X_s) \quad (16)$$

where  $h_{\text{dis,g}}$  is obtained as in Battistelli et al. (1997) from an equation due to Himmelblau (1959). For geologic sequestration we are primarily interested in liquid-like (high-pressure)  $\text{CO}_2$ , for which the specific enthalpy of dissolved  $\text{CO}_2$  may be written

$$h_{\text{CO}_2,\text{aq}}(T, P, X_s) = h_{\text{CO}_2,\text{l}}(T, P) + h_{\text{dis,l}}(T, X_s) \quad (17)$$

Here  $h_{\text{dis,l}}$  is the specific heat of dissolution for liquid-like  $\text{CO}_2$ . Along the  $\text{CO}_2$  saturation line, liquid and gaseous  $\text{CO}_2$  phases may co-exist, and the expressions Eqs. (16, 17) must be equal there. We obtain

$$h_{\text{dis,l}}(T, X_s) = h_{\text{dis,g}}(T, X_s) + h_{\text{CO}_2,\text{gl}}(T) \quad (18)$$

where  $h_{\text{CO}_2,\text{gl}}(T) = h_{\text{CO}_2,\text{g}}(T, P_s) - h_{\text{CO}_2,\text{l}}(T, P_s)$  is the specific enthalpy of vaporization of  $\text{CO}_2$ , and  $P_s = P_s(T)$  is the saturated vapor pressure of  $\text{CO}_2$  at temperature  $T$ . Depending upon whether  $\text{CO}_2$  is in gas or liquid conditions, we use Eq. (16) or (17) in Eq. (15) to calculate the specific enthalpy of dissolved  $\text{CO}_2$ . At the temperatures of interest here,  $h_{\text{dis,g}}$  is a negative quantity, so that dissolution of low-pressure  $\text{CO}_2$  is accompanied by an increase in temperature.  $h_{\text{CO}_2,\text{gl}}$  is a positive quantity, which will reduce or cancel out the heat-of-dissolution effects. This indicates that dissolution of liquid  $\text{CO}_2$  will produce less temperature increase than dissolution of gaseous  $\text{CO}_2$ , and may even cause a temperature decline if  $h_{\text{CO}_2,\text{gl}}$  is sufficiently large.



Application of Eqs. (15)-(18) is straightforward for conditions in which either a liquid or a gaseous CO<sub>2</sub>-rich phase is present;  $h_{\text{CO}_2,\text{l}}$  or  $h_{\text{CO}_2,\text{g}}$  is then obtained as a function of temperature and pressure through bivariate interpolation from a tabulation of Altunin's correlation (1975). If both liquid and gaseous CO<sub>2</sub>-rich phases are present,  $h_{\text{CO}_2,\text{l}}$  and  $h_{\text{CO}_2,\text{g}}$  are obtained by linear interpolation along the CO<sub>2</sub> saturation line. A complication arises for single-phase aqueous conditions, because it would not be correct to evaluate  $h_{\text{CO}_2,\text{l}}$  or  $h_{\text{CO}_2,\text{g}}$  at total pressure  $P$ , where equilibrium with a free CO<sub>2</sub>-rich phase would occur at a mass fraction  $X_{\text{aq}} > X$ . What is the proper pressure to use for evaluating CO<sub>2</sub> enthalpy? We assume that, for a given temperature, the enthalpy of aqueous CO<sub>2</sub> depends only on the dissolved mass fraction  $X$ , not on total fluid pressure. Accordingly, the enthalpy of dissolved aqueous CO<sub>2</sub> may be calculated from the enthalpy of a free CO<sub>2</sub>-rich phase, that would be in equilibrium with aqueous phase at a dissolved mass fraction  $X$ . In two-phase conditions with an aqueous and a CO<sub>2</sub>-rich phase at fixed temperature, the dissolved aqueous CO<sub>2</sub> mass fraction  $X$  increases monotonically as a function of total pressure  $P$ . Therefore, when dissolved aqueous CO<sub>2</sub> mass fraction  $X$  is smaller than would correspond to phase equilibrium with a CO<sub>2</sub>-rich phase, the total pressure  $P_2$  at which a free CO<sub>2</sub>-rich phase would evolve is smaller than  $P$ ,  $P_2 < P$ . To obtain  $P_2$  it is necessary to invert the Spycher and Pruess (2005) phase partitioning relation  $X = X(P_2; T, X_s)$ . Prior to doing this, we evaluate dissolved aqueous CO<sub>2</sub> concentration at a pressure of  $P_0 = 1$  bar,  $X_{\text{aq}}(1 \text{ bar})$ ; the subsequent approach for obtaining  $P_2$  is different depending upon whether  $X$  does or does not exceed  $X_{\text{aq}}(1 \text{ bar})$ . If  $X \geq X_{\text{aq}}(1 \text{ bar})$ ,  $P_2$  is obtained by iterative bisection in the interval (1 bar,  $P$ ) followed by Newtonian iteration. Specific enthalpy of the CO<sub>2</sub>-rich phase in the two-phase system is then calculated as  $h_{\text{CO}_2} = h_{\text{CO}_2}(T, P_2)$ , and specific enthalpy of dissolved CO<sub>2</sub> is  $h_{\text{CO}_2} + h_{\text{dis}}$  from Eq. (16) or (17).

A different approach is required for small CO<sub>2</sub> concentrations with  $X < X_{\text{aq}}(1 \text{ bar})$ , corresponding to  $P_2 < 1$  bar, because our tabular equation of state for CO<sub>2</sub> typically only starts at a pressure of 1 bar. For small CO<sub>2</sub> concentrations, where no tabular data are available, ECO2M obtains  $P_2$  from Henry's law, with Henry's constant computed at a pressure of 1 bar. The enthalpy of a free CO<sub>2</sub>-rich phase corresponding to  $P_2 < 1$  bar is calculated from the same polynomial fit as in the EWASG code (Battistelli et al., 1997).

A somewhat subtle problem arises when the dissolved aqueous CO<sub>2</sub> mass fraction  $X$  is such that the corresponding CO<sub>2</sub> pressure  $P_2$  is “near” the CO<sub>2</sub> saturation line,  $P_2 \approx P_{\text{sat,CO}_2}(T)$ . As noted above, for fixed temperature  $X$  increases monotonically as a function of  $P_2$ , and at the saturation line we have  $X_{\text{aq,l}} = X_{\text{aq,g}}$ . In ECO2M we define the CO<sub>2</sub> saturation line  $P_{\text{sat,CO}_2}(T)$  based on the correlations of Altunin (1975), which is slightly different from the saturation line implicit in the phase partitioning correlations of Spycher and Pruess (2005). Because of this difference, the monotonicity and uniqueness properties of dissolved aqueous mass fraction as a function of pressure are slightly violated. Table 5 shows that for  $T \leq 20$  °C, there is a finite albeit small gap between  $X_{\text{aq,l}}$  and  $X_{\text{aq,g}}$ , while for  $T \geq 25$  °C there is an overlap with  $X_{\text{aq,l}} < X_{\text{aq,g}}$ . The discrepancies are small, but will cause the iterative determination of  $P_2$  from  $X$  to fail if there is a gap  $X_{\text{aq,g}} < X_{\text{aq,l}}$ , and if  $X$  is such as to fall into this gap:  $X_{\text{aq,g}} < X < X_{\text{aq,l}}$ . One might think that such an occurrence is rare; however, our experience with CO<sub>2</sub> migrating upwards from depth indicates that there are strong mechanisms at play that tend to push thermodynamic conditions to the vicinity of the CO<sub>2</sub> saturation line (e.g., Pruess, 2005b, 2008), and it is necessary to cope with the slight violation of the monotonicity and uniqueness properties of dissolved aqueous CO<sub>2</sub> mass fraction. ECO2M has coding to recognize when  $X$  falls into a gap between  $X_{\text{aq,g}}$  and  $X_{\text{aq,l}}$ , and simply assigns  $P_2 = P_{\text{sat,CO}_2}(T)$  in that case.

Table 5. Dissolved aqueous CO<sub>2</sub> mass fractions along the CO<sub>2</sub> saturation line.

T (°C)	$P_{\text{sat,CO}_2}$ (Pa)	$X_{\text{aq,g}}$	$X_{\text{aq,l}}$	$X_{\text{aq,l}}$ vs. $X_{\text{aq,g}}$
5	.397230E+07	.691135E-01	.737777E-01	gap
10	.450567E+07	.661992E-01	.696398E-01	gap
15	.508953E+07	.633831E-01	.656093E-01	gap
20	.573314E+07	.606913E-01	.616303E-01	gap
25	.643866E+07	.579773E-01	.577475E-01	overlap
30	.721982E+07	.543894E-01	.534334E-01	overlap
31.0	.738389E+07	.533000E-01	.532595E-01	overlap
31.03	.738881E+07	.532748E-01	.532647E-01	overlap

#### **4. Heat Exchange with Impermeable Regions**

CO<sub>2</sub> flow in geologic storage reservoirs often may be approximated as isothermal, but very strong non-isothermal effects may occur in the vicinity of the injection point, and when leaking CO<sub>2</sub> migrates to shallower horizons. These effects arise principally from two mechanisms, (1) latent heat effects when liquid CO<sub>2</sub> boils into gas, and (2) strong cooling upon decompression of gaseous CO<sub>2</sub>, the so-called Joule-Thomson effect (Katz and Lee, 1990; Pruess, 2004, 2005a, b, 2008; Oldenburg, 2007). CO<sub>2</sub> leakage may occur in diffuse manner through permeable media, but perhaps more importantly may occur along localized preferential pathways, such as fracture zones and faults, that are surrounded by media of much lower permeability. For diffuse permeation, non-isothermal effects will be spatially dispersed as is the CO<sub>2</sub> flow, while in the latter case, cooling occurs in localized permeable regions. Such cooling will give rise to heat transfer in the adjacent media, which will be primarily conductive in nature due to their low permeability.

One possible approach for modeling heat exchange with conductive regions is to simply extend the computational grid into those regions, and assign them appropriately small or vanishing permeability. This way heat transfer would be treated on an equal footing with fluid flow in the reservoir. A drawback of this approach is that, even for modest accuracy requirements, the number of grid blocks in the thermal conduction domain could easily become comparable to, or even larger than, the number of grid blocks in the permeable regions, leading to a very inefficient calculation. A much more efficient alternative involves application of a semi-analytical method, which requires no grid blocks outside of the fluid flow domain, and permits better accuracy for short- and long-term heat exchange. TOUGH2/ECO2M provides an option to use the method of Vinsome and Westerveld (1980), which gives excellent accuracy for heat exchange between permeable regions and adjacent impermeable conductive domains.

Observing that the process of heat conduction tends to dampen out temperature variations, Vinsome and Westerveld reasoned that temperatures in the conduction zone would vary smoothly even for strong and rapid temperature changes at the boundary of the flow region. Arguing that heat conduction perpendicular to the conductive boundary is more important than

parallel to it, they proposed to represent the temperature profile in a semi-infinite conductive half-space with a simple trial function, as follows:

$$T(x,t) - T_i = (T_f - T_i + px + qx^2) \exp(-x/d) \quad (19)$$

Here  $x$  is the distance from the permeable boundary,  $T_i$  is initial temperature in the conductive domain (assumed uniform),  $T_f$  is the time-varying temperature at the boundary of the permeable domain,  $p$  and  $q$  are time-varying fit parameters, and  $d$  is the penetration depth for heat conduction, given by

$$d = \sqrt{\Theta t}/2 \quad (20)$$

where  $\Theta = \lambda/\rho C$  is the thermal diffusivity,  $\lambda$  the thermal conductivity,  $\rho$  the density of the medium, and  $C$  the specific heat. In the context of a finite-difference simulation of nonisothermal flow, each grid block in the computational grid for the permeable region may have an associated temperature profile in the adjacent impermeable rock as given by Eq. (19). The coefficients  $p$  and  $q$  will be different for each grid block; they are determined concurrently with the flow simulation from the physical constraints of (1) continuity of heat flux across the boundary, and (2) energy conservation for the reservoir/confining layer system.

As originally conceived by Vinsome and Westerveld (1980) and used in standard TOUGH2, the semi-analytical approach for modeling conductive heat exchange was designed for confining beds with low permeability, such as cap rocks and base rocks. In that case the boundary of the permeable region typically occurs at a fixed vertical depth, and the initial temperature  $T_i$  at the boundary of the conduction zone is approximately the same for all grid blocks that have an interface with the conduction zone. For such applications, the entire conduction zone may be considered to have the same initial temperature. The situation may be quite different in  $\text{CO}_2$  leakage, where the pathways are more likely to be (sub-)vertical, and the initial temperature distribution along the leakage path would be given by a geothermal gradient. Accordingly, TOUGH2/ECO2M offers the possibility of modeling temperature gradients along

the boundary to the conduction zone by specifying the initial temperature of the conductive half-spaces to be different for different grid blocks; i.e., initial temperature in the conductive domain can be a function of grid block index  $n$ , and is denoted by  $T_i(n)$ .

There is no separate input data block for invoking a semi-analytical heat exchange calculation. Instead, a number of parameters have to be specified in different blocks to engage this option, as follows. In order to activate a semi-analytical heat loss calculation, the parameter MOP(15) in record PARAM.1 must be set equal to 1. The heat capacity and conductivity of the conductive zone is specified by means of data provided for the very last volume element in data block ELEME. (A “dummy” inactive element should be used for this purpose; this is an element that is not connected to any part of the simulation domain, having the sole purpose of serving as a vehicle for transferring thermal parameters.) Heat capacity and conductivity are taken from data provided in block ROCKS for the particular domain to which the last element belongs. The temperature with which this last element is initialized is taken as the uniform default value for the initial temperature in the conductive region(s), but this value can be superseded if element-specific  $T_i(n)$  data are provided; see below. Thus, if a semi-analytical heat exchange calculation is desired, the user would append an additional inactive element in block ELEME, and provide the desired parameters as initial conditions and domain data, respectively, for this element.

If it is desired to employ different temperatures for the conductive half-spaces attached to different elements, then these temperature specifications must be provided through a disk file that is written to the same specifications as a TOUGH2 INCON file, except that the file should not have a first record “INCON;” instead, it should start immediately with the data for the first grid block. For simplicity we use the file MINC, that normally would be used for geometric data, as a means to convey the element-specific temperature information to TOUGH2/ECO2M. In practice, prior to simulating CO<sub>2</sub> storage and leakage, the user would generate steady state conditions for the flow system with the appropriate geothermal gradient and hydrostatic pressure profile. The SAVE file representing these conditions would be used as file INCON to initialize the flow simulation, and the same file, with header “INCON” omitted, would also be provided as file MINC to initialize the temperatures in the conductive domain. Note that the file MINC must include data for all grid blocks, regardless of whether or not they have conductive domains

attached to them, and the grid blocks must appear in exactly the same order as in the ELEM data in the input file (or in file MESH). Finally, it is necessary to specify interface areas with the conductive domains. This information is input as parameter AHTX in columns 31-40 of volume element data in block ELEM. Generating a computational grid using MESHMAKER will automatically assign proper data for the interface areas. Volume elements for which a zero-interface area is specified will not be subject to semi-analytical heat exchange.

When semi-analytical heat transfer is engaged, the temperature data for elements subjected to semi-analytical heat transfer will be printed to the output file at the beginning of a simulation run, along with the initial temperatures of their associated conductive domains. This is useful for checking and plotting. At the termination of a run the data necessary for continuing the heat exchange calculation in a TOUGH2 continuation run are written onto a disk file TABLE. When restarting a problem, this file has to be provided under the name TABLE. If file TABLE is absent, TOUGH2 assumes that no prior heat exchange with conductive zones has taken place, and takes their temperatures to be uniform and equal to their initial temperatures. Also, a continuation run requires the same file MINC with data on the initial temperatures in the conductive region. Examples of the application of a semi-analytical treatment for heat exchange are given in sample problem 3 and 4, below.

## **5. Preparation of Input Data**

Most of TOUGH2/ECO2M input specifications correspond to the general TOUGH2 input formats as given in the TOUGH2 user's guide (Pruess et al., 1999). This information is not duplicated in the present report; here we discuss only parameter choices specific to ECO2M.

### **5.1 Initialization Choices with ECO2N-style Primary Variables**

Initialization of a simulation with TOUGH2/ECO2M would normally be made with the internally used primary variables as listed in Table 2. As a convenience to users, ECO2M provides the possibility to initialize flow problems with the same primary variables as used in ECO2N; see Table 6. This capability is engaged by omitting the data block INDEX. ECO2N-style primary variables are internally converted to ECO2M style in the initialization phase of a

TOUGH2/ECO2M run. ECO2M also retains the same capabilities as ECO2N for initialization with additional parameter choices; see below.

Table 6. ECO2N-style primary variables

single fluid phase (only aqueous, or only CO <sub>2</sub> -rich phase)#&	(P, X <sub>sm</sub> , X, T)
two fluid phases (aqueous and CO <sub>2</sub> -rich phase)#&	(P, X <sub>sm</sub> , S <sub>C</sub> +10, T)
<u>Primary Variables</u>	
P -	pressure (Pa)
X <sub>sm</sub> -	salt mass fraction X <sub>s</sub> in two-component water-salt system, or solid saturation S <sub>s</sub> +10; when X <sub>sm</sub> < 0, it specifies NaCl molality as m = -X <sub>sm</sub>
X -	CO <sub>2</sub> mass fraction in the aqueous phase, or in the CO <sub>2</sub> -rich phase, in the three-component system water-salt-CO <sub>2</sub>
T -	temperature (°C)
S <sub>C</sub> -	saturation of CO <sub>2</sub> -rich phase (liquid or gas)

- # When discussing fluid phase conditions, we refer to the potentially mobile (aqueous and CO<sub>2</sub>-rich) phases only; in all cases solid salt may precipitate or dissolve, adding another active phase to the system.
- & Depending on temperature and pressure conditions, the CO<sub>2</sub>-rich phase may be either liquid or gas.

The ECO2N primary variables are (P, X<sub>sm</sub>, X, T) for grid blocks with a single (aqueous or CO<sub>2</sub>-rich) phase, and (P, X<sub>sm</sub>, S<sub>C</sub>+10, T) for grid blocks with two phases (aqueous and CO<sub>2</sub>-rich; see Table 6). Here X is the mass fraction of CO<sub>2</sub> in the single (aqueous or CO<sub>2</sub>-rich) fluid phase, and S<sub>C</sub> is the saturation of the CO<sub>2</sub>-rich phase. As had been discussed above, for conditions of interest to geologic sequestration of CO<sub>2</sub>, X is restricted to small values  $0 \leq X \leq X_{aq,C}$  (a few percent) for single-phase aqueous conditions, or to values near 1 ( $X_{C,eq} \leq X \leq 1$ , with  $X_{C,eq} > 0.99$  typically) when only a single CO<sub>2</sub>-rich phase is present (Fig. 6). (Here and in the remainder of Sec. 5.1, we denote the CO<sub>2</sub>-rich phase by “C,” which may be either liquid or gas. All equations given in this section are valid regardless of whether the CO<sub>2</sub>-rich phase happens to be liquid or gaseous.) Intermediate values  $X_{aq,C} < X < X_{C,eq}$  correspond to two-phase conditions, and thus should be initialized by specifying S<sub>C</sub>+10 as third primary variable. As a

convenience to users, ECO2N allows initial conditions to be specified in the full range  $0 \leq X \leq 1$ , and this capability is retained when initializing ECO2M with ECO2N-style variables. During the initialization phase of a simulation, a check is made whether  $X = X3$  is in fact within the range of mass fractions that correspond to single-phase (aqueous or CO<sub>2</sub>-rich phase) conditions. If this is found not to be the case, the conditions are recognized as being two-phase, and the corresponding phase saturations are calculated from the phase equilibrium constraint.

$$X(S_{\text{aq}}\rho_{\text{aq}} + S_{\text{C}}\rho_{\text{C}}) = S_{\text{aq}}\rho_{\text{aq}}X_{\text{aq,C}} + S_{\text{C}}\rho_{\text{C}}X_{\text{C,eq}} \quad (21)$$

Using  $S_{\text{aq}} = 1 - S_{\text{C}} - S_{\text{s}}$ , with  $S_{\text{s}}$  the "solid saturation" (fraction of pore space occupied by solid salt), we obtain

$$S_{\text{C}} = A \times (1 - S_{\text{s}}) \quad (22)$$

and the third primary variable is reset internally to  $X3 = S_{\text{C}} + 10$ , prior to eventually being converted to internal ECO2M usage. Here the parameter  $A$  is given by

$$A = \frac{(X - X_{\text{aq,C}})\rho_{\text{aq}}}{(X - X_{\text{aq,C}})\rho_{\text{aq}} + (X_{\text{C,eq}} - X)\rho_{\text{C}}} \quad (23)$$

Users may think of specifying single-phase aqueous conditions by setting  $X3 = 10$  (corresponding to  $S_{\text{C}} = 0$ ), and single-phase liquid CO<sub>2</sub> conditions by setting  $X3 = 11 - S_{\text{s}}$  (corresponding to  $S_{\text{aq}} = 0$ ). Strictly speaking this is not permissible, because ECO2N-style two-phase initialization requires that both  $S_{\text{C}} > 0$  and  $S_{\text{aq}} > 0$ . Single-phase states should instead be initialized by specifying primary variable  $X3$  as CO<sub>2</sub> mass fraction. However, as a convenience to users, when ECO2N-style primary variables are used, ECO2M accepts initialization of single-phase aqueous conditions by specifying  $X3 = 10$ . Such specification will be converted internally to two-phase in the initialization phase by adding a small number ( $10^{-11}$ ) to the third primary variable, changing conditions to two-phase with a small saturation  $S_{\text{C}} = 10^{-11}$  of the CO<sub>2</sub>-rich phase.



Salt concentration (or saturation of solid salt, if present) is characterized in ECO2M by means of the second primary variable  $X_{sm}$ . When no solid phase is present,  $X_{sm}$  denotes  $X_s$ , the mass fraction of NaCl referred to the two-component system water-NaCl. This is restricted to the range  $0 \leq X_{sm} \leq XEQ$ , where  $XEQ = XEQ(T)$  is the solubility of salt. For  $X_{sm} > 10$  this variable means  $S_s + 10$ , solid saturation plus 10. Users also have the option to specify salt concentration by means of molality  $m$  by assigning  $X_{sm} = -m$ . Such specification will in the initialization phase be internally converted to  $X_s$  by using Eq. (1). When salt concentration (as a fraction of total  $H_2O + NaCl$  mass) exceeds  $XEQ$ , this corresponds to conditions in which solid salt will be present in addition to dissolved salt in the aqueous phase. Such states should be initialized with a second primary variable  $X_{sm} = S_s + 10$ . However, ECO2M accepts initialization with  $X_{sm} > XEQ$ , recognizes this as corresponding to presence of solid salt, and converts the second primary variable internally to the appropriate solid saturation that will result in total salt mass fraction in the binary system water-salt being equal to  $X_{sm}$ . The conversion starts from the following equation.

$$X_{sm} = \frac{XEQ \times S_{aq} \rho_{aq} (1 - X) + S_s \rho_s}{S_{aq} \rho_{aq} (1 - X) + S_s \rho_s} \quad (24)$$

where  $X$  is dissolved  $CO_2$  mass fraction in the aqueous phase, and the numerator gives the total salt mass per unit volume, in aqueous and solid phases, while the denominator gives the total mass of salt plus water. Substituting  $S_{aq} = 1 - S_c - S_s$ , this can be solved for  $S_s$  to yield

$$S_s = \frac{B \times (1 - S_c)}{1 + B} \quad (25)$$

where the parameter  $B$  is given by

$$B = \frac{(X_{sm} - XEQ) \rho_{aq} (1 - X)}{\rho_s (1 - X_{sm})} \quad (26)$$

The most general conditions arise when both the second and third primary variables are initialized as mass fractions, nominally corresponding to single-phase fluid conditions with no solid phase present, but both mass fractions being in the range corresponding to two-phase fluid conditions with precipitated salt. Under these conditions, Eqs. (22) and (25) are solved simultaneously in ECO2M for  $S_s$  and  $S_c$ , yielding

$$S_c = \frac{A}{1 + B \times (1 - A)} \quad (27)$$

and

$$S_s = \frac{B \times (1 - A)}{1 + B \times (1 - A)} \quad (28)$$

Then both second and third primary variables are first converted to phase saturations,  $S_s + 10$  and  $S_c + 10$ , respectively, and subsequently the third primary variable is converted from ECO2N to ECO2M conventions. Examples of different initialization choices are given in sample problem 1, below.

## 5.2 Permeability Change from Precipitation and Dissolution of Salt

ECO2M offers several choices for the functional dependence of relative change in permeability,  $k/k_0$ , on relative change in active flow porosity.

$$\frac{k}{k_0} = f\left(\frac{\phi_f}{\phi_0}\right) \equiv f(1 - S_s) \quad (29)$$

The simplest model that can capture the converging-diverging nature of natural pore channels consists of alternating segments of capillary tubes with larger and smaller radii, respectively; see Fig. 8. While in straight capillary tube models permeability remains finite as long as porosity is non-zero, in models of tubes with different radii in series, permeability is reduced to zero at a finite porosity. From the tubes-in-series model shown in Fig. 8, the following relationship can be derived (Verma and Pruess, 1988)

$$\frac{k}{k_0} = \theta^2 \frac{1-\Gamma+\Gamma/\omega^2}{1-\Gamma+\Gamma[\theta/(\theta+\omega-1)]^2} \quad (30)$$

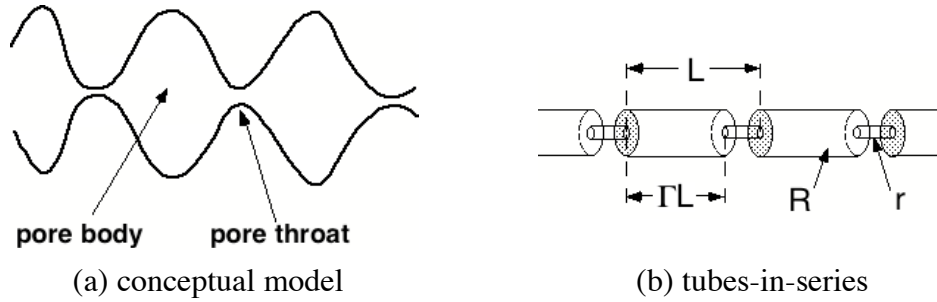


Figure 8. Model for converging-diverging pore channels.

Here

$$\theta = \frac{1-S_s - \phi_r}{1 - \phi_r} \quad (31)$$

depends on the fraction  $1-S_s$  of original pore space that remains available to fluids, and on a parameter  $\phi_r$ , which denotes the fraction of original porosity at which permeability is reduced to zero.  $\Gamma$  is the fractional length of the pore bodies, and the parameter  $\omega$  is given by

$$\omega = 1 + \frac{1/\Gamma}{1/\phi_r - 1} \quad (32)$$

Therefore, Eq. (30) has only two independent geometric parameters that need to be specified,  $\phi_r$  and  $\Gamma$ . As an example, Fig. 9 shows the permeability reduction factor from Eq. (30), plotted against  $\phi/\phi_0 \equiv (1-S_s)$ , for parameters of  $\phi_r = \Gamma = 0.8$ .

For parallel-plate fracture segments of different aperture in series, a relationship similar to Eq. (30) is obtained, the only difference being that the exponent 2 is replaced everywhere by 3

(Verma and Pruess, 1988). If only straight capillary tubes of uniform radius are considered, we have  $\phi_r = 0$ ,  $\Gamma = 0$ , and Eq. (30) simplifies to

$$k/k_0 = (1-S_s)^2 \quad (33)$$

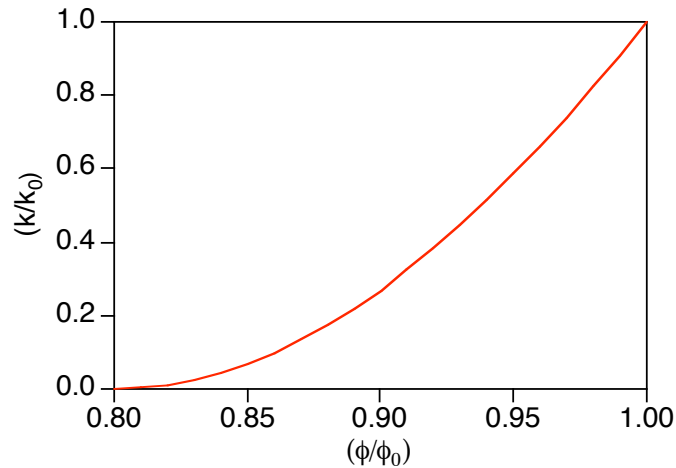


Figure 9. Porosity-permeability relationship for tubes-in-series model, after Verma and Pruess (1988).

### 5.3 Choice of Program Options

Various options for ECO2M can be selected through parameter specifications in data block SELEC. Default choices corresponding to various selection parameters set equal to zero provide the most comprehensive thermophysical property model. Certain functional dependencies can be turned off or replaced by simpler and less accurate models, see below. These options are offered to enable users to identify the role of different effects in a flow problem, and to facilitate comparison with other simulation programs that may not include full dependencies of thermophysical properties.

#### INDEX

A record with INDEX typed in columns 1-5 tells the code that ECO2M-style initial condition data are read in the input file. This affects

- (1) default initial conditions specified in data block PARAM;
- (2) domain-specific initial conditions specified in data block INDOM; and
- (3) element-specific initial conditions specified in data block INCON.

The assignment is hierarchical, with INDOM overriding defaults, and being itself overridden by INCON specifications.

Default initial conditions in data block PARAM.

In standard-TOUGH2, default initial conditions are entered in Record PARAM.4. When keyword INDEX is present, Record PARAM.4 will instead hold the phase index (a number between 1 and 7; see Table 2), and an additional Record PARAM.5 will be read for the four primary variables, whose significance depends on the phase conditions specified (see Table 2). The data formats are as follows.

Record PARAM.4 phase index (see Table 2)

Format(I5)  
INDEX

Record PARAM.5 primary variables (see Table 2)

Format(4E20.14)  
X1, X2, X3, X4

A set of four primary variables (Table 2), assigned as defaults to all grid blocks.

Domain-specific initial conditions in data block INDOM.

**INDOM** introduces domain-specific initial conditions.

Record INDOM.1

Format(A5, I5)  
MAT, INDEX

**MAT** name of a reservoir domain, as specified in data block ROCKS.

**INDEX** phase index (see Table 2).

Record INDOM.2

Format(4E20.14)  
X1, X2, X3, X4

A set of four primary variables (see Table 2), assigned to all grid blocks in the domain specified in INDOM.1.

Record INDOM.3

A blank record closes the INDOM data block.

**INCON** introduces element-specific initial conditions.

Record INCON.1

Format (A3, I2, 2I5, E15.9, I2)  
EL, NE, NSEQ, NADD, PORX, INDEX

EL, NE code name of element.

NSEQ number of additional elements with the same initial conditions.

NADD increment between the code numbers of two successive elements with identical initial conditions.

PORX porosity; if zero or blank, porosity will be taken as specified in block ROCKS if option START is used.

INDEX integer variable to assign phase compositions for specific grid blocks (see Table 2).

Record INCON.2 specifies primary variables.

Format (4E20.14)  
X1, X2, X3, X4

A set of four primary variables (see Table 2), assigned to all grid blocks in the domain specified in INCON.1.

Record INCON.3

A blank record closes the INCON data block. Alternatively, initial condition information may terminate on a record with '+++' typed in the first three columns, followed by time stepping information. This feature is used for a continuation run from a previous TOUGH2/ECO2M simulation.

**SELECTION** keyword to introduce a data block with parameters for ECO2M.

Record SELEC.1

Format(16I5)  
IE(I), I=1,16

- IE(1) set equal to 1, to read one additional data record (a larger value with more data records is acceptable, but only one additional record will be used by ECO2M).
- IE(7) allows choice of additional element-by-element printout.
- 0: print out only one basic set of parameters for elements.  
 >0: print out an additional set of parameters.
- IE(8) allows choice of the manner in which phase assignments are handled for supercritical temperatures. (Recall that for  $T > T_{crit}$ , points with  $P \geq P_{crit}$  are arbitrarily assigned as liquid, points with  $P < P_{crit}$  as gas.)
- 0: the a-l  $\rightleftharpoons$  a-g phase transition will always be made, based on comparing  $P$  with  $P_{crit}$ .
- >0: the a-l  $\rightleftharpoons$  a-g phase transitions for supercritical  $T$  will only be made for the first few Newtonian iterations (iteration counter  $ITER \leq IE(8)$ ).
- IE(9) allows choice of a finite window for certain phase transitions. A “hairtrigger” criterion (see Sec. 2.4) will be applied for  $ITER < IE(9)$ , while for  $ITER \geq IE(9)$ , phase transitions will only be made when pressure  $P$  or mass fraction  $X$  is outside a finite window.
- The l  $\rightleftharpoons$  l-g and a-l  $\rightleftharpoons$  a-l-g transition will only be made when  $P < (1 - FE(3)) * P_{s,CO_2}$ .
- The a-g  $\rightleftharpoons$  a-l-g transition will only be made when  $P > (1 + FE(3)) * P_{s,CO_2}$ .
- The l  $\rightleftharpoons$  a-l transition will only be made when  $X < X_{l,eq} * (1 - FE(3))$ .
- The a  $\rightleftharpoons$  a-l transition will only be made when  $X > X_{aq,l} * (1 + FE(4))$ .
- The a  $\rightleftharpoons$  a-g transition will only be made when  $X > X_{aq,g} * (1 + FE(4))$ .
- IE(11) selects dependence of permeability on the fraction  $\phi_f / \phi_0 = (1 - S_s)$  of original pore space that remains available to fluids.
- 0: permeability does not vary with  $\phi_f$ .
- 1:  $k/k_0 = (1 - S_s)^\gamma$ , with  $\gamma = FE(1)$  (record SELEC.2).
- 2: fractures in series, i.e., Eq. (30) with exponent 2 everywhere replaced by 3.
- 3: tubes-in-series, i.e., Eq. (30).

- IE(12) allows choice of model for water solubility in CO<sub>2</sub>.
- 0: after Spycher and Pruess (2005).  
 1: evaporation model; i.e., water density in the CO<sub>2</sub>-rich phase is calculated as density of saturated water vapor at prevailing temperature and salinity.
- IE(13) allows choice of dependence of brine density on dissolved CO<sub>2</sub>.
- 0: brine density varies with dissolved CO<sub>2</sub>-concentration, according to García's (2001) correlation (Eqs. 13-14) for temperature dependence of molar volume of dissolved CO<sub>2</sub>.  
 1: brine density is independent of CO<sub>2</sub> concentration.
- IE(14) allows choice of treatment of thermophysical properties as a function of salinity.
- 0: full dependence.  
 1: no salinity dependence of thermophysical properties (except for brine enthalpy; salt solubility constraints are maintained).
- IE(15) allows choice of correlation for brine enthalpy at saturated vapor pressure.
- 0: after Lorenz et al. (2000).  
 1: after Michaelides (1981).  
 2: after Miller (1978).
- Record SELEC.2 introduces parameters for functional dependence of permeability on solid saturation, and for finite phase change windows.
- Format(8E10.4)  
 FE(1), FE(2), FE(3), FE(4), FE(5)
- FE(1) parameter  $\gamma$  (for IE(11)=1); parameter  $\phi_r$  (for IE(11) = 2, 3)
- FE(2) parameter  $\Gamma$  (for IE(11) = 2, 3)
- FE(3) if set to a small non-zero number (e.g., 10<sup>-5</sup> to 10<sup>-3</sup>), will specify a finite window for some phase changes (see IE(9)).
- FE(4) if set to a small non-zero number (e.g., 10<sup>-5</sup> to 10<sup>-3</sup>), will specify a finite window for some phase changes (see IE(9)).
- FE(5) Parameter  $S_{aq,l} = FE(5)$  for handling potential disappearance of aqueous phase. If specified as a non-zero number, typically of order 0.2, will



proceed to reduce time step  $\Delta t$  if aqueous phase disappearance is diagnosed from conditions in which  $S_{aq} > S_{aq,l}$ . In some highly non-linear flow problems, aqueous phase disappearance may occur during the Newtonian iteration from initially large aqueous phase saturation. Such transitions rarely lead to a converged time step. Setting FE(5) to something like 0.2 will allow the Newtonian iteration to continue following an aqueous phase disappearance only when initial aqueous phase saturation in the grid block in question was reasonably small,  $S_{aq} \leq S_{aq,l}$ . This avoids numerical work and diagnostic printouts associated with excessively large saturation changes.

The ECO2M module includes a customized version of a subroutine FG TAB that supersedes the default version provided as part of the main TOUGH2 module t2f.f. FG TAB can write data files FOFT, COFT, and GOFT with time series of conditions at user-selected grid blocks and connections for plotting. The parameters written out in comma-delimited format at each time step are as follows.

FOFT: (1) fluid pressure (first primary variable), (2) temperature, (3) liquid saturation, (4) gas saturation, (5) dissolved CO<sub>2</sub> mass fraction in aqueous phase;

COFT: flow rates of (1) aqueous phase, (2) liquid phase, (3) gas phase, and (4) total CO<sub>2</sub> (as free phase(s) and dissolved in aqueous phase);

GOFT: (1) well mass flow rate, (2) flowing enthalpy, (3) flowing CO<sub>2</sub> mass fraction, (4) fractional flow in CO<sub>2</sub>-rich phases (liquid plus gaseous), (5) flowing wellbore pressure (production wells only).

## 6. Sample Problems

This section presents a number of sample problems for TOUGH2/ECO2M. The problems were chosen to demonstrate the preparation of input data, to illustrate code capabilities, and to provide benchmarks for proper code installation. These problems include a basic injection problem (Section 6.2), and a basic fault leakage problem (Section 6.3). The injection problem was taken from a code intercomparison study, in which ten groups from six countries had exercised different simulation codes to generate results for a suite of test problems (Pruess et al., 2002, 2004). In order to provide some context and perspective the current TOUGH2/ECO2M results are compared with results previously obtained with TOUGH2/ECO2N.

### 6.1 Problem No. 1 (\*rtab\*) - Demonstration of Initialization Options

The input file as given in Fig. 10 demonstrates initialization of a TOUGH2/ECO2M run with ECO2N-type primary variables. This type of initialization is enabled by omitting the single-line data block INDEX that is required when initializing with the primary variables internally used in ECO2M (Table 2). The input file is completely identical to the corresponding input file for ECO2N, except for one single change in the third parameter in data block MULTI. This parameter specifies the number of phases treated by the fluid property module, and is NPH=3 for ECO2N, while it is NPH=4 in ECO2M. These NPH specifications are necessary, regardless of how many phases are actually present in a flow problem. The input file performs just a single infinitesimal time step ( $\Delta t = 10^{-9}$  s) and includes neither flow connections between grid blocks nor sinks or sources. Therefore, there is no flow and no changes in the initially specified thermodynamic conditions. The purpose of this problem is simply to demonstrate different options for initializing thermodynamic conditions.

```

*rtab* ... initialization test for ECO2M
ROCKS-----1-----2-----3-----4-----5-----6-----7-----8
SANDS  2 2600.e00      .35 100.e-15 100.e-15 100.e-15      2.51      920.
4.5e-10
  7      .457      .30      1.      .05
  7      .457      .00      5.1e-5      1.e7      .999

MULTI-----1-----2-----3-----4-----5-----6-----7-----8
  3  4  4  6
START-----1-----2-----3-----4-----5-----6-----7-----8
-----*-----1 MOP: 123456789*123456789*1234 -----*-----5-----*-----6-----*-----7-----*-----8
PARAM-----1-----2-----3-----4-----5-----6-----7-----8
  1  1      110 0900000000 4  3
      -1.
      1.e-9
      1.E-5      1.E00
      60.e5
SELEC...2...3...4...5...6...7...8...9...10...11...12...13...14...15...16
  1
      .8      .8
ELEME-----1-----2-----3-----4-----5-----6-----7-----8
a  1  10  1SANDS      1.
A  14  7  1SANDS      1.

CONNE-----1-----2-----3-----4-----5-----6-----7-----8

INCON-----1-----2-----3-----4-----5-----6-----7-----8
a  1
a  2      40.0e5      0.0      3.9e-2      30.
a  3      40.0e5      0.0      3.9e-1      30.
a  4      340.0e5      0.0      6.6e-2      30.
a  5      340.0e5      0.3      6.6e-1      30.
a  6      140.0e5      0.10466      3.6e-2      30.
a  7      140.0e5      0.10466      3.6e-1      30.
a  8      140.0e5      0.50      3.6e-2      30.
a  9      140.0e5      0.50      3.6e-1      30.
a  10     140.0e5      10.50      0.99      30.
a  11     140.0e5      10.50      0.999      30.
a  12     140.0e5      0.50      0.99      30.
A  14     216.18e5      0.05      10.50      45.0
A  15     216.18e5      10.05      10.50      45.0
A  16     216.18e5      0.50000      10.50      45.0
A  17     216.18e5      0.50000      0.50      45.0
A  18     216.18e5      10.2      0.50      45.0
A  19     216.18e5      10.2      10.50      45.0
A  20     216.18e5      -2.0      10.50      45.0
A  21     216.18e5      -6.0      10.50      45.0

GENER-----1-----2-----3-----4-----5-----6-----7-----8
ENDCY-----1-----2-----3-----4-----5-----6-----7-----8

```

Figure 10. TOUGH2/ECO2M input file for sample problem 1.

Initialization with standard ECO2N-style primary variables (Table 6) is made for a number of grid blocks in single-phase aqueous conditions (\*a 1\*, \*a 3\*, \*a 5\*), a single CO<sub>2</sub>-rich phase (\*a 10\*), and two-phase fluid (\*A 14\*, \*A 15\*, \*A 19\*). Several grid blocks are initialized with single-phase type primary variables, but with a CO<sub>2</sub> mass fraction (primary variable #3) that is larger than can be dissolved in the aqueous phase, and smaller than required for single-phase gas conditions (\*a 2\*, \*a 6\*, \*a 9\*, \*A 18\*). The CO<sub>2</sub> mass fractions for these blocks correspond to two-phase (aqueous-liquid or aqueous-gas) fluid conditions (see Fig. 6 and Section 5.1), and are internally converted to the appropriate phase saturations during initialization. Grid block \*A 16\* is initialized with primary variable #3 corresponding to internal ECO2N usage, but primary variable #2 is larger than saturated salt mass fraction in the binary system water-salt. This specification corresponds to presence of solid salt, and is internally converted to  $S_s + 10$ . In some grid blocks both primary variables #2 and #3 are specified with conventions applicable for single-phase liquid conditions, but with salt mass fraction exceeding the solubility limit, and CO<sub>2</sub> mass fraction being in the intermediate range between the liquid and gas phase limits (\*a 4\*, \*a 7\*, \*a 8\*, \*a 11\*, \*A 17\*). Salt as well as CO<sub>2</sub> mass fractions for these blocks are converted to the appropriate internally used saturation variables. Finally, there are grid blocks (\*A 20\*, \*A 21\*) in which primary variable #2 is specified as salt molality (counted by convention as undissociated) in the binary water-salt system, which is internally converted to salt mass fraction. The internally used ECO2M-style primary variables generated from the ECO2N-style INCON data given in Fig. 10 are shown in Fig. 11, where phase indices are printed following the pound sign (#). Fig. 12 shows part of the printed output for this problem, with phase indices appearing in the column following the element index (header I). Results agree closely with ECO2N (Pruess, 2005).

We emphasize that the preferred and recommended option is to initialize flow problems by means of the internally used primary variables (Table 2). The options of using ECO2N-style initialization and allowing salt and CO<sub>2</sub> mass fractions to go out of range are provided as a convenience to users.

PRIMARY VARIABLES

AT ELEMENT	*a	1*	---	#1	.400000E+07	.000000E+00	.390000E-01	.300000E+02
AT ELEMENT	*a	2*	---	#5	.400000E+07	.000000E+00	.134589E+00	.300000E+02
AT ELEMENT	*a	3*	---	#1	.340000E+08	.000000E+00	.660000E-01	.300000E+02
AT ELEMENT	*a	4*	---	#4	.340000E+08	.100080E+02	.293994E+00	.300000E+02
AT ELEMENT	*a	5*	---	#1	.140000E+08	.104660E+00	.360000E-01	.300000E+02
AT ELEMENT	*a	6*	---	#4	.140000E+08	.104660E+00	.605318E+00	.300000E+02
AT ELEMENT	*a	7*	---	#4	.140000E+08	.101996E+02	.776503E+00	.300000E+02
AT ELEMENT	*a	8*	---	#4	.140000E+08	.101265E+02	.492210E+00	.300000E+02
AT ELEMENT	*a	9*	---	#4	.140000E+08	.105000E+02	.306639E-02	.300000E+02
AT ELEMENT	*a	10*	---	#2	.140000E+08	.105000E+02	.999000E+00	.300000E+02
AT ELEMENT	*a	11*	---	#4	.140000E+08	.100016E+02	.612312E-02	.300000E+02
AT ELEMENT	*A	14*	---	#4	.216180E+08	.500000E-01	.500000E+00	.450000E+02
AT ELEMENT	*A	15*	---	#4	.216180E+08	.100500E+02	.450000E+00	.450000E+02
AT ELEMENT	*A	16*	---	#4	.216180E+08	.101016E+02	.398434E+00	.450000E+02
AT ELEMENT	*A	17*	---	#4	.216180E+08	.100957E+02	.375591E+00	.450000E+02
AT ELEMENT	*A	18*	---	#4	.216180E+08	.102000E+02	.332287E+00	.450000E+02
AT ELEMENT	*A	19*	---	#4	.216180E+08	.102000E+02	.300000E+00	.450000E+02
AT ELEMENT	*A	20*	---	#4	.216180E+08	.104661E+00	.500000E+00	.450000E+02
AT ELEMENT	*A	21*	---	#4	.216180E+08	.259637E+00	.500000E+00	.450000E+02

Figure 11. Primary variables internally used in ECO2M for the INCON data given in Fig. 10. Phase indices are shown as #1 etc.

OUTPUT DATA AFTER ( 1, 1)-2-TIME STEPS THE TIME IS .115741E-13 DAYS

\*\*\*\*\*

TOTAL TIME	KCYC	ITER	ITERC	KON	DX1M	DX2M	DX3M	MAX. RES.	NER	KER	DELTEX
.100000E-08	1	1	1	2	.00000E+00	.00000E+00	.00000E+00	.00000E+00	0	0	.10000E-08

\*\*\*\*\*

ELEM	INDEX	I	P	T	SAQ	SLIQ	SGAS	XCO2AQ	DLIQ	VISLIQ	DGAS	VISGAS
			(PA)	(DEG.C)					(KG/M3)	(PA-S)	(KG/M3)	(PA-S)
a	1	1	.400000E+07	30.0000	.100000E+01	.000000E+00	.000000E+00	.390000E-01	.00	.100000E+01	.00	.100000E+01
a	2	2	.400000E+07	30.0000	.134589E+00	.000000E+00	.865411E+00	.396862E-01	.00	.100000E+01	89.85	.164334E-04
a	3	3	.340000E+08	30.0000	.100000E+01	.000000E+00	.000000E+00	.660000E-01	.00	.100000E+01	.00	.100000E+01
a	4	4	.340000E+08	30.0000	.293994E+00	.697993E+00	.000000E+00	.181907E-01	966.06	.110621E-03	.00	.100000E+01
a	5	5	.140000E+08	30.0000	.100000E+01	.000000E+00	.000000E+00	.360000E-01	.00	.100000E+01	.00	.100000E+01
a	6	6	.140000E+08	30.0000	.605318E+00	.394682E+00	.000000E+00	.369151E-01	836.43	.787401E-04	.00	.100000E+01
a	7	7	.140000E+08	30.0000	.776503E+00	.238643E-01	.000000E+00	.153895E-01	836.43	.787401E-04	.00	.100000E+01
a	8	8	.140000E+08	30.0000	.492210E+00	.381246E+00	.000000E+00	.153895E-01	836.43	.787401E-04	.00	.100000E+01
a	9	9	.140000E+08	30.0000	.306639E-02	.496934E+00	.000000E+00	.153895E-01	836.43	.787401E-04	.00	.100000E+01
a	10	10	.140000E+08	30.0000	.000000E+00	.500000E+00	.000000E+00	.153895E-01	836.43	.787401E-04	.00	.100000E+01
a	11	11	.140000E+08	30.0000	.612312E-02	.992303E+00	.000000E+00	.153895E-01	836.43	.787401E-04	.00	.100000E+01
A	14	12	.216180E+08	45.0000	.500000E+00	.500000E+00	.000000E+00	.464753E-01	829.66	.775389E-04	.00	.100000E+01
A	15	13	.216180E+08	45.0000	.450000E+00	.500000E+00	.000000E+00	.158536E-01	829.66	.775389E-04	.00	.100000E+01
A	16	14	.216180E+08	45.0000	.398434E+00	.500000E+00	.000000E+00	.158536E-01	829.66	.775389E-04	.00	.100000E+01
A	17	15	.216180E+08	45.0000	.375591E+00	.528666E+00	.000000E+00	.158536E-01	829.66	.775389E-04	.00	.100000E+01
A	18	16	.216180E+08	45.0000	.332287E+00	.467713E+00	.000000E+00	.158536E-01	829.66	.775389E-04	.00	.100000E+01
A	19	17	.216180E+08	45.0000	.300000E+00	.500000E+00	.000000E+00	.158536E-01	829.66	.775389E-04	.00	.100000E+01
A	20	18	.216180E+08	45.0000	.500000E+00	.500000E+00	.000000E+00	.358200E-01	829.66	.775389E-04	.00	.100000E+01
A	21	19	.216180E+08	45.0000	.500000E+00	.500000E+00	.000000E+00	.164893E-01	829.66	.775389E-04	.00	.100000E+01

\*\*\*\*\*

Figure 12. Output data for sample problem 1.

## 6.2 Problem No. 2 (\*rcc3\*) - Radial Flow from a CO<sub>2</sub> Injection Well

This is a basic problem of CO<sub>2</sub> injection into a saline aquifer, examining two-phase flow with CO<sub>2</sub> displacing (saline) water under conditions that may be encountered in brine aquifers at a depth of the order of 1.2 km. A CO<sub>2</sub> injection well fully penetrates a homogeneous, isotropic, infinite-acting aquifer of 100 m thickness (Fig. 13), at conditions of 120 bar pressure, 45 °C temperature, and a salinity of 15 % by weight. CO<sub>2</sub> is injected uniformly at a constant rate of 100 kg/s. This problem had been included as test problem #3 in a code intercomparison study (Pruess et al., 2002, 2004).

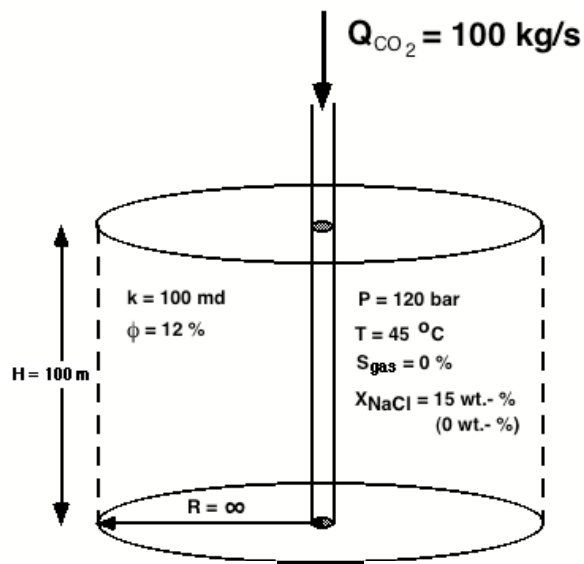


Figure 13. Schematic of sample problem 2.

The TOUGH2 input file used for grid generation is shown in Fig. 14. The well is modeled as a circular grid element of  $R = 0.3 \text{ m}$  ( $\approx 12''$ ). The numerical grid is extended to a large distance of 100 km, so that the system would be infinite-acting for the time period simulated (10,000 days, 27.38 years). Prior to the flow simulation, a minor amount of editing is performed on the MESH file. The well block is assigned to a domain #2, with a view on facilitating running of a non-isothermal variation of the problem. Further, the nodal distance corresponding to the well block was changed to an infinitesimal value. A fragment of the modified MESH file is shown in Fig. 15, and the TOUGH2/ECO2M input file used for the simulation is shown in Fig. 16. The input file is identical to the one for TOUGH2/ECO2N,

```

*rccc3* ... Code Intercomparison problem3: Radial flow from a CO2 Injection Well
MESHMAKER1-----2-----3-----4-----5-----6-----7-----8
RZ2D
RADII
  1
    0.
EQUID
  1      .3
LOGAR
  200    1.E3
LOGAR
  100    3.E3
LOGAR
  100    1.E4
LOGAR
  34     1.E5
LAYER-----1-----2-----3-----4-----5-----6-----7-----8
  1
    100.
ENDFI-----1-----2-----3-----4-----5-----6-----7-----8

```

Figure 14. TOUGH2 input file for grid generation for radial injection problem.

```

ELEME --- 435    1    1 434    .00000100000.000
A1  1      2 .2827E+02 .5655E+00      .3000E+00      -.5000E+02
A1  2      1 .8728E+02 .1746E+01      .4532E+00      -.5000E+02
A1  3      1 .1501E+03 .3002E+01      .7630E+00      -.5000E+02
A1  4      1 .2169E+03 .4339E+01      .1079E+01      -.5000E+02
...
...
CONNE
A1  1A1  2      1 .1500E-05 .1532E+00 .1885E+03
A1  2A1  3      1 .1532E+00 .1565E+00 .3811E+03
A1  3A1  4      1 .1565E+00 .1599E+00 .5778E+03
...

```

Figure 15. Modified MESH file for radial injection problem.

except that in data block MULTI the number of possible active phases is specified as NPH=4, as compared to NPH=3 for ECO2N. The simulation is performed in isothermal mode (NEQ = 3 in data block MULTI). A separate ROCKS domain 'well ' with "infinite" rock grain density was included in the input file to enable running of a non-isothermal variation simply by setting NEQ = 4; the well block "A1 1" is assigned to domain 'well ' with "infinite" rock grain density, so that CO<sub>2</sub> injection would effectively occur at initial temperature of 45 °C, obviating the need for specifying an injection enthalpy. Part of the output generated from this problem is shown in Fig. 17. As can be seen salt is precipitating around the injection well (solid saturation is  $S_s = 1 - SAQ - SLIQ - SGAS > 0$ ), but associated permeability reduction is turned off (IE(11) = 0). Simulation results agree closely with those previously obtained with ECO2N (Pruess, 2005). We also

present results for a run that includes permeability reduction due to solids precipitation. This requires just a single change in the input file of Fig. 16, namely, we set IE(11)=3 to select the “tubes in series” model for relating porosity reduction from precipitation to permeability change (see Figs. 8, 9). In addition we also set parameter IE(7)=1, to obtain printout of additional parameters at elements (grid blocks), including solid saturations and permeability reduction factors “k-red.” Fig. 18 provides some printed output after 1,000 days of simulation time. Precipitation is observed to start in time step 42; results through time step 41 ( $t = 4.055 \times 10^3$  s)

```

*rccc3* ... Code Intercomparison problem3: Radial flow from a CO2 Injection Well
ROCKS-----1-----*-----2-----*-----3-----*-----4-----*-----5-----*-----6-----*-----7-----*-----8
SAND      2      2600.e00          .12  100.e-15  100.e-15  100.e-15          2.51      920.
          4.5e-10
          7          .457          .30          1.          .05
          7          .457          .00          5.1e-5          1.e7          .999
well      2      2600.e40          .12  100.e-15  100.e-15  100.e-15          2.51      920.
          4.5e-10
          7          .457          .30          1.          .05
          7          .457          .00          5.1e-5          1.e7          .999

MULTI-----1-----*-----2-----*-----3-----*-----4-----*-----5-----*-----6-----*-----7-----*-----8
          3      3      4      6
SELEC.....2.....3.....4.....5.....6.....7.....8.....9...10...11...12...13...14...15...16
          1
          .8          .8
SOLVR-----1-----*-----2-----*-----3-----*-----4-----*-----5-----*-----6-----*-----7-----*-----8
5 Z1 O0      8.0e-1      1.0e-7
START-----1-----*-----2-----*-----3-----*-----4-----*-----5-----*-----6-----*-----7-----*-----8
-----*-----1 MOP: 123456789*123456789*1234 -----*-----5-----*-----6-----*-----7-----*-----8
PARAM-----1-----*-----2-----*-----3-----*-----4-----*-----5-----*-----6-----*-----7-----*-----8
          1 999          9991000300000000 4      3
          8.64e8          -1.
          1.
          1.E-5          1.E00
          120.e5          .15          0.0          45.
FOFT -----1-----*-----2-----*-----3-----*-----4-----*-----5-----*-----6-----*-----7-----*-----8
A1 49          1 .1745E+04 .2685E+03          .2570E+02          -.6500E+01
A12 2          1 .3080E+08 .4738E+07          .1080E+04          -.6500E+01

GENER-----1-----*-----2-----*-----3-----*-----4-----*-----5-----*-----6-----*-----7-----*-----8
A1 linj 1          COM3          100.

INCON-----1-----*-----2-----*-----3-----*-----4-----*-----5-----*-----6-----*-----7-----*-----8

TIMES-----1-----*-----2-----*-----3-----*-----4-----*-----5-----*-----6-----*-----7-----*-----8
          4
          2.592E+06  8.64E+06  8.64E+07  8.64E+08
ENDCY-----1-----*-----2-----*-----3-----*-----4-----*-----5-----*-----6-----*-----7-----*-----8

```

Figure 16. TOUGH2/ECO2M input file for radial injection problem.



are completely identical to those without allowing for permeability reduction, as they should. Fluid pressures exceed those of Fig. 17 by only a few bars. This modest effect is due to the relatively small solid saturations of around  $S_s = 1 - SLIQ \approx 4\%$  near the injection well.

```

...ITERATING... AT [ 1, 1] --- DELTEX = .100000E+01 MAX. RES. = .353732E+01 AT ELEMENT A1 1 EQUATION 3
$$$ 1 ---> 4 $$$ LIQ. EVOLVES AT *A1 1* XCO2AQ = .267978E-01 TX = .450000E+02 PX = .136627E+08 Ps,CO2 =
...ITERATING... AT [ 1, 2] --- DELTEX = .100000E+01 MAX. RES. = .246617E-01 AT ELEMENT A1 2 EQUATION 3
$$$ 4 ---> 1 $$$ LIQ. DISAPP. AT ELEMENT *A1 1* $$$$$$ SAQ = .100009E+01
...ITERATING... AT [ 1, 3] --- DELTEX = .100000E+01 MAX. RES. = .614306E-02 AT ELEMENT A1 2 EQUATION 3
...ITERATING... AT [ 1, 4] --- DELTEX = .100000E+01 MAX. RES. = .783833E-04 AT ELEMENT A1 1 EQUATION 3
Al 2( 1, 5) ST = .100000E+01 DT = .100000E+01 DX1= .115906E+07 DX2= .226407E-15 T = 45.000 P = 13159061. S = .100000E+01
...ITERATING... AT [ 2, 1] --- DELTEX = .100000E+01 MAX. RES. = .100000E+01 AT ELEMENT A1 1 EQUATION 3
$$$ 1 ---> 4 $$$ LIQ. EVOLVES AT *A1 1* XCO2AQ = .515157E-01 TX = .450000E+02 PX = .141315E+08 Ps,CO2 =
...ITERATING... AT [ 2, 2] --- DELTEX = .100000E+01 MAX. RES. = .986667E+00 AT ELEMENT A1 1 EQUATION 3
...ITERATING... AT [ 2, 3] --- DELTEX = .100000E+01 MAX. RES. = .910155E+00 AT ELEMENT A1 2 EQUATION 3
...ITERATING... AT [ 2, 4] --- DELTEX = .100000E+01 MAX. RES. = .172937E+00 AT ELEMENT A1 2 EQUATION 3
...ITERATING... AT [ 2, 5] --- DELTEX = .100000E+01 MAX. RES. = .112589E-01 AT ELEMENT A1 2 EQUATION 3
...ITERATING... AT [ 2, 6] --- DELTEX = .100000E+01 MAX. RES. = .116588E-03 AT ELEMENT A1 2 EQUATION 3
Al 2( 2, 7) ST = .200000E+01 DT = .100000E+01 DX1= .111159E+07 DX2= .974700E-07 T = 45.000 P = 14270651. S = .100000E+01
...ITERATING... AT [ 3, 1] --- DELTEX = .100000E+01 MAX. RES. = .496177E+00 AT ELEMENT A1 1 EQUATION 3
...ITERATING... AT [ 3, 2] --- DELTEX = .100000E+01 MAX. RES. = .124120E-01 AT ELEMENT A1 1 EQUATION 3
...ITERATING... AT [ 3, 3] --- DELTEX = .100000E+01 MAX. RES. = .252253E-04 AT ELEMENT A1 2 EQUATION 3
Al 1( 3, 4) ST = .300000E+01 DT = .100000E+01 DX1= .158370E+07 DX2= .972615E-05 T = 45.000 P = 17948923. S = .927782E+00
...ITERATING... AT [ 4, 1] --- DELTEX = .200000E+01 MAX. RES. = .661797E+00 AT ELEMENT A1 1 EQUATION 3
...ITERATING... AT [ 4, 2] --- DELTEX = .200000E+01 MAX. RES. = .745778E+00 AT ELEMENT A1 2 EQUATION 3
...ITERATING... AT [ 4, 3] --- DELTEX = .200000E+01 MAX. RES. = .679967E-01 AT ELEMENT A1 2 EQUATION 3
...ITERATING... AT [ 4, 4] --- DELTEX = .200000E+01 MAX. RES. = .594899E-03 AT ELEMENT A1 2 EQUATION 3
Al 2( 4, 5) ST = .500000E+01 DT = .200000E+01 DX1= .259505E+06 DX2= -.563856E-06 T = 45.000 P = 14951272. S = .100000E+01
...
...
OUTPUT DATA AFTER ( 362, 4)-2-TIME STEPS THE TIME IS .100000E+04 DAYS
#####
TOTAL TIME KCYC ITER ITERC KON DX1M DX2M DX3M MAX. RES. NER KER DELTEX
.864000E+08 362 4 2489 2 .12193E+06 .60601E-01 .91557E-01 .26750E-07 1 3 .12097E+07
#####

ELEM INDEX I P T SAQ SLIQ SGAS XCO2AQ DLIQ VISLIQ DGAS VISGAS
(PA) (DEG.C) (KG/M3) (PA-S) (KG/M3) (PA-S)
A1 1 1 2 .223198E+08 45.0000 .000000E+00 .932082E+00 .000000E+00 .159723E-01 836.06 .787746E-04 .00 .100000E+01
A1 2 2 2 .222432E+08 45.0000 .000000E+00 .956191E+00 .000000E+00 .159593E-01 835.37 .786410E-04 .00 .100000E+01
A1 3 3 2 .221667E+08 45.0000 .000000E+00 .958953E+00 .000000E+00 .159465E-01 834.68 .785076E-04 .00 .100000E+01
A1 4 4 2 .221152E+08 45.0000 .000000E+00 .959150E+00 .000000E+00 .159378E-01 834.22 .784177E-04 .00 .100000E+01
A1 5 5 2 .220761E+08 45.0000 .000000E+00 .960482E+00 .000000E+00 .159313E-01 833.87 .783497E-04 .00 .100000E+01
A1 6 6 2 .220446E+08 45.0000 .000000E+00 .961052E+00 .000000E+00 .159261E-01 833.59 .782947E-04 .00 .100000E+01
A1 7 7 2 .220181E+08 45.0000 .000000E+00 .962298E+00 .000000E+00 .159217E-01 833.35 .782484E-04 .00 .100000E+01
A1 8 8 2 .219951E+08 45.0000 .000000E+00 .961570E+00 .000000E+00 .159179E-01 833.14 .782081E-04 .00 .100000E+01
A1 9 9 2 .219748E+08 45.0000 .000000E+00 .962568E+00 .000000E+00 .159143E-01 832.95 .781721E-04 .00 .100000E+01
A1 10 10 2 .219565E+08 45.0000 .000000E+00 .962082E+00 .000000E+00 .159112E-01 832.79 .781397E-04 .00 .100000E+01
A1 11 11 2 .219399E+08 45.0000 .000000E+00 .962001E+00 .000000E+00 .159083E-01 832.63 .781102E-04 .00 .100000E+01
A1 12 12 2 .219247E+08 45.0000 .000000E+00 .960881E+00 .000000E+00 .159057E-01 832.49 .780832E-04 .00 .100000E+01
A1 13 13 2 .219106E+08 45.0000 .000000E+00 .963763E+00 .000000E+00 .159033E-01 832.36 .780582E-04 .00 .100000E+01
A1 14 14 2 .218974E+08 45.0000 .000000E+00 .963087E+00 .000000E+00 .159010E-01 832.24 .780348E-04 .00 .100000E+01
A1 15 15 2 .218851E+08 45.0000 .000000E+00 .960868E+00 .000000E+00 .158989E-01 832.13 .780130E-04 .00 .100000E+01

```

Figure 17. Part of printed output for radial flow problem.



### 6.3 Problem No. 3 (\*r1d\*) - Upflow of CO<sub>2</sub> along a Deep Fault Zone

We consider leakage of CO<sub>2</sub> from a deep storage reservoir along a vertical fault zone of 5 m thickness. The fault is assumed to intersect the CO<sub>2</sub> reservoir at a depth of  $Z = -1500$  m. Fault zone permeability is assumed as  $k = 100 \times 10^{-15} \text{ m}^2$ , porosity  $\phi = 15 \%$ , with wall rocks assumed completely impermeable. Initial conditions in the fault correspond to hydrostatic equilibrium in a typical geothermal gradient, as shown in Fig. 19.

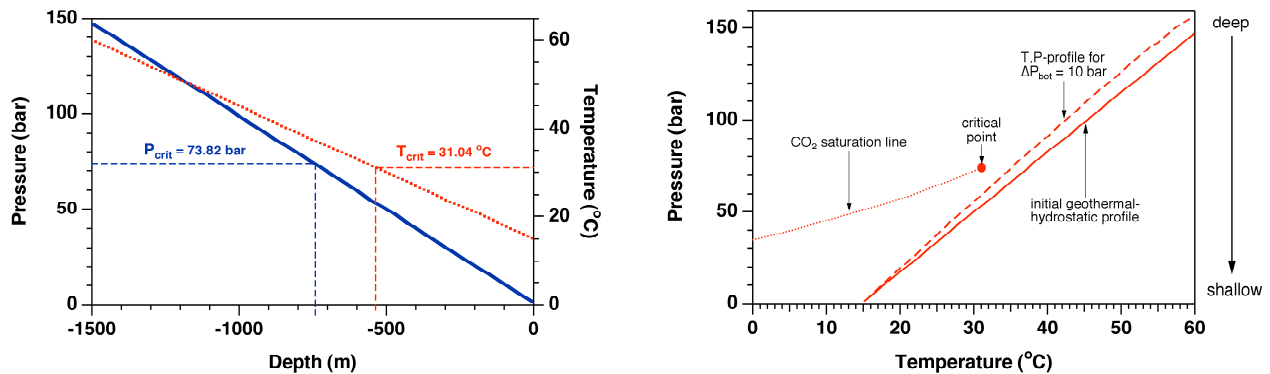


Figure 19. T,P-diagram of a typical geothermal-hydrostatic profile, as used in the present problem. The CO<sub>2</sub> saturation line is also shown, as is a profile that corresponds to a pressure increase of  $\Delta P = 10$  bar at 1500 m depth.

Setup and solution of the problem involves several steps, (1) MESH generation followed by some hand-editing, (2) generation of a geothermal-hydrostatic profile as initial conditions for the CO<sub>2</sub> leakage scenario, and (3) upflow of CO<sub>2</sub> along the fault zone. We will now give a detailed description of these steps.

#### 6.3.1 MESH Generation

The scenario considered here does not model the CO<sub>2</sub> storage reservoir as such; instead, we assume that a CO<sub>2</sub> plume from a nearby storage reservoir reaches the bottom of a fault zone at some pressure in excess of hydrostatic. We model a 1 m long section of the fault as a 1-D vertical flow system. The TOUGH2 input file shown in Fig. 20 specifies generation of a 1-D grid in Y-direction; the X-increment of 1 m represents the section of fault length that is modeled, while the Z-increment of 5 m represents the fault thickness. We also specify that the Y-axis will be rotated by 90 degrees, to make the 1-D grid vertical. The reason for generating a grid in Y-

direction and rotating it, rather than making a grid in Z-direction, is that the grid generation process automatically places interface areas for conductive heat exchange with impermeable half spaces in the XY-planes at the topmost and bottommost grid blocks. With a Y-direction grid, these interface areas are generated in such a way that after rotation by 90 degrees they represent the (vertical) wall rocks of the fault zone, which is what we desire in this problem. In addition to 150 Y-increments of 10 m each, the input data also specify very small grid blocks with  $\Delta Y = 10^{-3}$  m at the beginning and end, which will be used to impose top and bottom boundary conditions; see below.

```
*r1d* - 1-D vertical flow channel, for ECO2M
MESHMAKER1-----*-----2-----*-----3-----*-----4-----*-----5-----*-----6-----*-----7-----*-----8
XYZ
          90.
NX         1         1.
NY         1         1.e-3
NY        150         10.
NY         1         1.e-3
NZ         1         5.

ENDFI-----1-----*-----2-----*-----3-----*-----4-----*-----5-----*-----6-----*-----7-----*-----8
```

Figure 20. TOUGH2 input file for generating a 1-D vertical grid for a fault zone.

Prior to the flow simulation, some hand-editing is performed on the MESH file, see Fig. 21. The topmost grid block [A11 1], which we intend to use for maintaining atmospheric boundary conditions at the top of the fault, is assigned to a domain ‘atmos’ and is made inactive by moving it to the end of the ELEME-block and preceding it with a “dummy” grid block [ina ] with zero volume. The bottommost grid block [E1C 1] is assigned to a domain ‘botom’, that will be used for imposing bottom boundary conditions, but is kept in an active position.

### 6.3.2 Obtaining Initial Conditions

The first task of flow simulation is to obtain a static geothermal-hydrostatic profile, as shown in Fig. 19, above. This simulation uses the modified MESH file as shown in Fig. 21, and the TOUGH2/ECO2M input file shown in Fig. 22. The input file does not include a data block ‘INDEX’ and accordingly uses ECO2N-style initialization. The ‘atmos’ domain is initialized as single-phase water ( $X3=0$ ) without salinity ( $X2=0$ ) at a pressure of  $1.013 \times 10^5$  Pa and a

```

ELEME
A12 1          1 .5000E+02 .2000E+02          .5000E+00 .5001E+01-.2500E+01
A13 1          1 .5000E+02 .2000E+02          .5000E+00 .1500E+02-.2500E+01
A14 1          1 .5000E+02 .2000E+02          .5000E+00 .2500E+02-.2500E+01
A15 1          1 .5000E+02 .2000E+02          .5000E+00 .3500E+02-.2500E+01
...
E19 1          1 .5000E+02 .2000E+02          .5000E+00 .1475E+04-.2500E+01
E1A 1          1 .5000E+02 .2000E+02          .5000E+00 .1485E+04-.2500E+01
E1B 1          1 .5000E+02 .2000E+02          .5000E+00 .1495E+04-.2500E+01
E1C 1          botom .5000E-02 .2000E-02          .5000E+00 .1500E+04-.2500E+01
ina
A11 1          atmos .5000E-02 .2000E-02          .5000E+00 .5000E-03-.2500E+01

CONNE
A11 1A12 1          2 .5000E-03 .5000E+01 .5000E+01 .1000E+01
A12 1A13 1          2 .5000E+01 .5000E+01 .5000E+01 .1000E+01
A13 1A14 1          2 .5000E+01 .5000E+01 .5000E+01 .1000E+01
...

```

Figure 21. Modified MESH file for 1-D vertical fault leakage problem.

temperature of 15 °C. The domain ‘botom’ for the bottommost grid block of the MESH is initialized with a pressure of  $150 \times 10^5$  Pa and a temperature of 60 °C. Note that in the ‘botom’ domain we have increased rock grain density by 40 orders of magnitude relative to its “physical” value of  $2600 \text{ kg/m}^3$ . This was done to create an overwhelmingly large heat capacity in that domain, so that the initial temperature of 60 °C would remain unchanged during the flow simulation. The fluid in the fault is initialized with default initial conditions of single-phase pure water at a pressure of  $100 \times 10^5$  Pa and a temperature of 40 °C. In response to the sharp contrast in initial conditions at the top and bottom of the domain, we expect changes to be rapid initially and to slow down over time. Accordingly, we specify a sequence of strongly increasing time steps.

The CO<sub>2</sub> migration simulation to be conducted subsequent to obtaining the geothermal-hydrostatic equilibrium assumes a fault zone permeability of  $100 \times 10^{-15} \text{ m}^2$  (see below), and we wish to comment briefly on why here we choose a much smaller value of  $10^{-19} \text{ m}^2$  (Fig. 22). For the thermal parameters specified (thermal conductivity  $\lambda = 2.51 \text{ W/m/}^\circ\text{C}$ , rock grain density  $\rho_r = 2600 \text{ kg/m}^3$ , and rock specific heat  $C_r = 920 \text{ J/kg/}^\circ\text{C}$ ), we have a thermal diffusivity  $\Theta = \lambda / \rho_r C_r = 1.049 \times 10^{-6} \text{ m}^2/\text{s}$ . In contrast, for a permeability  $k = 100 \times 10^{-15} \text{ m}^2$  and a porosity  $\phi = 15 \%$ , the pressure diffusivity  $D_p = k / (\phi c \mu)$  in single-phase water at average conditions of  $(T, P) = (37.5 \text{ }^\circ\text{C}, 75 \times 10^5 \text{ Pa})$ , is about  $2.215 \text{ m}^2/\text{s}$ , more than 6 orders of magnitude larger. (Applicable water properties include a compressibility of  $c = 4.42 \times 10^{-10} \text{ Pa}^{-1}$  and a viscosity of  $\mu = 0.684 \text{ cP}$ .) The

eventual geothermal-hydrostatic equilibrium does not depend on the value of permeability, and through reducing permeability by six orders of magnitude, to  $k = 10^{-19} \text{ m}^2$ , we force pressure and thermal diffusivities to be of comparable magnitude, which allows for a more stable and efficient simulation. The simulation progresses well through rapidly increasing time steps, see Fig. 23, and terminates automatically when steady state criteria are met after 16 time steps and a very large total time of  $1.27 \times 10^{16} \text{ s} = 4.03 \times 10^8 \text{ yr}$ . The equilibrated temperature and pressure profiles are shown in Fig. 19; the pressure at 1500 m depth is found to be  $P = 147.476 \text{ bar}$ .

```

*rld* - 1-D vertical flow channel, for ECO2M
ROCKS-----1-----*-----2-----*-----3-----*-----4-----*-----5-----*-----6-----*-----7-----*-----8
fault      2  2600.e00      .15      1.e-19      1.e-19      1.e-19      2.51      920.
          0.0e-10
          12      .300      .01      .01      3.
          8      0.000      1.84      3.16      3.48
atmos      2  2600.e00      .15      1.e-19      1.e-19      1.e-19      2.51      920.
          0.0e-10
          12      .300      .01      .01      3.
          8      0.000      1.84      3.16      3.48
botom      2  2600.e40      .15      1.e-19      1.e-19      1.e-19      2.51      920.
          0.0e-10
          12      .300      .01      .01      3.
          8      0.000      1.84      3.16      3.48

MULTI-----1-----*-----2-----*-----3-----*-----4-----*-----5-----*-----6-----*-----7-----*-----8
          3      4      4      6
SELEC.....2.....3.....4.....5.....6.....7.....8.....9...10...11...12...13...14...15...16
          1
          .8      .8      1.e-3
START-----1-----*-----2-----*-----3-----*-----4-----*-----5-----*-----6-----*-----7-----*-----8
-----*-----1 MOP: 123456789*123456789*1234 -----*-----5-----*-----6-----*-----7-----*-----8
PARAM-----1-----*-----2-----*-----3-----*-----4-----*-----5-----*-----6-----*-----7-----*-----8
          1  30      51000300000200003
          -1.
          1.e6      1.e8      1.e9      1.e10      1.e11      1.e12      1.e13      1.e14
          1.e-6
          100.e5      0.0      0.0      40.
SOLVR-----1-----*-----2-----*-----3-----*-----4-----*-----5-----*-----6-----*-----7-----*-----8
5 Z1 O0      8.0e-1      1.0e-7
INDOM-----1-----*-----2-----*-----3-----*-----4-----*-----5-----*-----6-----*-----7-----*-----8
atmos
          1.013e5      0.0      0.0      15.
botom
          150.e5      0.0      0.0      60.

INCON-----1-----*-----2-----*-----3-----*-----4-----*-----5-----*-----6-----*-----7-----*-----8
GENER-----1-----*-----2-----*-----3-----*-----4-----*-----5-----*-----6-----*-----7-----*-----8
ENDCY-----1-----*-----2-----*-----3-----*-----4-----*-----5-----*-----6-----*-----7-----*-----8

```

Figure 22. TOUGH2/ECO2M input file for generating a static geothermal-hydrostatic profile.

```

...ITERATING... AT [ 1, 1] --- DELTEX = .100000E+07 MAX. RES. = .140447E+01 AT ELEMENT E1C 1 EQUATION 1
...ITERATING... AT [ 1, 2] --- DELTEX = .100000E+07 MAX. RES. = .381971E-03 AT ELEMENT E1C 1 EQUATION 1
E1C 1( 1, 3) ST = .100000E+07 DT = .100000E+07 DX1= -.458000E+07 DX2= .000000E+00 T = 60.000 P = 10419999. S = .100000E+01
...ITERATING... AT [ 2, 1] --- DELTEX = .100000E+09 MAX. RES. = .116674E+01 AT ELEMENT A12 1 EQUATION 4
...ITERATING... AT [ 2, 2] --- DELTEX = .100000E+09 MAX. RES. = .296035E-02 AT ELEMENT A12 1 EQUATION 1
...ITERATING... AT [ 2, 3] --- DELTEX = .100000E+09 MAX. RES. = .402307E-05 AT ELEMENT A12 1 EQUATION 4
A12 1( 2, 4) ST = .101000E+09 DT = .100000E+09 DX1= -.810646E+07 DX2= .000000E+00 T = 26.283 P = 968610. S = .100000E+01
...ITERATING... AT [ 3, 1] --- DELTEX = .100000E+10 MAX. RES. = .501326E+01 AT ELEMENT A12 1 EQUATION 4
...ITERATING... AT [ 3, 2] --- DELTEX = .100000E+10 MAX. RES. = .370777E-02 AT ELEMENT E1C 1 EQUATION 1
...ITERATING... AT [ 3, 3] --- DELTEX = .100000E+10 MAX. RES. = .246912E-04 AT ELEMENT E1C 1 EQUATION 1
E1C 1( 3, 4) ST = .110100E+10 DT = .100000E+10 DX1= .177769E+07 DX2= .000000E+00 T = 60.000 P = 18364724. S = .100000E+01
...ITERATING... AT [ 4, 1] --- DELTEX = .100000E+11 MAX. RES. = .471419E+01 AT ELEMENT A13 1 EQUATION 4
...ITERATING... AT [ 4, 2] --- DELTEX = .100000E+11 MAX. RES. = .414352E-02 AT ELEMENT A13 1 EQUATION 1
...ITERATING... AT [ 4, 3] --- DELTEX = .100000E+11 MAX. RES. = .177162E-03 AT ELEMENT E16 1 EQUATION 1
E1C 1( 4, 4) ST = .111010E+11 DT = .100000E+11 DX1= .126972E+07 DX2= .000000E+00 T = 60.000 P = 19634446. S = .100000E+01
...ITERATING... AT [ 5, 1] --- DELTEX = .100000E+12 MAX. RES. = .456361E+01 AT ELEMENT A16 1 EQUATION 4
...ITERATING... AT [ 5, 2] --- DELTEX = .100000E+12 MAX. RES. = .377943E-02 AT ELEMENT A17 1 EQUATION 1
...ITERATING... AT [ 5, 3] --- DELTEX = .100000E+12 MAX. RES. = .157762E-03 AT ELEMENT D1W 1 EQUATION 1
E1C 1( 5, 4) ST = .111101E+12 DT = .100000E+12 DX1= .113997E+07 DX2= .000000E+00 T = 60.000 P = 20774412. S = .100000E+01

```

Figure 23. Part of printed output for obtaining a geothermal-hydrostatic profile.

### 6.3.3 Simulating CO<sub>2</sub> Upflow Along the Fault

The simulation of CO<sub>2</sub> upflow is initialized using the SAVE file with the geothermal-hydrostatic conditions obtained above, with only one essential change: the conditions at the bottom boundary (grid block [E1C 1]) are changed “by hand” from single-phase water at P = 147.476 bar to single-phase CO<sub>2</sub> at a 10 bar overpressure, P = 157.476 bar. In addition to changing the pressure in the SAVE file, this requires to change the third primary variable (CO<sub>2</sub> mass fraction) from X = 0 to X = 1, and to change the phase index from 1 (aqueous) to 2 (liquid CO<sub>2</sub>). In order to maintain these boundary conditions for the CO<sub>2</sub> migration simulation, we move the bottommost grid block [E1C 1] into inactive position at the end of the ELEME data block in the MESH file, and we place it in the same (last) position in the INCON file. The same INCON file with header removed is used as file MINC to provide the initial temperatures in the semi-infinite conductive domains that are attached to every grid block of the fault (see Sec. 4). The TOUGH2/ECO2M input file for the CO<sub>2</sub> migration simulation is shown in Fig. 24. A semi-analytical heat exchange calculation is engaged by specifying MOP(15) = 1. Note that the thermal parameters for the conductive domains ( $\lambda$ ,  $\rho_r$ ,  $C_r$ ) are taken from the domain ‘botom’ of the last grid block (E1C 1), and rock grain density in this domain was restored to its physical value  $\rho_r = 2600 \text{ kg/m}^3$ . The three-phase relative permeability and capillary pressure functions used are described in Appendices A and B. By specifying IE(9) = 3 and FE(3) = 1.e-3 we invoke a finite window for phase transitions, see Sec. 2.4. MOP(16) = 4 invokes automatic time stepping, with  $\Delta t$  doubling whenever a time step converges in 4 or fewer iterations. The problem initialization by means of the INCON file generated in the geothermal-hydrostatic equilibration run, above, uses internal ECO2M-style primary variables (Table 2), and a single-record data

```

*rld* - 1-D vertical flow channel, for ECO2M
ROCKS-----1-----*-----2-----*-----3-----*-----4-----*-----5-----*-----6-----*-----7-----*-----8
fault      2  2600.e00      .15  100.e-15  100.e-15  100.e-15      2.51      920.
          0.0e-10
          12      .300      .01      .01      3.
          8      0.000      1.84      3.16      3.48
atmos      2  2600.e00      .15  100.e-15  100.e-15  100.e-15      2.51      920.
          0.0e-10
          12      .300      .01      .01      3.
          8      0.000      1.84      3.16      3.48
botom      2  2600.e00      .15  100.e-15  100.e-15  100.e-15      2.51      920.
          0.0e-10
          12      .300      .01      .01      3.
          8      0.000      1.84      3.16      3.48

MULTI-----1-----*-----2-----*-----3-----*-----4-----*-----5-----*-----6-----*-----7-----*-----8
          3      4      4      6
SELEC.....2.....3.....4.....5.....6.....7.....8.....9...10...11...12...13...14...15...16
          1
          .8      .8      1.e-3
INDEX-----1-----*-----2-----*-----3-----*-----4-----*-----5-----*-----6-----*-----7-----*-----8
START-----1-----*-----2-----*-----3-----*-----4-----*-----5-----*-----6-----*-----7-----*-----8
-----*-----1 MOP: 123456789*123456789*1234 -----*-----5-----*-----6-----*-----7-----*-----8
PARAM-----1-----*-----2-----*-----3-----*-----4-----*-----5-----*-----6-----*-----7-----*-----8
          1 500      501000300000200014
                  -1.                      9.81
          1.e2
          1.e-6
          1
          100.e5                      0.0                      0.0                      40.
SOLVR-----1-----*-----2-----*-----3-----*-----4-----*-----5-----*-----6-----*-----7-----*-----8
5 Z1 00      8.0e-1      1.0e-7
FOFT -----1-----*-----2-----*-----3-----*-----4-----*-----5-----*-----6-----*-----7-----*-----8
A12 1      1 .1000E+02 .2000E+02      .5000E+00 .5001E+01-.5000E+00
B1H 1      1 .1000E+02 .2000E+02      .5000E+00 .5050E+03-.5000E+00
C1W 1      1 .1000E+02 .2000E+02      .5000E+00 .1005E+04-.5000E+00
E1B 1      1 .1000E+02 .2000E+02      .5000E+00 .1495E+04-.5000E+00

COFT -----1-----*-----2-----*-----3-----*-----4-----*-----5-----*-----6-----*-----7-----*-----8
A11 1A12 1      2 .5000E-03 .5000E+01 .1000E+01 .1000E+01

iNCON-----1-----*-----2-----*-----3-----*-----4-----*-----5-----*-----6-----*-----7-----*-----8

GENER-----1-----*-----2-----*-----3-----*-----4-----*-----5-----*-----6-----*-----7-----*-----8

ENDCY-----1-----*-----2-----*-----3-----*-----4-----*-----5-----*-----6-----*-----7-----*-----8

```

Figure 24. TOUGH2/ECO2M input file for CO<sub>2</sub> migration along a fault zone.

block INDEX is required to allow proper reading of these data. Note that default initial conditions in data block PARAM then also need to be supplied using ECO2M-style primary variables, with an added record with phase INDEX preceding the primary variables, even though these default initial conditions will be ignored, as all initial conditions are supplied through the



INCON file. Nonetheless, data in proper format need to be provided to allow proper reading of the input file. The input file also includes some FOFT and COFT data to generate time series of thermodynamic conditions and fluid and heat flows for plotting.

The pressurization from the step change in bottom boundary conditions rapidly migrates up the fault; the resulting T,P-profile is shown as a dashed line in the right frame of Fig. 19. In response to CO<sub>2</sub> injection water is being pushed upward, and a front of free-phase CO<sub>2</sub> is advancing towards the land surface. The simulation accounts for non-isothermal effects that arise from (1) upflow of warmer (T = 60 °C) fluid into colder regions, (2) Joule-Thomson cooling as upflowing CO<sub>2</sub> expands (Katz and Lee, 1990), (3) boiling of liquid CO<sub>2</sub> into gas, and (4) mutual dissolution of H<sub>2</sub>O and CO<sub>2</sub>. Conductive heat exchange with the wall rocks is an important aspect of system evolution. After the 500 time steps specified in the input file, the simulation reaches a time of  $6.10 \times 10^8$  s = 19.33 yr. Fig. 25 shows parts of the printed output. We then perform a continuation run, using the SAVE file generated after 500 time steps as INCON, using the file TABLE generated in the 500 time step run to pass on the history of thermal perturbations in the conductive domains, and using virtually the same input file as shown in Fig. 24, except that we allow 1000 time steps, and specify the first time step as  $10^5$  s. The continuation run stops after time step 1302 at a simulation time of  $1.12 \times 10^9$  s = 35.56 yr, after time steps get cut repeatedly in response to temperatures dropping down to 1 °C in grid block [A1T 1] at a depth of 275 m. A portion of the output appears in Fig. 26. The strong temperature decline near grid block [A1T 1] occurs in response to persistent boiling of liquid CO<sub>2</sub> into gas; see the transition from aqueous-liquid conditions (phase index I=4 in Fig. 26) in [A1T 1] and below to aqueous-gas conditions (phase index I=5) at [A1S 1] and above.

```

...ITERATING... AT [ 1, 1] --- DELTEX = .100000E+03 MAX. RES. = .262001E+01 AT ELEMENT E1B 1 EQUATION 3
...ITERATING... AT [ 1, 2] --- DELTEX = .100000E+03 MAX. RES. = .902673E-03 AT ELEMENT E1B 1 EQUATION 4
E1B 1( 1, 3) ST = .100000E+03 DT = .100000E+03 DX1= .949484E+06 DX2= .000000E+00 T = 59.868 P = 15648572. S = .100000E+01
...ITERATING... AT [ 2, 1] --- DELTEX = .200000E+03 MAX. RES. = .350382E+00 AT ELEMENT E1B 1 EQUATION 3
...ITERATING... AT [ 2, 2] --- DELTEX = .200000E+03 MAX. RES. = .574395E-04 AT ELEMENT E1A 1 EQUATION 3
E1B 1( 2, 3) ST = .300000E+03 DT = .200000E+03 DX1= .448990E+05 DX2= .000000E+00 T = 59.874 P = 15693471. S = .100000E+01
...ITERATING... AT [ 3, 1] --- DELTEX = .400000E+03 MAX. RES. = .238365E+00 AT ELEMENT E1B 1 EQUATION 3
...ITERATING... AT [ 3, 2] --- DELTEX = .400000E+03 MAX. RES. = .671538E-04 AT ELEMENT E1A 1 EQUATION 3
E1B 1( 3, 3) ST = .700000E+03 DT = .400000E+03 DX1= .854930E+04 DX2= .000000E+00 T = 59.882 P = 15702021. S = .100000E+01
...ITERATING... AT [ 4, 1] --- DELTEX = .800000E+03 MAX. RES. = .300646E+00 AT ELEMENT E1B 1 EQUATION 3
...ITERATING... AT [ 4, 2] --- DELTEX = .800000E+03 MAX. RES. = .112113E-03 AT ELEMENT E1A 1 EQUATION 3
E1B 1( 4, 3) ST = .150000E+04 DT = .800000E+03 DX1= .392338E+04 DX2= .000000E+00 T = 59.893 P = 15705944. S = .100000E+01
...ITERATING... AT [ 5, 1] --- DELTEX = .160000E+04 MAX. RES. = .439526E+00 AT ELEMENT E1B 1 EQUATION 3
...ITERATING... AT [ 5, 2] --- DELTEX = .160000E+04 MAX. RES. = .215756E-03 AT ELEMENT E1A 1 EQUATION 3
E1B 1( 5, 3) ST = .310000E+04 DT = .160000E+04 DX1= .243120E+04 DX2= .000000E+00 T = 59.911 P = 15708375. S = .100000E+01
...
E1B 1( 9, 3) ST = .511000E+05 DT = .256000E+05 DX1= .520613E+03 DX2= .000000E+00 T = 60.501 P = 15712368. S = .100000E+01
...ITERATING... AT [ 10, 1] --- DELTEX = .512000E+05 MAX. RES. = .809612E+00 AT ELEMENT E1B 1 EQUATION 3
$$$ 1 ----> 4 $$$ LIQ. EVOLVES AT *E1A 1* X3 = .128541E+00 XCO2aq = .491300E-01 TX = .622284E+02 PX = .157127E+08
...ITERATING... AT [ 10, 2] --- DELTEX = .512000E+05 MAX. RES. = .755252E+00 AT ELEMENT E1B 1 EQUATION 3
...ITERATING... AT [ 10, 3] --- DELTEX = .512000E+05 MAX. RES. = .730977E-02 AT ELEMENT E1B 1 EQUATION 3
E1A 1( 10, 4) ST = .102300E+06 DT = .512000E+05 DX1= .550080E+04 DX2= .000000E+00 T = 59.558 P = 15606611. S = .100000E+01
...
...ITERATING... AT [ 14, 1] --- DELTEX = .819200E+06 MAX. RES. = .165135E+01 AT ELEMENT E1A 1 EQUATION 3
$$$ 1 ----> 4 $$$ LIQ. EVOLVES AT *E1A 1* X3 = .128541E+00 XCO2aq = .493597E-01 TX = .612091E+02 PX = .156235E+08
...ITERATING... AT [ 14, 2] --- DELTEX = .819200E+06 MAX. RES. = .250817E+01 AT ELEMENT E1A 1 EQUATION 3
...ITERATING... AT [ 14, 3] --- DELTEX = .819200E+06 MAX. RES. = .106214E+01 AT ELEMENT E19 1 EQUATION 3
...ITERATING... AT [ 14, 4] --- DELTEX = .819200E+06 MAX. RES. = .131243E-01 AT ELEMENT E19 1 EQUATION 3
...ITERATING... AT [ 14, 5] --- DELTEX = .819200E+06 MAX. RES. = .160165E-05 AT ELEMENT E19 1 EQUATION 3
E1B 1( 14, 6) ST = .163830E+07 DT = .819200E+06 DX1= .264060E+03 DX2= .000000E+00 T = 60.344 P = 15715968. S = .748272E+00
...ITERATING... AT [ 15, 1] --- DELTEX = .819200E+06 MAX. RES. = .885202E+00 AT ELEMENT E19 1 EQUATION 3
...ITERATING... AT [ 15, 2] --- DELTEX = .819200E+06 MAX. RES. = .383161E+01 AT ELEMENT E19 1 EQUATION 3
...ITERATING... AT [ 15, 3] --- DELTEX = .819200E+06 MAX. RES. = .271578E+00 AT ELEMENT E19 1 EQUATION 3
...ITERATING... AT [ 15, 4] --- DELTEX = .819200E+06 MAX. RES. = .854221E-03 AT ELEMENT E19 1 EQUATION 3
E19 1( 15, 5) ST = .245750E+07 DT = .819200E+06 DX1= .666931E+04 DX2= .000000E+00 T = 59.909 P = 15528792. S = .100000E+01
...ITERATING... AT [ 16, 1] --- DELTEX = .819200E+06 MAX. RES. = .817948E+00 AT ELEMENT E19 1 EQUATION 3
$$$ 1 ----> 4 $$$ LIQ. EVOLVES AT *E19 1* X3 = .114473E+00 XCO2aq = .490062E-01 TX = .620841E+02 PX = .155346E+08
...ITERATING... AT [ 16, 2] --- DELTEX = .819200E+06 MAX. RES. = .163967E+01 AT ELEMENT E19 1 EQUATION 3
...ITERATING... AT [ 16, 3] --- DELTEX = .819200E+06 MAX. RES. = .480272E+00 AT ELEMENT E18 1 EQUATION 3
...ITERATING... AT [ 16, 4] --- DELTEX = .819200E+06 MAX. RES. = .917734E-02 AT ELEMENT E19 1 EQUATION 3
...ITERATING... AT [ 16, 5] --- DELTEX = .819200E+06 MAX. RES. = .122046E-04 AT ELEMENT E18 1 EQUATION 3
E19 1( 16, 6) ST = .327670E+07 DT = .819200E+06 DX1= .141000E+05 DX2= .000000E+00 T = 59.869 P = 15542892. S = .915558E+00
...
...
OUTPUT DATA AFTER ( 500, 5)-2-TIME STEPS THE TIME IS .706081E+04 DAYS
#####
TOTAL TIME KCYC ITER ITCR KON DX1M DX2M DX3M MAX. RES. NER KER DELTEX
.610054E+09 500 5 3083 2 .67753E+05 .00000E+00 .57948E-01 .28322E-06 49 3 .65536E+07
#####
ELEM INDEX I P T SAQ SLIQ SGAS XCO2AQ DLIQ VISLIQ DGAS VISGAS
(PA) (DEG.C) (KG/M3) (PA-S) (KG/M3) (PA-S)
A12 1 1 5 .323812E+06 11.5902 .432462E+00 .000000E+00 .567538E+00 .648484E-02 .00 .100000E+01 6.18 .143531E-04
A13 1 2 5 .604535E+06 12.2855 .462756E+00 .000000E+00 .537244E+00 .115992E-01 .00 .100000E+01 11.67 .144361E-04
A14 1 3 5 .829970E+06 13.0833 .479844E+00 .000000E+00 .520156E+00 .153071E-01 .00 .100000E+01 16.18 .145184E-04
A15 1 4 5 .102569E+07 13.7026 .492181E+00 .000000E+00 .507819E+00 .183495E-01 .00 .100000E+01 20.21 .145902E-04
A16 1 5 5 .120240E+07 14.1978 .501769E+00 .000000E+00 .498231E+00 .209416E-01 .00 .100000E+01 23.90 .146537E-04

```

Figure 25. Part of printed output for fault leakage problem.

```

...ITERATING... AT [ 501, 1] --- DELTEX = .100000E+06 MAX. RES. = .149760E-02 AT ELEMENT B1E 1 EQUATION 1
...ITERATING... AT [ 501, 2] --- DELTEX = .100000E+06 MAX. RES. = .190763E-04 AT ELEMENT B1D 1 EQUATION 3
B1E 1( 501, 3) ST = .610154E+09 DT = .100000E+06 DX1= -.460688E+03 DX2= .000000E+00 T = 26.217 P = 5120766. S = .591994E+00
...ITERATING... AT [ 502, 1] --- DELTEX = .200000E+06 MAX. RES. = .307501E-02 AT ELEMENT B1E 1 EQUATION 1
...ITERATING... AT [ 502, 2] --- DELTEX = .200000E+06 MAX. RES. = .170107E-03 AT ELEMENT B1D 1 EQUATION 3
B1E 1( 502, 3) ST = .610354E+09 DT = .200000E+06 DX1= -.828839E+03 DX2= .000000E+00 T = 26.216 P = 5119937. S = .593901E+00
...ITERATING... AT [ 503, 1] --- DELTEX = .400000E+06 MAX. RES. = .642575E-02 AT ELEMENT B1E 1 EQUATION 1
...ITERATING... AT [ 503, 2] --- DELTEX = .400000E+06 MAX. RES. = .153333E-02 AT ELEMENT B1D 1 EQUATION 3
B1D 1( 503, 3) ST = .610754E+09 DT = .400000E+06 DX1= -.346067E+04 DX2= .000000E+00 T = 25.988 P = 5036071. S = .540780E+00
...ITERATING... AT [ 504, 1] --- DELTEX = .800000E+06 MAX. RES. = .136035E-01 AT ELEMENT B1E 1 EQUATION 1
...ITERATING... AT [ 504, 2] --- DELTEX = .800000E+06 MAX. RES. = .149929E-01 AT ELEMENT B1E 1 EQUATION 3
...ITERATING... AT [ 504, 3] --- DELTEX = .800000E+06 MAX. RES. = .104410E-04 AT ELEMENT B1D 1 EQUATION 3
B1E 1( 504, 4) ST = .611554E+09 DT = .800000E+06 DX1= -.177195E+04 DX2= .000000E+00 T = 26.207 P = 5116806. S = .606442E+00
...ITERATING... AT [ 505, 1] --- DELTEX = .160000E+07 MAX. RES. = .279618E-01 AT ELEMENT B1E 1 EQUATION 1
...ITERATING... AT [ 505, 2] --- DELTEX = .160000E+07 MAX. RES. = .113877E+00 AT ELEMENT B1E 1 EQUATION 3
...ITERATING... AT [ 505, 3] --- DELTEX = .160000E+07 MAX. RES. = .713452E-03 AT ELEMENT B1D 1 EQUATION 3
B1C 1( 505, 4) ST = .613154E+09 DT = .160000E+07 DX1= -.148967E+05 DX2= .000000E+00 T = 25.774 P = 4953426. S = .525572E+00
...ITERATING... AT [ 506, 1] --- DELTEX = .320000E+07 MAX. RES. = .486746E-01 AT ELEMENT B1E 1 EQUATION 1
...ITERATING... AT [ 506, 2] --- DELTEX = .320000E+07 MAX. RES. = .670741E+00 AT ELEMENT B1C 1 EQUATION 3
...ITERATING... AT [ 506, 3] --- DELTEX = .320000E+07 MAX. RES. = .286049E-01 AT ELEMENT B1E 1 EQUATION 3
...ITERATING... AT [ 506, 4] --- DELTEX = .320000E+07 MAX. RES. = .249026E-04 AT ELEMENT B1E 1 EQUATION 3
B1E 1( 506, 5) ST = .616354E+09 DT = .320000E+07 DX1= .663283E+03 DX2= .000000E+00 T = 26.169 P = 5116223. S = .634664E+00
...
...
OUTPUT DATA AFTER (1302, 1)-2-TIME STEPS THE TIME IS .129900E+05 DAYS
#####
TOTAL TIME KCYC ITER ITCR KON DX1M DX2M DX3M MAX. RES. NER KER DELTEX
.112234E+10 1302 1 8192 2 .000000E+00 .000000E+00 .000000E+00 .31680E-06 28 4 .19073E+00
#####
ELEM INDEX I P T SAQ SLIQ SGAS XCO2AQ DLIQ VISLIQ DGAS VISGAS
(PA) (DEG.C) (KG/M3) (PA-S) (KG/M3) (PA-S)
A12 1 1 5 .269174E+06 10.2051 .359580E+00 .000000E+00 .640420E+00 .562728E-02 .00 .100000E+01 5.16 .142759E-04
A13 1 2 5 .481190E+06 10.3745 .384256E+00 .000000E+00 .615744E+00 .978592E-02 .00 .100000E+01 9.26 .143190E-04
A14 1 3 5 .648962E+06 11.2890 .396871E+00 .000000E+00 .603129E+00 .127497E-01 .00 .100000E+01 12.62 .143957E-04
A15 1 4 5 .793645E+06 12.0508 .405707E+00 .000000E+00 .594293E+00 .150931E-01 .00 .100000E+01 15.51 .144608E-04
A16 1 5 5 .923714E+06 12.6620 .412561E+00 .000000E+00 .587439E+00 .170841E-01 .00 .100000E+01 18.12 .145165E-04
A17 1 6 5 .104348E+07 13.2013 .418609E+00 .000000E+00 .581391E+00 .188876E-01 .00 .100000E+01 20.63 .145697E-04
...
A1Q 1 25 5 .366797E+07 16.8512 .641202E+00 .000000E+00 .358798E+00 .493955E-01 .00 .100000E+01 88.61 .157410E-04
A1R 1 26 5 .380221E+07 16.6548 .640571E+00 .000000E+00 .359429E+00 .508754E-01 .00 .100000E+01 93.44 .158220E-04
A1S 1 27 5 .391964E+07 8.6693 .648431E+00 .000000E+00 .351569E+00 .626476E-01 .00 .100000E+01 106.68 .156788E-04
A1T 1 28 4 .401465E+07 1.0000 .592995E+00 .407005E+00 .000000E+00 .759259E-01 120.51 .237459E-04 .00 .100000E+01
A1U 1 29 4 .410117E+07 5.0169 .585097E+00 .414903E+00 .000000E+00 .738498E-01 896.43 .921949E-04 .00 .100000E+01
A1V 1 30 4 .421946E+07 6.0161 .566981E+00 .433019E+00 .000000E+00 .730134E-01 889.91 .906190E-04 .00 .100000E+01
A1W 1 31 4 .433528E+07 7.4865 .563734E+00 .436266E+00 .000000E+00 .717817E-01 879.54 .881418E-04 .00 .100000E+01
A1X 1 32 4 .444953E+07 8.8554 .564914E+00 .435086E+00 .000000E+00 .706382E-01 869.53 .858400E-04 .00 .100000E+01
A1Y 1 33 4 .456271E+07 10.1422 .567776E+00 .432224E+00 .000000E+00 .695540E-01 859.67 .836737E-04 .00 .100000E+01
A1Z 1 34 4 .467541E+07 11.3633 .572697E+00 .427303E+00 .000000E+00 .685483E-01 850.15 .816263E-04 .00 .100000E+01
B11 1 35 7 .479197E+07 12.5081 .576071E+00 .406545E+00 .173847E-01 .676042E-01 840.92 .797197E-04 147.63 .168274E-04
B12 1 36 7 .492416E+07 13.6259 .577532E+00 .399334E+00 .231336E-01 .667013E-01 831.88 .779065E-04 153.55 .170400E-04
B13 1 37 7 .505364E+07 14.7018 .586788E+00 .401950E+00 .112622E-01 .658416E-01 822.92 .761551E-04 159.52 .172553E-04
B14 1 38 4 .518177E+07 15.7093 .599701E+00 .400299E+00 .000000E+00 .650345E-01 814.21 .745159E-04 .00 .100000E+01

```

Figure 26. Part of printed output for continuation run of fault leakage problem.

### 6.3.4 Presentation and Discussion of Results

Fig. 27 shows profiles of temperature and CO<sub>2</sub> phase saturations at different times. The saturation profile at t = 6.42 yr gives a snapshot just prior to commencement of CO<sub>2</sub> discharge at the land surface at 6.425 yr. Note a sharp transition from liquid to gaseous CO<sub>2</sub> at 540 m depth. As will be seen below (Fig. 30), this transition occurs almost exactly at the critical point of CO<sub>2</sub>. Over time the system experiences predominant cooling effects, and evolves an extended region with 3-phase fluid conditions (aqueous - liquid CO<sub>2</sub> - gaseous CO<sub>2</sub>). After t = 27.33 yr, three-phase conditions are seen to extend from - 240 m to -460 m depth (note that an aqueous phase is present throughout, which is not shown in Fig. 27). There is a precipitous temperature decline in the three-phase zone, reflecting heat loss as liquid CO<sub>2</sub> boils into gas. Lowest temperatures are reached at the liquid CO<sub>2</sub> front, where rates of boiling and associated heat loss are largest. We note that saturations of liquid CO<sub>2</sub> increase to large values beneath the three-phase zone. This

represents buoyant accumulation of less dense fluid (liquid CO<sub>2</sub>) beneath a region of low effective permeability. The three-phase zone acts as a mobility block, because in three-phase conditions, relative permeabilities are small for all phases. Within the three-phase zone, liquid and gas saturations show strong fluctuations, which are due to the interplay between multiphase flow and conductive heat transfer in the fault walls with different time constants. Aqueous phase saturation  $S_{aq} = 1 - (S_{liq} + S_{gas})$  shows much smaller fluctuations than either  $S_{liq}$  or  $S_{gas}$ .

At early times, outflow at the land surface is just aqueous phase. A large “burp” of water outflow occurs as free CO<sub>2</sub> approaches the land surface, reflecting the strong volume expansion there (Fig. 28). CO<sub>2</sub> flux at the land surface shows non-monotonic behavior. Periods of large CO<sub>2</sub> outflow correlate with declining temperatures of the discharge (Fig. 28). The largest CO<sub>2</sub> flux approaches  $2 \times 10^{-3}$  kg/s/m<sup>2</sup>, which for the assumed fault zone thickness of 5 m translates into an outflow rate of somewhat less than  $10^{-2}$  kg/s per meter fault length, or 1 kg/s per 100 m fault length. During periods when the CO<sub>2</sub> outflow rate is relatively small, three-phase conditions migrate upward, and the region with three-phase conditions thickens (Fig. 29). As CO<sub>2</sub> outflow rates increase, the upward extension of three-phase conditions slows and eventually turns around when liquid CO<sub>2</sub> is boiled off the top of the three-phase zone at large rates.

Additional insight into the system dynamics can be gained by examining the evolution of profiles in T,P-space. Fig. 30 shows that, as a consequence of the pressure increase and temperature decline during CO<sub>2</sub> migration, the T,P-profile is rapidly shifted towards the CO<sub>2</sub> saturation line. Thermodynamic conditions get drawn towards the critical point and then approximately follow the saturation line. Note that three-phase points must fall right on the saturation line, while in the vicinity of three-phase zones, thermodynamic conditions will plot near the saturation line. At time  $t = 27.33$  yr we have a large extent of three-phase conditions (Figs. 27, 29), and a correspondingly large region of T,P-conditions overlapping with the saturation line. Temperatures have a local minimum at the lowest pressure (shallowest depth) with three-phase conditions (Fig. 30). Temperatures increase near the bottom of the overlying two-phase aqueous-gas zone, but resume enhanced decline due to Joule-Thomson cooling as the gas expands during upward flow.

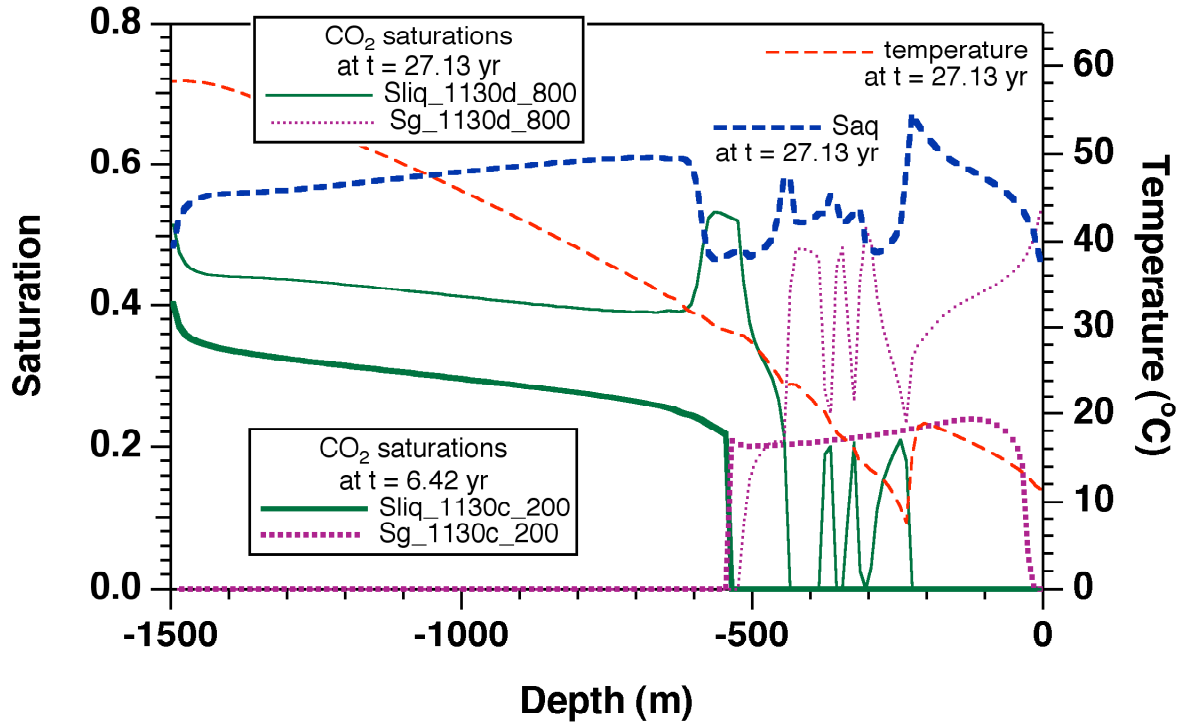


Figure 27. Saturation and temperature profiles at different times.

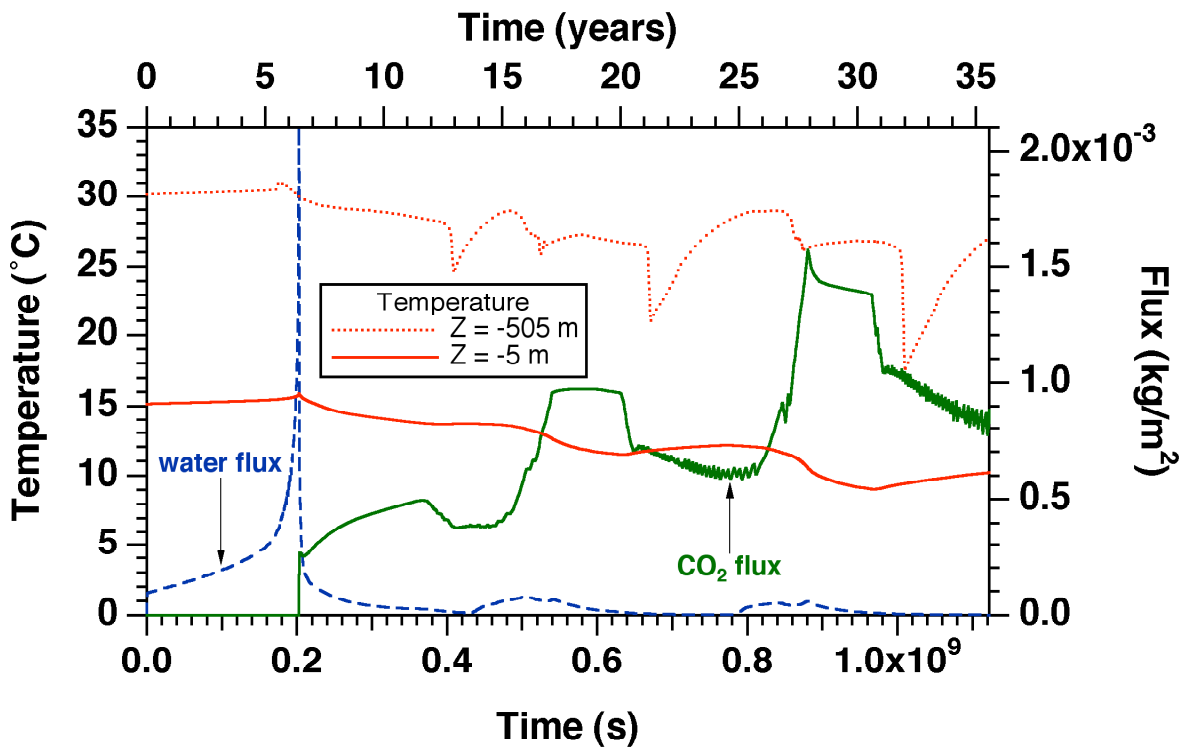


Figure 28. Time dependence of water and CO<sub>2</sub> outflow at the land surface, and temperatures at two different depths.

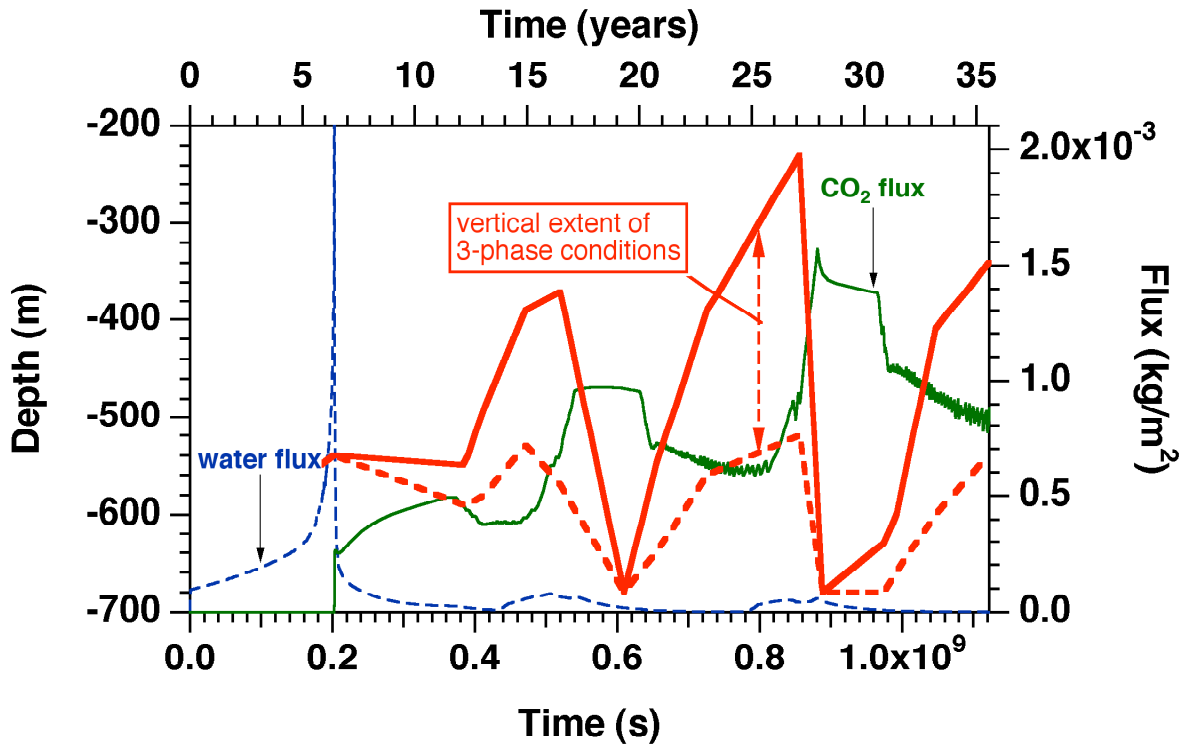


Figure 29. Water and CO<sub>2</sub> fluxes as shown in Fig. 28, with the heavy superposed lines indicating the top and bottom of three-phase conditions, respectively.

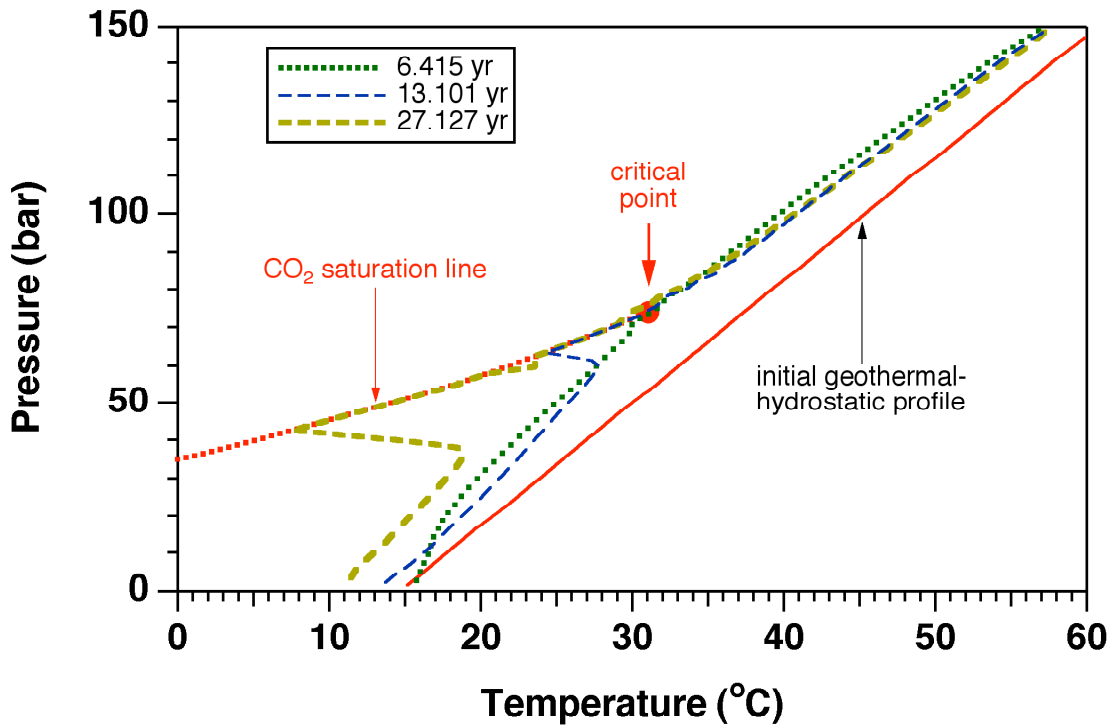


Figure 30. Temperature-pressure profiles at different times.

#### 6.4 Problem No. 4 (\*rwaf\*) - Migration of a CO<sub>2</sub> Plume in a Sloping Aquifer, Intersected by a Fault

The purpose of this problem is to illustrate application of TOUGH2/ECO2M to a scenario that includes the primary CO<sub>2</sub> storage reservoir, as well as a leakage pathway that extends all the way to the land surface. The preparation of the computational grid for such a scenario, and the development of appropriate initial conditions, entails a number of processing steps that involve TOUGH2 runs as well as some hand-editing of files. We will only summarize the workflow here, and will not present input files and outputs for all of the preprocessing steps.

The problem considered explores the large-scale long-time migration of a CO<sub>2</sub> plume in a sloping aquifer that is intersected by a leaky fault. Aquifer parameters are patterned after the Carrizo-Wilcox aquifer at the Texas Gulf coast (Nicot, 2008; Hesse et al., 2008). We assume that a substantial number of CO<sub>2</sub> storage projects will be operating in the Wilcox, and we consider a 2-D vertical section along the dip of the aquifer. The aquifer is modeled as a rectangular domain of 200 m thickness and 110 km length, sandwiched between impermeable cap and base rocks, and tilted with an angle of  $\alpha = 1.5^\circ$  against the horizontal (Fig. 31). We consider the upper right hand corner of the domain to be at the land surface; the lower left hand corner is then at a depth of  $110,000 \sin(\alpha) + 200 \cos(\alpha)$ , which for a tilt angle of  $\alpha = 1.5^\circ$  corresponds to 3,079.4 m. Formation properties include a uniform and isotropic permeability of 500 mD, a porosity of 15 %, and a compressibility of  $4.5 \times 10^{-10} \text{ Pa}^{-1}$  (similar to compressibility of water at ambient conditions). The 2-D computational grid for the aquifer models a section of 1 m thickness; it has

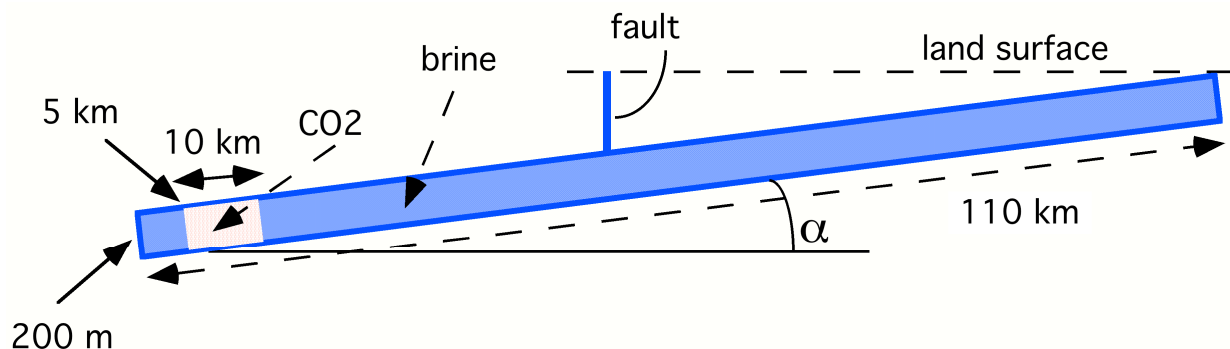


Figure 31. Geometric dimensions of the 2-D rectangular domain modeled. The domain is dipping upward by an angle  $\alpha$ . The initial CO<sub>2</sub> plume is shown by light shading.

7300 blocks with a basic space discretization of 10 m in the sub-vertical and 1000 m in the sub-horizontal direction (Fig. 32). The grid was refined to  $\Delta Z = 1$  m near the top, to better resolve the  $\text{CO}_2$  plume, and to  $\Delta Y = 10$  m in the Y-direction near  $Y = 50$  km where a vertical fault intersects the aquifer at a depth of 1570.75 m. The fault zone has a thickness of 10 m. Vertical discretization in the fault is also  $\Delta Z = 10$  m, hydrogeologic properties are assumed identical to those in the aquifer, and land surface conditions of  $(T_0, P_0) = (10 \text{ }^\circ\text{C}, 1.013 \times 10^5 \text{ Pa})$  are maintained at the top of the fault. The grids for the aquifer and the fault were generated

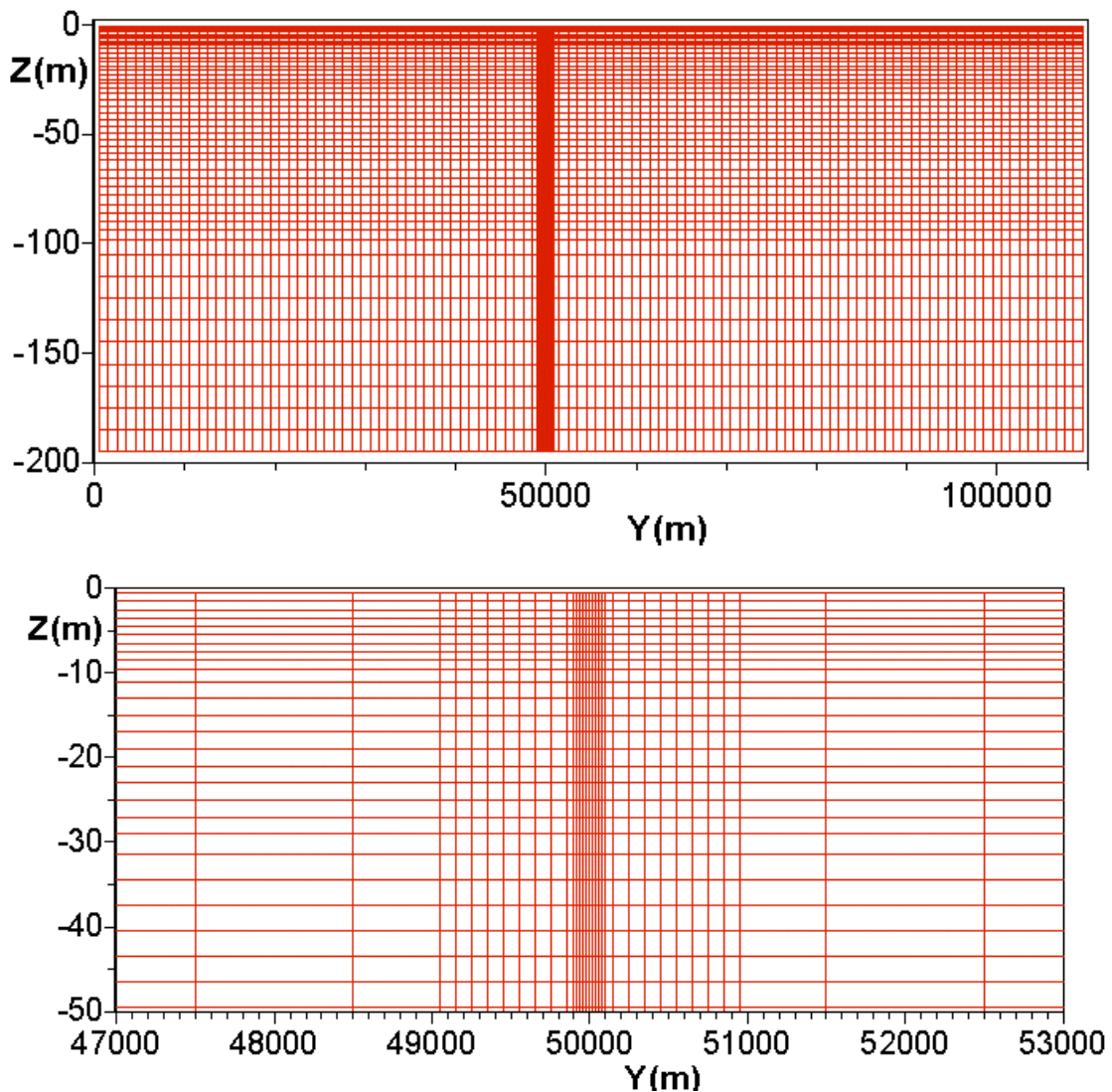


Figure 32. Computational grid showing the entire aquifer (top) and a zoom into the region with refined gridding (bottom).



separately using the MESHMAKER facility of TOUGH2, and some hand-editing was performed to connect the fault and aquifer grids, and to assign different portions of the grid to different domains in data block ROCKS.

Boundary conditions for the aquifer are “no flow” everywhere, except for the fault connection and at the upper right hand corner, which is held at land surface conditions. (In the calculational grid for the aquifer, land surface boundary conditions are actually implemented in the upper rightmost grid block [I16 1], whose nodal point is at a true depth of 13.588 m, with conditions of  $T = 10.4076$  °C,  $P = 2.37183$  bar.) The flow system is initialized as a fully (fresh-) water-saturated medium in hydrostatic equilibrium, held in a geothermal gradient of  $\text{grad}(T) = 30$  °C/km relative to a land surface temperature of 10 °C. The initialization is accomplished in several steps. We use a free-standing utility program to read in the 2-D TOUGH2 MESH file and write out an INCON file with temperature and pressure data assigned as  $T(Z) = T_0 + \text{grad}(T)*Z$ ,  $P(Z) = P_0 + \text{grad}(P)*Z$ . Here,  $Z$  is the elevation difference relative to a reference point with conditions  $(T_0, P_0)$ , and an approximate value of  $\text{grad}(P) \approx 10^4$  Pa/m is used. Subsequently we initialize a TOUGH2 simulation with these INCON data, maintaining temperatures at their initial values, and allowing pressures to come to an accurate gravitational equilibrium relative to a pressure of  $1.013 \times 10^5$  Pa at the land surface. A similar procedure is followed for the 1-D grid of the fault.

The CO<sub>2</sub> plume is emplaced instantaneously by using another utility program to assign a uniform gas saturation of  $S_g = 80$  % to the subdomain labeled “CO2” in Fig. 31, corresponding to aqueous phase at irreducible saturation of  $S_{ir} = 20$  %; for the CO<sub>2</sub> emplacement, pressures and temperatures are kept unchanged at their initial values. Plume evolution takes place under the combined action of gravity and pressure forces, with CO<sub>2</sub> buoyancy due to lower density being the primary driving force. For the simulations reported here we neglect capillary pressures in the aquifer domain, but include them in the fault zone. As in the previous fault upflow problem (\*r1d\*), conductive heat exchange across the fault walls is an important part of the evolution of the system, and is again modeled with the semi-analytical technique of Vinsome and Westerveld (1980; see Sec. 4); conductive heat exchange between the aquifer and cap and base rocks is less significant, but is included as well.

We now proceed to highlight selected parameters in the TOUGH2/ECO2M input file as shown in Fig. 33. In the aquifer (domains WILCO and co2in) we specify two-phase van Genuchten (1980) relative permeability functions, whereas in the fault zone the same three-phase relative permeability and capillary pressure functions are used as in sample problem 3 (\*r1d\*). When the CO<sub>2</sub> plume migrates updip it will eventually reach sub-critical pressure conditions, and when that happens, three-phase conditions may evolve. Our specification of two-phase relative permeabilities in the aquifer limits us to simulation times prior to evolution of three-phase conditions there. The choice of the parameter IE(9)=3 in block SELEC means that a finite window for certain phase transitions will be applied for ITER ≥ 3 during the Newtonian iteration at each time step; see Sec. 2.4. The window size is set to 10<sup>-3</sup> in parameters FE(3) and FE(4). For the scenario modeled here, extended regions of the fault evolve thermodynamic conditions that are very close to or right on the CO<sub>2</sub>-saturation line, and a finite window for phase change is essential for being able to move the simulation forward at time steps sufficiently large to permit an analysis of the long-time migration of the CO<sub>2</sub> plume. Parameter MOP(15)=1 in block PARAM engages the semi-analytical technique for heat exchange with impermeable wallrocks. MOP(16)=4 specifies automatic time step control, with time step size doubling whenever convergence is achieved in ITER ≤ 4 Newtonian iterations. The FOFT block will generate time series of thermophysical parameters at grid blocks of particular interest: [A12 2], [B1H 2] and [E1H 2] that are located at the top, at 509 m depth, and at the bottom of the fault, respectively, as well as at aquifer grid blocks next to the intersection with the fault. [C1X 1] is centered at Y = 49,995 m, while [C1W 1] and [C1Y 1] are 10 m downslope and upslope, respectively. (The four digits printed in the input file for nodal point coordinates include roundoff and do not accurately reflect these parameters.) The COFT block specifies writing of flow data at the top and bottom of the fault, respectively (connections [A11 2, A12 2] and [E1H 2, C1X 1]), as well as in the top of the aquifer near the fault intersection. Keywords for data blocks are case-sensitive, and “iNCON” is (intentionally) not a valid keyword and will be ignored, as initial condition data are supplied through an external INCON data file. The same INCON data file with its header removed is also supplied as file “MINC” to initialize the initial temperatures in the semi-infinite conductive half-spaces attached to the fault, and to the top and bottom of the aquifer. The thermal parameters used for the wallrocks are taken from the domain of the very last grid block in the ELEME-data, which is [I16 1] in domain WILCO.

```

*rwaf* ... Wilcox aquifer with vertical fault
ROCKS-----1-----*-----2-----*-----3-----*-----4-----*-----5-----*-----6-----*-----7-----*-----8
WILCO   2  2600.e00      .15  500.e-15  500.e-15  500.e-15      2.51      920.
  4.5e-10
  7          .457      .20          1.          .20
  10
co2in   2  2600.e00      .15  500.e-15  500.e-15  500.e-15      2.51      920.
  4.5e-10
  7          .457      .20          1.          .20
  10
fault   2  2600.e00      .15  500.e-15  500.e-15  500.e-15      2.51      920.
  4.5e-10
  12         .300      .01          .01          3.
  8          0.000      1.84         3.16         3.48

MULTI---1---*---2---*---3---*---4---*---5---*---6---*---7---*---8
  3  4  4  6
SELEC...2...3...4...5...6...7...8...9...10...11...12...13...14...15...16
  1          .8          .8          1.e-3          1.e-3          3  0  0  0  0  0  0
INDEX---1---*---2---*---3---*---4---*---5---*---6---*---7---*---8
START---1---*---2---*---3---*---4---*---5---*---6---*---7---*---8
----*-----1 MOP: 123456789*123456789*1234 ----*-----5-----*-----6-----*-----7-----*-----8
PARAM---1---*---2---*---3---*---4---*---5---*---6---*---7---*---8
  12000      25010 0 00000000 14  3
          -1.          9.81
          1.e3      9.e3      9.e4      9.e6
          1.E-5      1.E00
  1
          135.e5          1.e-6          1.e-6          50.0
FOFT ---1---*---2---*---3---*---4---*---5---*---6---*---7---*---8
A12 2          fault0.1000E+030.2000E+02          0.5000E+000.9318E+01-.5000E+01
B1H 2          fault0.1000E+030.2000E+02          0.5000E+000.5093E+03-.5000E+01
E1H 2          fault0.5000E+020.1000E+02          0.5000E+000.1557E+04-.5000E+01
C1W 1          1 .1000E+02 .1000E+02          .5000E+00 .4998E+05-.5000E+00
C1X 1          1 .1000E+02 .1000E+02          .5000E+00 .5000E+05-.5000E+00
C1Y 1          1 .1000E+02 .1000E+02          .5000E+00 .5000E+05-.5000E+00

COFT ---1---*---2---*---3---*---4---*---5---*---6---*---7---*---8
A11 2A12 2          30.2159E+010.5000E+010.1000E+020.1000E+01
E1H 2C1X 1          30.2500E+010.5000E+000.1000E+020.1000E+01
C1W 1C1X 1          2 .5000E+01 .5000E+01 .1000E+01-.2618E-01
C1X 1C1Y 1          2 .5000E+01 .5000E+01 .1000E+01-.2618E-01
C1X 1C2X 1          3 .5000E+00 .5000E+00 .1000E+02 .9997E+00

iNCON---1---*---2---*---3---*---4---*---5---*---6---*---7---*---8

GENER---1---*---2---*---3---*---4---*---5---*---6---*---7---*---8

ENDCY---1---*---2---*---3---*---4---*---5---*---6---*---7---*---8

```

Figure 33. TOUGH2/ECO2M input file for a problem of CO<sub>2</sub> plume migration in a sloping aquifer that is intersected by a vertical fault.

### 6.4.1 Results

A detailed discussion of the plume migration problem without a leaky fault present and simulated with TOUGH2/ECO2N is available in a laboratory report (Pruess, 2009) and in a journal publication (Pruess and Nordbotten, 2011). Here we primarily highlight features of the TOUGH2/ECO2M simulation that pertain to the role of the leaky fault. Fig. 34 shows part of the printed output generated at the beginning of the run for only those grid blocks that are subjected to semi-analytical heat exchange; i.e., having a non-zero heat transfer area AHT in the ELEME data. The list includes all the blocks in the fault ([A12 2] through [E1H 2]), but only the top and bottom layer blocks in the aquifer portion of the grid. Fig. 35 shows selected printed output from the flow simulation, including (1) the beginning of the iteration sequence, (2) time step 855 when a CO<sub>2</sub>-rich (liquid) phase first enters the bottommost grid block [E1H 2] of the fault (at  $t = 5.88606 \times 10^9$  s = 186.5 yr), and (3) part of the output at the end of the run (2000 time steps, simulation time of  $t = 7.07838 \times 10^9$  s = 224.3 yr). It is seen that at this time the top part of the fault is in two-phase aqueous-gas conditions ( $I = 5$ ), the bottom part is at supercritical pressures ( $P_{\text{crit}} = 73.82$  bar) in two-phase aqueous-liquid conditions ( $I = 4$ ), and in between there are a few grid blocks in three-phase conditions ( $I = 7$ ).

```

PARAMETERS AT FIRST CALL TO QLOSS ( 1, 1)-TIME STEPS
THE TIME IS 0.000000E+00 DAYS
*****
TOTAL TIME   KCYC   ITER   ITCR   KON      DX1M      DX2M      DX3M      MAX. RES.   NER   KER   DELTEX
0.000000E+00 1       1       1       1       0.000000E+00 0.000000E+00 0.000000E+00 0.000000E+00 0 0 0.100000E+04
*****

ELEM  INDEX  I   P      XSM      X3      X4      TX      T00      AI(N)      PERRED
A12 2    1 1 0.307398E+06 0.125586E-09 0.125586E-11 0.106224E+02 10.6224 10.6224 0.000000E+00 0.100000E+01
A13 2    2 1 0.405479E+06 0.115553E-10 0.115552E-12 0.109224E+02 10.9224 10.9224 0.000000E+00 0.100000E+01
A14 2    3 1 0.503559E+06 0.946147E-12 0.946147E-14 0.112224E+02 11.2224 11.2224 0.000000E+00 0.100000E+01
A15 2    4 1 0.601640E+06 0.700643E-13 0.700646E-15 0.115223E+02 11.5223 11.5223 0.000000E+00 0.100000E+01
A16 2    5 1 0.699722E+06 0.271391E-14 0.271407E-16 0.118223E+02 11.8223 11.8223 0.000000E+00 0.100000E+01
A17 2    6 1 0.797803E+06 0.274902E-17 0.275425E-19 0.121223E+02 12.1223 12.1223 0.000000E+00 0.100000E+01
A18 2    7 1 0.895884E+06 0.250894E-22 0.250822E-24 0.124223E+02 12.4223 12.4223 0.000000E+00 0.100000E+01
...
E1E 2   153 1 0.151705E+08 0.532530E-19 0.532531E-21 0.562186E+02 56.2186 56.2186 0.000000E+00 0.100000E+01
E1F 2   154 1 0.152677E+08 0.596463E-17 0.596463E-19 0.565186E+02 56.5186 56.5186 0.000000E+00 0.100000E+01
E1G 2   155 1 0.153649E+08 0.983517E-15 0.983517E-17 0.568185E+02 56.8185 56.8185 0.000000E+00 0.100000E+01
E1H 2   156 1 0.154378E+08 0.443698E-12 0.443698E-14 0.570435E+02 57.0435 57.0435 0.000000E+00 0.100000E+01
A11 1   157 1 0.279604E+08 0.100000E-08 0.100000E-10 0.960063E+02 96.0063 96.0063 0.000000E+00 0.100000E+01
BF1 1   206 1 0.298148E+08 0.100000E-08 0.100000E-10 0.101839E+03 101.8393 101.8393 0.000000E+00 0.100000E+01
A12 1   207 1 0.277103E+08 0.100000E-08 0.100000E-10 0.952210E+02 95.2210 95.2210 0.000000E+00 0.100000E+01
BF2 1   256 1 0.295655E+08 0.100000E-08 0.100000E-10 0.101054E+03 101.0540 101.0540 0.000000E+00 0.100000E+01
A13 1   257 1 0.274601E+08 0.100000E-08 0.100000E-10 0.944357E+02 94.4357 94.4357 0.000000E+00 0.100000E+01
BF3 1   306 1 0.293160E+08 0.100000E-08 0.100000E-10 0.100269E+03 100.2687 100.2687 0.000000E+00 0.100000E+01
...
I13 1   7257 1 0.100751E+07 0.100000E-08 0.100000E-10 0.127636E+02 12.7636 12.7636 0.000000E+00 0.100000E+01
JF3 1   7306 1 0.291445E+07 0.100000E-08 0.100000E-10 0.185966E+02 18.5966 18.5966 0.000000E+00 0.100000E+01
I14 1   7307 1 0.750734E+06 0.100000E-08 0.100000E-10 0.119783E+02 11.9783 11.9783 0.000000E+00 0.100000E+01
JF4 1   7356 1 0.265773E+07 0.100000E-08 0.100000E-10 0.178113E+02 17.8113 17.8113 0.000000E+00 0.100000E+01
I15 1   7357 1 0.493957E+06 0.100000E-08 0.100000E-10 0.111930E+02 11.1930 11.1930 0.000000E+00 0.100000E+01
JF5 1   7406 1 0.240099E+07 0.100000E-08 0.100000E-10 0.170260E+02 17.0260 17.0260 0.000000E+00 0.100000E+01
JF6 1   7455 1 0.214424E+07 0.100000E-08 0.100000E-10 0.162406E+02 16.2406 16.2406 0.000000E+00 0.100000E+01

```

Figure 34. Part of printout of primary variables at beginning of run, for those grid blocks that are subject to semi-analytical heat exchange. T00 is the initial temperature of the conductive domains.

```

...ITERATING... AT [ 1, 1] --- DELTEX = 0.100000E+04 MAX. RES. = 0.249777E+00 AT ELEMENT A1F 1 EQUATION 3
...ITERATING... AT [ 1, 2] --- DELTEX = 0.100000E+04 MAX. RES. = 0.567619E-03 AT ELEMENT A15 1 EQUATION 3
A15 1( 1, 3) ST = 0.100000E+04 DT = 0.100000E+04 DX1= 0.269188E+03 DX2= -.293902E-16 T = 92.865 P = 26959612. S = 0.100000E+01
...ITERATING... AT [ 2, 1] --- DELTEX = 0.900000E+04 MAX. RES. = 0.357556E-01 AT ELEMENT A1E 1 EQUATION 3
...ITERATING... AT [ 2, 2] --- DELTEX = 0.900000E+04 MAX. RES. = 0.472905E-02 AT ELEMENT A05 1 EQUATION 3
...ITERATING... AT [ 2, 3] --- DELTEX = 0.900000E+04 MAX. RES. = 0.162493E-04 AT ELEMENT A05 1 EQUATION 4
A05 1( 2, 4) ST = 0.100000E+05 DT = 0.900000E+04 DX1= 0.361961E+04 DX2= -.245605E-15 T = 94.065 P = 27345559. S = 0.100000E+01
...ITERATING... AT [ 3, 1] --- DELTEX = 0.900000E+05 MAX. RES. = 0.194583E+00 AT ELEMENT A1G 1 EQUATION 3
...ITERATING... AT [ 3, 2] --- DELTEX = 0.900000E+05 MAX. RES. = 0.274123E-02 AT ELEMENT B6G 1 EQUATION 3
...ITERATING... AT [ 3, 3] --- DELTEX = 0.900000E+05 MAX. RES. = 0.102574E-04 AT ELEMENT B6G 1 EQUATION 4
A7G 1( 3, 4) ST = 0.100000E+06 DT = 0.900000E+05 DX1= 0.657998E+05 DX2= -.703333E-14 T = 84.412 P = 24350180. S = 0.100000E+01
...
E1H 2( 854, 9) ST = 0.588494E+10 DT = 0.112500E+07 DX1= -.927963E+03 DX2= -.665742E-13 T = 58.176 P = 15504472. S = 0.100000E+01
...ITERATING... AT [ 855, 1] --- DELTEX = 0.112500E+07 MAX. RES. = 0.856031E+00 AT ELEMENT E1H 2 EQUATION 3
...ITERATING... AT [ 855, 2] --- DELTEX = 0.112500E+07 MAX. RES. = 0.471307E+00 AT ELEMENT E1H 2 EQUATION 3
...ITERATING... AT [ 855, 3] --- DELTEX = 0.112500E+07 MAX. RES. = 0.463046E-02 AT ELEMENT E1H 2 EQUATION 3
E1H 2( 855, 4) ST = 0.588606E+10 DT = 0.112500E+07 DX1= 0.179457E+03 DX2= -.890390E-13 T = 58.396 P = 15504652. S = 0.986880E+00
...ITERATING... AT [ 856, 1] --- DELTEX = 0.225000E+07 MAX. RES. = 0.117474E+01 AT ELEMENT E1H 2 EQUATION 3
...ITERATING... AT [ 856, 2] --- DELTEX = 0.225000E+07 MAX. RES. = 0.369871E+02 AT ELEMENT E1G 2 EQUATION 3
...ITERATING... AT [ 856, 3] --- DELTEX = 0.225000E+07 MAX. RES. = 0.995087E+01 AT ELEMENT E1G 2 EQUATION 3
...ITERATING... AT [ 856, 4] --- DELTEX = 0.225000E+07 MAX. RES. = 0.200463E+01 AT ELEMENT E1G 2 EQUATION 3
...ITERATING... AT [ 856, 5] --- DELTEX = 0.225000E+07 MAX. RES. = 0.169750E+00 AT ELEMENT E1G 2 EQUATION 3
...ITERATING... AT [ 856, 6] --- DELTEX = 0.225000E+07 MAX. RES. = 0.162361E-02 AT ELEMENT E1G 2 EQUATION 3
E1G 2( 856, 7) ST = 0.588831E+10 DT = 0.225000E+07 DX1= 0.211036E+03 DX2= -.749364E-13 T = 57.838 P = 15431368. S = 0.100000E+01
...
OUTPUT DATA AFTER (2000, 7)-2-TIME STEPS THE TIME IS 0.819256E+05 DAYS
#####
TOTAL TIME KCYC ITER ITERC KON DX1M DX2M DX3M MAX. RES. NER KER DELTEX
0.707838E+10 2000 7 13000 2 0.20654E+05 0.35454E-11 0.27208E-01 0.76931E-05 74 3 0.11250E+07
#####
ELEM INDEX I P T SAQ SLIQ SGAS XCO2AQ DLIQ VISLIQ DGAS VISGAS
(PA) (DEG.C) (KG/M3) (PA-S) (KG/M3) (PA-S)
A12 2 1 5 0.305575E+06 10.2779 0.664561E+00 0.000000E+00 0.335439E+00 0.635468E-02 0.00 0.100000E+01 5.86 0.142855E-04
A13 2 2 5 0.385981E+06 10.2996 0.670722E+00 0.000000E+00 0.329278E+00 0.795447E-02 0.00 0.100000E+01 7.42 0.142997E-04
A14 2 3 5 0.467046E+06 10.5588 0.690845E+00 0.000000E+00 0.309155E+00 0.946704E-02 0.00 0.100000E+01 8.98 0.143257E-04
A15 2 4 5 0.550546E+06 10.9051 0.709655E+00 0.000000E+00 0.290345E+00 0.109924E-01 0.00 0.100000E+01 10.64 0.143579E-04
A16 2 5 5 0.636102E+06 11.2701 0.725166E+00 0.000000E+00 0.274834E+00 0.125148E-01 0.00 0.100000E+01 12.36 0.143923E-04
A17 2 6 5 0.723217E+06 11.6270 0.737815E+00 0.000000E+00 0.262185E+00 0.139982E-01 0.00 0.100000E+01 14.11 0.144265E-04
A18 2 7 5 0.811523E+06 11.9680 0.748364E+00 0.000000E+00 0.251636E+00 0.154405E-01 0.00 0.100000E+01 15.88 0.144602E-04
A19 2 8 5 0.900771E+06 12.2964 0.757349E+00 0.000000E+00 0.242651E+00 0.168393E-01 0.00 0.100000E+01 17.66 0.144934E-04
...
B1V 2 65 5 0.638489E+07 25.4581 0.878780E+00 0.000000E+00 0.121220E+00 0.574588E-01 0.00 0.100000E+01 233.14 0.201772E-04
B1W 2 66 5 0.648410E+07 26.0198 0.878632E+00 0.000000E+00 0.121368E+00 0.572006E-01 0.00 0.100000E+01 241.31 0.205093E-04
B1X 2 67 5 0.658304E+07 26.3099 0.878560E+00 0.000000E+00 0.121440E+00 0.571805E-01 0.00 0.100000E+01 255.50 0.210817E-04
B1Y 2 68 7 0.668162E+07 26.6065 0.777723E+00 0.165619E+00 0.566574E-01 0.564865E-01 685.05 0.545599E-04 269.54 0.216491E-04
B1Z 2 69 7 0.677859E+07 27.2390 0.779327E+00 0.176978E+00 0.436951E-01 0.560034E-01 673.78 0.531312E-04 280.61 0.221531E-04
C11 2 70 4 0.687553E+07 27.8339 0.832712E+00 0.167288E+00 0.000000E+00 0.555261E-01 661.53 0.516768E-04 0.00 0.100000E+01
C12 2 71 4 0.697321E+07 28.4026 0.836880E+00 0.163120E+00 0.000000E+00 0.551067E-01 650.26 0.503456E-04 0.00 0.100000E+01
C13 2 72 7 0.707111E+07 29.0937 0.816726E+00 0.163678E+00 0.195960E-01 0.545387E-01 631.31 0.481728E-04 325.57 0.243386E-04
C14 2 73 7 0.716784E+07 29.6832 0.836598E+00 0.157994E+00 0.540836E-02 0.536967E-01 581.85 0.433349E-04 368.71 0.267197E-04
C15 2 74 4 0.726454E+07 30.2431 0.849904E+00 0.150096E+00 0.000000E+00 0.533015E-01 535.53 0.388196E-04 0.00 0.100000E+01
C16 2 75 4 0.736144E+07 30.6906 0.855386E+00 0.144614E+00 0.000000E+00 0.531665E-01 501.20 0.355344E-04 0.00 0.100000E+01
C17 2 76 4 0.745843E+07 31.2485 0.856379E+00 0.143621E+00 0.000000E+00 0.530221E-01 500.17 0.361034E-04 0.00 0.100000E+01
C18 2 77 4 0.755544E+07 31.7821 0.854566E+00 0.145434E+00 0.000000E+00 0.528446E-01 502.92 0.377523E-04 0.00 0.100000E+01
C19 2 78 4 0.765245E+07 32.1218 0.854032E+00 0.145968E+00 0.000000E+00 0.527138E-01 503.32 0.380892E-04 0.00 0.100000E+01
...

```

Figure 35. Part of printed output for CO<sub>2</sub> plume migration and leakage problem.

Results presented in Figs. 36-38 include data from several continuation runs, which after a total of 10,000 time steps reach a simulation time of  $t = 9.86057 \times 10^9$  s (312.5 yr). We note that time steps are limited by the highly dynamic processes in the fault. Prior to CO<sub>2</sub> reaching the fault, a total of 855 time steps achieve a simulation time of 186.5 yr, while this time less than doubles during the next 9,145 time steps. Water flux at the bottom of the fault is small and positive (= upward) at early times, turning negative (downward) after CO<sub>2</sub> enters the fault at  $t = 186.5$  yr (Figs. 36, 37). The onset of CO<sub>2</sub> discharge at the top of the fault at  $t = 6.22585 \times 10^9$  s = 197.3 yr is preceded by a large “burp” of water outflow, in response to the strong volume expansion of CO<sub>2</sub> approaching the land surface. Water and CO<sub>2</sub> fluxes subsequently go through

cyclic variations, reflecting the interplay of processes on three different time scales, (1) multiphase flow in the fault, (2) heat exchange with the fault walls, and (3) coupling between fluid pressures and CO<sub>2</sub> upflow rates at the bottom of the fault. Up until the time when the CO<sub>2</sub> plume reaches the fault, its advancement is virtually identical to a case without a leaky fault, that had been simulated previously using TOUGH2/ECO2N (Pruess, 2009; Fig. 38). After the CO<sub>2</sub> plume reaches the fault its further advancement stalls for a while, but then resumes at an essentially unchanged rate. This behavior can be understood in terms of the variable plume thickness, see Fig. 39. The tip of the plume is very thin, and total CO<sub>2</sub> flow rate is small near the plume tip, allowing all of the advancing CO<sub>2</sub> to be leaked off when the plume first reaches the fault. At later time thicker portions of the plume approach the fault, total CO<sub>2</sub> flow rate increases, and only a fraction of the CO<sub>2</sub> plume can be captured by the fault. The CO<sub>2</sub> bypassing the fault then resumes its updip migration at the same speed as before the fault intercepted the plume. Fig. 38 also shows that CO<sub>2</sub> loss up the fault is substantial, amounting to almost 7 % of original CO<sub>2</sub> inventory over a 100-year period of fault leakage.

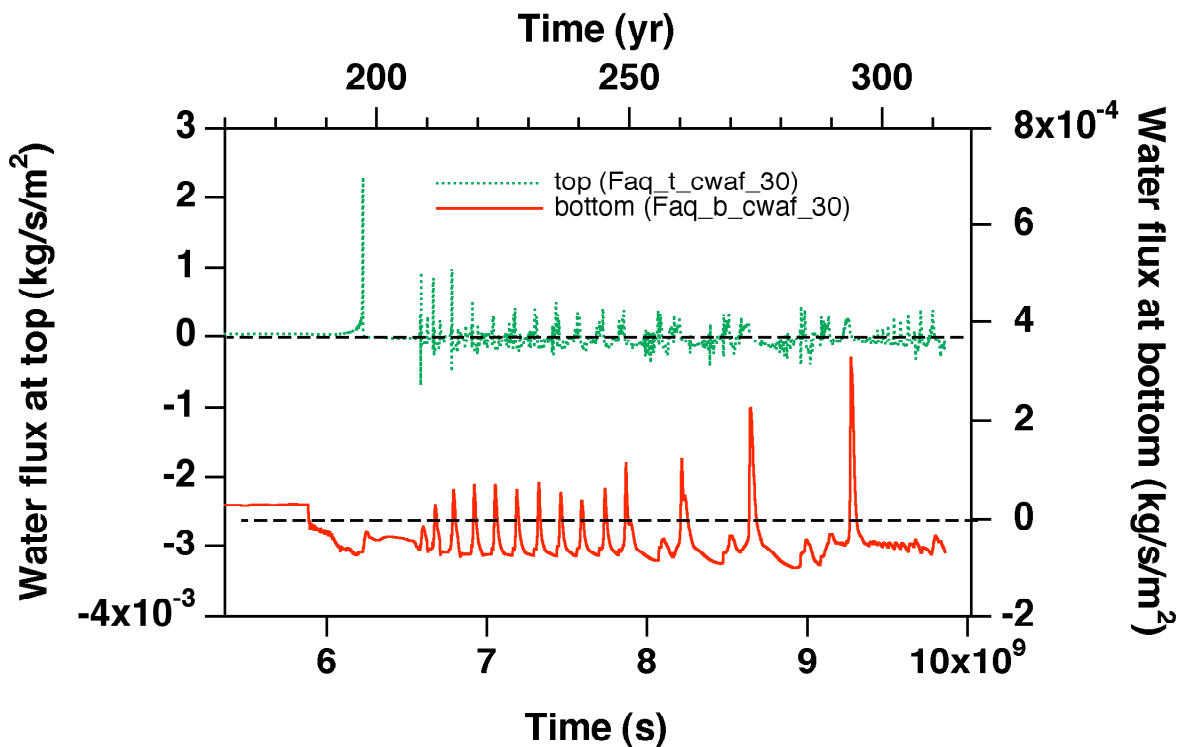


Figure 36. Water fluxes at the top and bottom of the fault.

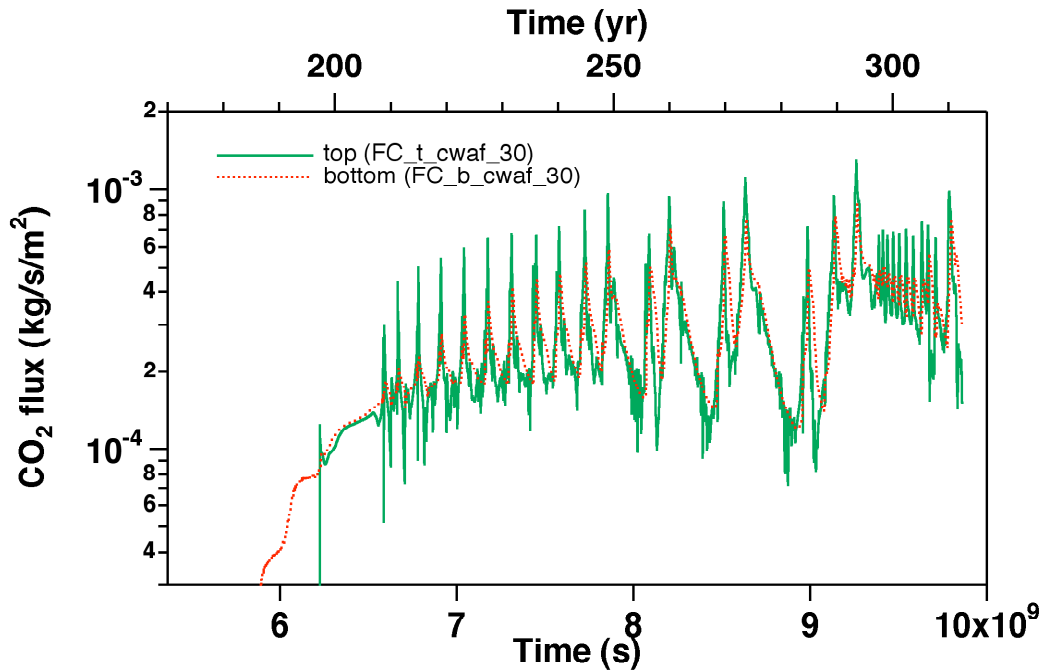


Figure 37. CO<sub>2</sub> fluxes at the top and bottom of the fault.

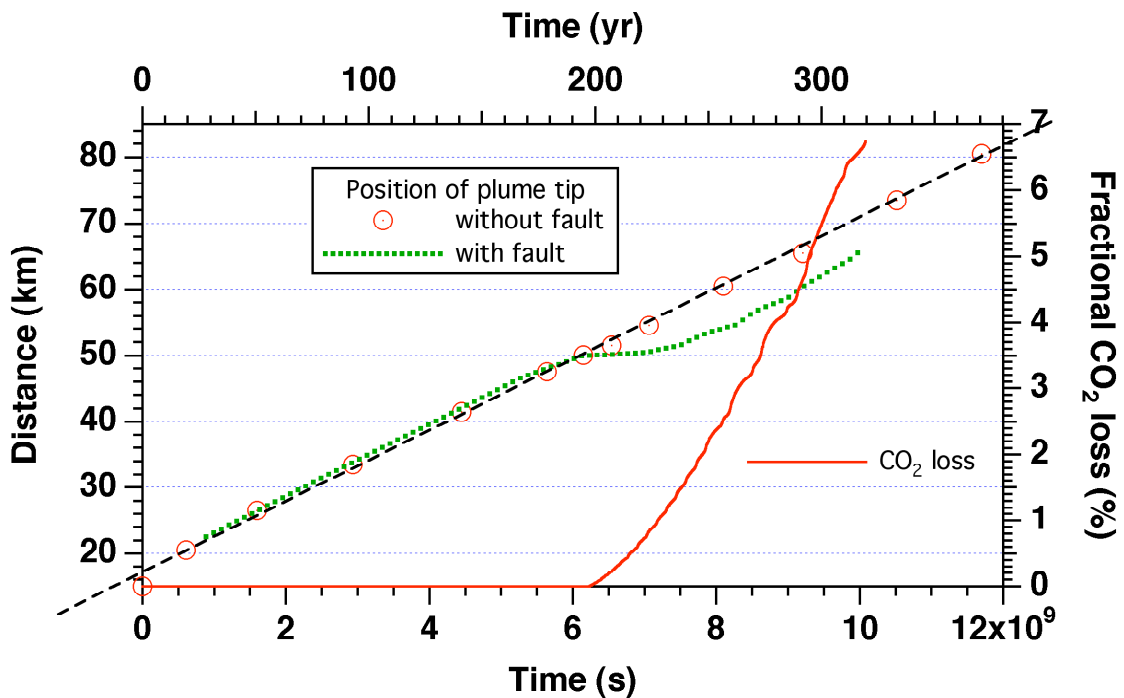


Figure 38. Advancement of the plume over time. The data for the case without a fault are from a TOUGH2/ECO2N simulation (Pruess, 2009), and the dashed straight line is an eye-fit to these data. CO<sub>2</sub> loss by leakage up the fault as fraction of initial inventory is also shown.

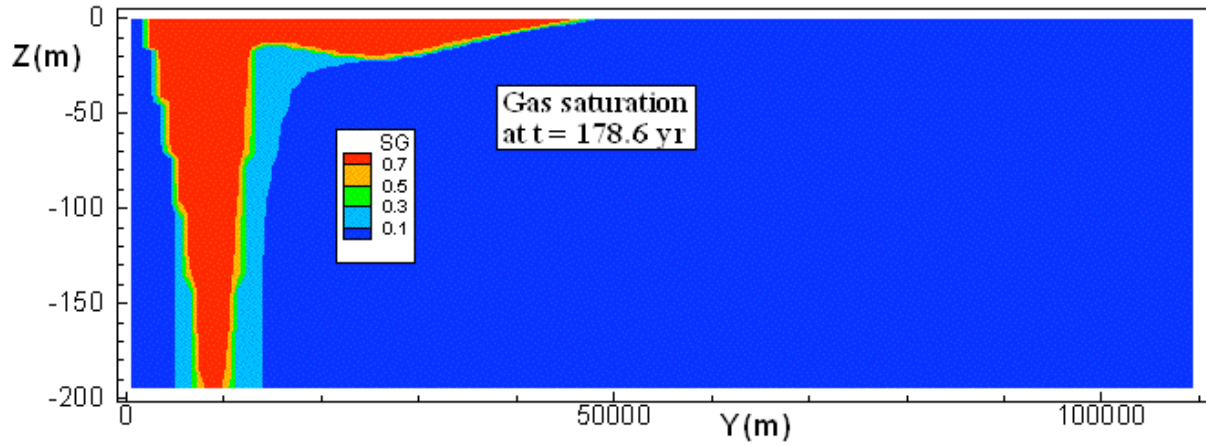


Figure 39. CO<sub>2</sub> plume at t = 178.6 yr, for a case without a leaky fault present, simulated with TOUGH2/ECO2N. (ECO2N does not distinguish between liquid and gaseous CO<sub>2</sub>-rich phases, and denotes the single CO<sub>2</sub>-rich phase modeled as “gas.” In ECO2M terminology, this is actually a “liquid CO<sub>2</sub>” phase.)



## 7. Concluding Remarks

We have extended a previously developed fluid property module “ECO2N” (Pruess and Spycher, 2007) to include all possible phase compositions of brine-CO<sub>2</sub> mixtures, including three-phase conditions of aqueous, liquid and gaseous CO<sub>2</sub> phases. Solid NaCl (halite) is included as a fourth active phase that may precipitate and dissolve in response to changes in aqueous NaCl concentrations. The new “ECO2M” fluid property module retains the original ECO2N-formulation for the compositions and properties of the aqueous and CO<sub>2</sub>-rich phases, and allows a seamless description of CO<sub>2</sub> storage and leakage systems for super- and sub-critical conditions in the temperature range  $10\text{ }^{\circ}\text{C} \leq T \leq 110\text{ }^{\circ}\text{C}$ , pressures up to 600 bar, and dissolved NaCl with salinity up to full halite saturation.

Leakage scenarios with CO<sub>2</sub> migrating from a deep storage reservoir to the land surface, either through direct preferential pathways or through secondary accumulations formed along the leakage path, give rise to a complex interplay of multiphase fluid flow and heat transfer. CO<sub>2</sub> rising towards the land surface may evolve into two-phase mixtures of liquid and gaseous CO<sub>2</sub> as temperatures and pressures decrease, inducing three-phase flow of CO<sub>2</sub>-brine mixtures, with strong cooling effects as liquid CO<sub>2</sub> boils into gas, and as gaseous CO<sub>2</sub> expands (Joule-Thomson effect; Katz and Lee, 1990). The ECO2M fluid property module for TOUGH2 was designed to model the entire range of fluid conditions in CO<sub>2</sub> storage and leakage systems, from CO<sub>2</sub> displacing brine in the deep storage reservoir, to upflowing CO<sub>2</sub> transitioning to sub-critical conditions and inducing three-phase flow of brine - liquid CO<sub>2</sub> - gaseous CO<sub>2</sub>, with strong coupling between fluid and heat flow.

ECO2M is a successor to and upward compatible with ECO2N, and can execute ECO2N input files with minimal modification (increasing the phase counter NPH in data block MULTI from 3 to 4). This report is intended as a reference to the physical and mathematical models used in ECO2M, and includes detailed instructions for preparing input data. A set of sample problems illustrates the use of the code, and provides templates for developing new applications.

Applications of TOUGH2/ECO2M to idealized CO<sub>2</sub> leakage scenarios demonstrate strong cooling effects from liquid CO<sub>2</sub> boiling into gas, and from Joule-Thomson cooling of

upflowing and expanding gas. The emergence of three-phase conditions (aqueous - liquid CO<sub>2</sub> - gaseous CO<sub>2</sub>) leads to low mobilities for all phases and acts to reduce CO<sub>2</sub> discharge rates. Coupling between multiphase flow and heat transfer on different time scales gives rise to non-linear feedbacks and a tendency towards cyclic variations of fluid discharges. For leakage scenarios, strong and highly non-linear feedbacks between fluid flow and heat transfer appear to be the norm rather than the exception. The interplay between fluid pressures and temperatures tends to push conditions towards the CO<sub>2</sub> saturation line, and towards the critical point at  $T_{\text{crit}} = 31.04$  °C,  $P_{\text{crit}} = 73.82$  bar. ECO2M has specific coding to cope with these processes, such as employing “finite windows” for phase transitions.

### **Acknowledgement**

Thanks are due to Curt Oldenburg, Tianfu Xu and Jacob Gudbjerg for reviewing the manuscript, testing the TOUGH2/ECO2M code, and suggesting improvements. This work was supported by the Director, Office of Science, Office of Basic Energy Sciences of the U.S. Department of Energy, and by the Assistant Secretary for Fossil Energy, Office of Coal and Power R&D, through the National Energy Technology Laboratory under Contract No. DE-AC02-05CH11231 with the U.S. Department of Energy.

## References

- Altunin, V.V. *Thermophysical Properties of Carbon Dioxide*, Publishing House of Standards, 551 pp., Moscow, 1975 (in Russian).
- Andersen, G., A. Probst, L. Murray and S. Butler. An Accurate PVT Model for Geothermal Fluids as Represented by H<sub>2</sub>O-NaCl-CO<sub>2</sub> Mixtures, *Proceedings 17th Workshop on Geothermal Reservoir Engineering*, pp. 239 - 248, Stanford, CA, 1992.
- Battistelli, A., C. Calore and K. Pruess. The Simulator TOUGH2/EWASG for Modeling Geothermal Reservoirs with Brines and Non-Condensable Gas, *Geothermics*, Vol. 26, No. 4, pp. 437 - 464, 1997.
- Chou, I.M. Phase Relations in the System NaCl-KCl-H<sub>2</sub>O: III: Solubilities of Halite in Vapor-Saturated Liquids Above 445 °C and Redetermination of Phase Equilibrium Properties in the System NaCl-H<sub>2</sub>O, *Geochim. Cosmochim. Acta*, Vol. 51, pp. 1965-1975, 1987.
- Corey, A.T. The Interrelation Between Gas and Oil Relative Permeabilities, *Producers Monthly*, pp. 38 - 41, November 1954.
- Evans, R.D. *The Atomic Nucleus*, Reprint Edition, Robert E. Krieger Publ. Co., Malabar, FL, 1982.
- García, J.E. Density of Aqueous Solutions of CO<sub>2</sub>, Lawrence Berkeley National Laboratory Report LBNL-49023, Berkeley, CA, 2001.
- García, J.E. *Fluid Dynamics of Carbon Dioxide Disposal into Saline Aquifers*, PhD Thesis, University of California at Berkeley, December 2003.
- Haas, J.L. Jr. Physical Properties of the Coexisting Phases and Thermochemical Properties of the H<sub>2</sub>O Component in Boiling NaCl solutions, *USGS Bulletin 1421-A*, Washington, DC, 73 pp., 1976.
- Hesse, M.A., F.M. Orr, Jr., and H.A. Tchelepi. Gravity Currents with Residual Trapping, *J. Fluid Mech.*, Vol. 611, pp. 35-60, 2008.
- Himmelblau, D.M. Partial Molal Heats and Entropies of Solution for Gases Dissolved in Water from the Freezing to the Near Critical Point, *J. of Phys. Chem.*, Vol. 63, pp. 1803-1808, 1959.
- International Formulation Committee. *A Formulation of the Thermodynamic Properties of Ordinary Water Substance*, IFC Secretariat, Düsseldorf, Germany, 1967.
- Katz, D.L. and R.L. Lee. *Natural Gas Engineering*, McGraw-Hill Publ. Comp., New York, NY 1990.

- Lorenz, S., D. Maric and C. Rirschl. Eine analytische Funktion zur Bestimmung der Enthalpie wässriger NaCl Lösungen, draft report, Institut für Sicherheitstechnologie, Köln, Germany, April 2000.
- Michaelides, E.E. Thermodynamic Properties of Geothermal Fluids, *Geothermal Resources Council Transactions*, Vol. 5, pp. 361 - 364, 1981.
- Miller, A.B. A Brine-Steam Properties Computer Program for Geothermal Energy Calculations, Lawrence Livermore National Laboratory Report UCRL-52495, Livermore, CA, June 1978.
- Nicot, J.-P. Evaluation of Large-Scale CO<sub>2</sub> Storage on Fresh-Water Sections of Aquifers: An Example from the Texas Gulf Coast Basin, *Int. J. Greenhouse Gas Control*, Vol. 2, Issue 4, pp. 583–593, 2008.
- Oldenburg, C.M. Joule-Thomson cooling due to CO<sub>2</sub> injection into natural gas reservoirs, *Energy Conversion and Management*, 48, 1808-1815, 2007.
- Phillips, S.L., A. Igbene, J.A. Fair, H. Ozbek and M. Tavana. A Technical Databook for Geothermal Energy Utilization, Lawrence Berkeley National Laboratory Report LBL-12810, Berkeley, CA, 46 pp., 1981.
- Parker, J.C., R.J. Lenhard and T. Kuppusamy. A Parametric Model for Constitutive Properties Governing Multiphase Flow in Porous Media, *Water Resour. Res.*, Vol. 23, No. 4, pp. 618 - 624, 1987.
- Pruess, K. The TOUGH Codes—A Family of Simulation Tools for Multiphase Flow and Transport Processes in Permeable Media, *Vadose Zone J.*, Vol. 3, pp. 738 - 746, 2004.
- Pruess, K. Numerical Simulation of CO<sub>2</sub> Leakage from a Geologic Disposal Reservoir, Including Transitions from Super- to Sub-Critical Conditions, and Boiling of Liquid CO<sub>2</sub>, *Soc. Pet. Eng. J.*, pp. 237 - 248, June 2004.
- Pruess, K. ECO2N: A TOUGH2 Fluid Property Module for Mixtures of Water, NaCl, and CO<sub>2</sub>, Lawrence Berkeley National Laboratory Report LBNL-57952, Berkeley, CA, June 2005.
- Pruess, K. Numerical Simulations Show Potential for Strong Non-isothermal Effects During Fluid Leakage from a Geologic Disposal Reservoir for CO<sub>2</sub>, B. Faybishenko, P.A. Witherspoon and J. Gale (eds.), *Dynamics of Fluids and Transport in Fractured Rock*, Geophysical Monograph 162, pp. 81–89, American Geophysical Union, Washington, DC, 2005a.
- Pruess, K. Numerical Studies of Fluid Leakage from a Geologic Disposal Reservoir for CO<sub>2</sub> Show Self-Limiting Feedback between Fluid Flow and Heat Transfer, *Geophys. Res. Lett.*, Vol. 32, No. 14, L14404, doi:10.1029/2005GL023250, July 2005b.

- Pruess, K. On CO<sub>2</sub> Fluid Flow and Heat Transfer Behavior in the Subsurface, Following Leakage from a Geologic Storage Reservoir, *Env. Geol.*, Vol. 54, No. 8, pp. 1677–1686, DOI 10.1007/s00254-007-0945-x, June 2008.
- Pruess, K. Numerical Simulation Experiments on the Long-term Evolution of a CO<sub>2</sub> Plume Under a Sloping Caprock, Lawrence Berkeley National Laboratory Report LBNL-2542E, September 2009.
- Pruess, K., C. Oldenburg and G. Moridis. TOUGH2 User's Guide, Version 2.0, Lawrence Berkeley National Laboratory Report LBNL-43134, Berkeley, CA, November 1999.
- Pruess, K. and J. García. Multiphase Flow Dynamics During CO<sub>2</sub> Injection into Saline Aquifers, *Environmental Geology*, Vol. 42, pp. 282 - 295, 2002.
- Pruess, K. and A. Battistelli. TMVOC, A Numerical Simulator for Three-Phase Non-Isothermal Flows of Multicomponent Hydrocarbon Mixtures in Saturated-Unsaturated Heterogeneous Media, Lawrence Berkeley National Laboratory Report LBNL-49375, Berkeley, CA 94720, April 2002.
- Pruess, K., J. García, T. Kavscek, C. Oldenburg, J. Rutqvist, C. Steefel and T. Xu. Intercomparison of Numerical Simulation Codes for Geologic Disposal of CO<sub>2</sub>, Lawrence Berkeley National Laboratory Report LBNL-51813, Berkeley, CA 94720, December 2002.
- Pruess, K., J. García, T. Kavscek, C. Oldenburg, J. Rutqvist, C. Steefel and T. Xu. Code Intercomparison Builds Confidence in Numerical Simulation Models for Geologic Disposal of CO<sub>2</sub>, *Energy*, Vol. 29, Issues 9-10, pp. 1431-1444, doi:10.1016/j.energy.2004.03.077, July-August 2004.
- Pruess K. and N. Spycher. ECO2N – A Fluid Property Module for the TOUGH2 Code for Studies of CO<sub>2</sub> Storage in Saline Aquifers, *Energy Conversion and Management*, Vol. 48, No. 6, pp. 1761–1767, doi:10.1016/j.enconman.2007.01.016, 2007.
- Pruess, K. and J. Nordbotten. Numerical Simulation Studies of the Long-term Evolution of a CO<sub>2</sub> Plume in a Saline Aquifer with a Sloping Caprock, *Transport in Porous Media*, DOI: 10.1007/s11242-011-9729-6, 2011.
- Span, R. and W. Wagner. A New Equation of State for Carbon Dioxide Covering the Fluid Region from the Triple-Point Temperature to 1100 K at Pressures up to 800 MPa, *J. Phys. Chem. Ref. Data*, Vol. 25, No. 6, pp. 1509 - 1596, 1996.
- Spycher, N. and K. Pruess. CO<sub>2</sub>-H<sub>2</sub>O Mixtures in the Geological Sequestration of CO<sub>2</sub>. II. Partitioning in Chloride Brines at 12–100 °C and up to 600 bar, *Geochim. Cosmochim. Acta*, Vol. 69, No. 13, pp. 3309–3320, doi:10.1016/j.gca.2005.01.015, 2005.
- Stone, H.L. Probability Model for Estimating Three-Phase Relative Permeability, *Trans. SPE of AIME*, 249, 214-218, 1970.
- van Genuchten, M.Th. A Closed-Form Equation for Predicting the Hydraulic Conductivity of

Unsaturated Soils, *Soil Sci. Soc. Am. J.*, Vol. 44, pp. 892 - 898, 1980.

Vargaftik, N.B. *Tables on the Thermophysical Properties of Liquids and Gases*, 2nd Ed., John Wiley & Sons, New York, NY, 1975.

Verma, A. and K. Pruess. Thermohydrologic Conditions and Silica Redistribution Near High-Level Nuclear Wastes Emplaced in Saturated Geological Formations, *Journal of Geophysical Res.*, Vol. 93 (B2), pp. 1159-1173, 1988.

Vinsome, P.K.W. and J. Westerveld. A Simple Method for Predicting Cap and Base Rock Heat Losses in Thermal Reservoir Simulators, *J. Canadian Pet. Tech.*, 19 (3), 87-90, July-September 1980.

## Appendix A. Relative Permeability Functions

Several relative permeability functions are provided in ECO2M for problems involving three-phase flow of aqueous, liquid CO<sub>2</sub> and gaseous CO<sub>2</sub> phases. For indices IRP = 1, 2, 3, 4, 7 and 8, the original TOUGH2 two-phase functions have been retained (see Pruess et al., 1999). This is only applicable to domains in which an aqueous phase and just a single CO<sub>2</sub>-rich phase may be present. An example is provided in sample problem 4, migration of a CO<sub>2</sub> plume in a sloping aquifer (Sec. 6.4). For the duration of the simulation, the CO<sub>2</sub> plume is confined in the aquifer to depths where pressures remain supercritical; so there is only a single CO<sub>2</sub>-rich phase present in the aquifer, and the two-phase van Genuchten (1980) and Corey (1954) relative permeabilities are used in the aquifer sub-domain. However, in the attached fault zone three-phase conditions evolve, and three-phase relative permeabilities must be used in the fault sub-domain. If one of the TOUGH2 two-phase functions is chosen, the relative permeability of the CO<sub>2</sub>-rich phase will be the same function of saturation, regardless whether the CO<sub>2</sub>-rich phase is liquid or gas. The notation used below is:  $k_{ra}$  - aqueous phase relative permeability;  $k_{rl}$  - liquid phase relative permeability;  $k_{rg}$  - gas phase relative permeability.  $S_a$ ,  $S_l$ , and  $S_g = 1 - S_a - S_l - S_s$  are the saturations of aqueous, liquid and gas phases, respectively, with  $S_s$  the saturation of solid salt.

IRP = 5      "All perfectly mobile"

$$k_{rg} = 1$$

$$k_{rw} = 1$$

$$k_{rn} = 1$$

no parameters.

IRP = 6      Modified version of Stone's first three-phase method (Stone, 1970).

$$k_{rg} = \left[ \frac{S_g - S_{gr}}{1 - S_{ar}} \right]^n$$

$$k_{ra} = \left[ \frac{S_a - S_{ar}}{1 - S_{ar}} \right]^n$$

$$k_{rl} = \left[ \frac{1 - S_g - S_a - S_{lr}}{1 - S_g - S_{ar} - S_{lr}} \right] \left[ \frac{1 - S_{ar} - S_{lr}}{1 - S_a - S_{lr}} \right] \left[ \frac{(1 - S_g - S_{ar} - S_{lr})(1 - S_a)}{(1 - S_{ar})} \right]^n$$

When  $S_l = 1 - S_a - S_g - S_s$  is near irreducible liquid saturation,  $S_{lr} \leq S_l \leq S_{lr} + .005$ , liquid relative permeability is taken to be

$$k'_{rl} = k_{rl} \cdot \frac{S_l - S_{lr}}{.005}$$

Parameters are  $S_{ar} = \text{RP}(1)$ ,  $S_{lr} = \text{RP}(2)$ ,  $S_{gr} = \text{RP}(3)$ ,  $n = \text{RP}(4)$ .

IRP = 9 three-phase functions of Parker et al. (1987).

$$m = 1 - 1/n$$

$$\bar{S}_g = S_g / (1 - S_m)$$

$$\bar{S}_a = (S_a - S_m) / (1 - S_m)$$

$$\bar{S}_l = (S_a + S_l - S_m) / (1 - S_m)$$

$$k_{rg} = \sqrt{\bar{S}_g} [1 - (\bar{S}_l)^{1/m}]^{2m}$$

$$k_{ra} = \sqrt{\bar{S}_a} \left\{ 1 - [1 - (\bar{S}_a)^{1/m}]^m \right\}^2$$

$$k_{rl} = \sqrt{\bar{S}_l - \bar{S}_a} \left\{ [1 - (\bar{S}_a)^{1/m}]^m - [1 - (\bar{S}_l)^{1/m}]^m \right\}^2$$

where  $k_{ra}$ ,  $k_{rg}$ , and  $k_{rl}$  are limited to values between 0 and 1, with  $S_m = \text{RP}(1)$ , and  $n = \text{RP}(2)$ .

IRP = 10 power-law relative permeabilities for all phases  $\beta = a, l, g$ :



$$k_{r\beta} = \left[ \frac{S_{\beta} - S_{\beta r}}{1 - S_{\beta r}} \right]^n$$

Parameters are  $S_{ar} = RP(1)$ ,  $S_{lr} = RP(2)$ ,  $S_{gr} = RP(3)$ ,  $n = RP(4)$ .

IRP = 11 functions used by Faust (1985) for two-phase Buckley-Leverett problem

$$k_{ra} = (S_a - 0.16)^2/0.64$$

$$k_{rg} = 0$$

$$k_{rl} = (0.8 - S_a)^2/0.64$$

where  $k_{ra}$  and  $k_{rl}$  are limited to values between 0 and 1, no parameters.

IRP = 12 same as IRP = 6, except a correction factor is applied to  $k_{rl}$  such as to make  $k_{rl}$  equal to  $k_{rg}$  for two-phase conditions with the same aqueous phase saturation.

The relative permeability functions listed above should be considered preliminary. TOUGH2/ECO2M users are encouraged to follow ongoing research into three-phase relative permeabilities, and to add suitable formulations into subroutine RELP. This routine has the following structure:

```

SUBROUTINE RELP(SA,SG,REPA,REPG,REPL,NMAT)
C
...
...
...
C
GOTO (10,11,12, ...),IRP(NMAT)
C
...
...
C
10 CONTINUE
...
...
REPA= ...
REPL= ...
REPG= ...
RETURN
C

```

(IRP = 1)

```

11 CONTINUE                                | (IRP = 2) |
      ...
      ...
      ...
      REPA= ...
      REPL= ...
      REPG= ...
      RETURN
C
12 CONTINUE
      ...
      ...
      ...
C
      END

```

Here,  $S_A$  and  $S_G$  are the aqueous and gas phase saturations (note that for liquid saturation we have  $S_L = 1 - S_A - S_G$ ).  $REPA$ ,  $REPL$ , and  $REPG$  are, respectively, the relative permeabilities of aqueous, liquid, and gas phases.  $NMAT$  is the index of the domain to which the grid block belongs, and  $IRP(NMAT)$  is the index number of the relative permeability function in that domain.

We mention that effects of a possible solid phase with saturation  $S_s$  are considered in subroutine `EOS` prior to calling `RELP`. This is done by scaling fluid phase saturations by a factor  $1/(1-S_s)$  prior to calling `RELP`, so that within `RELP` the fluid phase saturations sum to 1:  $S_a + S_l + S_g = 1$ .

To code an additional relative permeability function, the user needs to insert a code segment analogous to those shown above, beginning with a statement number that would also appear in the `GOTO` statement. The relative permeabilities  $REPA$ ,  $REPL$ , and  $REPG$  need to be defined as functions of the phase saturations. The  $RP( )$  data read in the input file can be utilized as parameters in these functional relationships.

## Appendix B. Capillary Pressure Functions

A three-phase capillary pressure function has been included in ECO2M. The original TOUGH2 two-phase functions have been retained, and if one of the TOUGH2 two phase functions is chosen, the gas-liquid capillary pressure will be assumed to be equal to zero. The notation used below is:  $P_{cgl} = P_l - P_g$  = gas-liquid capillary pressure;  $P_{cga} = P_a - P_g$  = gas-aqueous capillary pressure. It should be noted that the capillary pressure between the liquid and the aqueous phase,  $P_{cla}$ , is given by  $P_{cla} = P_{cga} - P_{cgl} = P_a - P_l$ .

ICP = 8      no capillary pressure

ICP = 9      three-phase capillary functions from Parker et al. (1987).

$$m = 1 - 1/n$$

$$\bar{S}_a = (S_a - S_m)/(1 - S_m)$$

$$\bar{S}_l = (S_a + S_l - S_m)/(1 - S_m)$$

$$P_{cgl} = - \frac{\rho_a g}{\alpha_{gl}} [(\bar{S}_l)^{-1/m} - 1]^{1/n}$$

$$P_{cga} = - \frac{\rho_a g}{\alpha_{la}} [(\bar{S}_a)^{-1/m} - 1]^{1/n} - \frac{\rho_a g}{\alpha_{gl}} [(\bar{S}_l)^{-1/m} - 1]^{1/n}$$

where  $S_m = CP(1)$ ;  $n = CP(2)$ ;  $\alpha_{gl} = CP(3)$ ;  $\alpha_{la} = CP(4)$ .

These functions have been modified so that the capillary pressures remain finite at low aqueous saturations. This is done by calculating the slope of the capillary pressure functions at  $\bar{S}_a$  and  $\bar{S}_l = 0.1$ . If  $\bar{S}_a$  or  $\bar{S}_l$  is less than 0.1, the capillary pressures are calculated as linear functions in this region with slopes equal to those calculated at scaled saturations of 0.1.

ICP = 10      as ICP = 9, except that the strength coefficients are directly provided as inputs, rather than being calculated from the parameters  $\alpha_{gl}$  and  $\alpha_{la}$ . The capillary pressure functions are then

$$P_{cgl} = -P_{cgl,0} [(\bar{S}_l)^{-1/m} - 1]^{1/n}$$

$$P_{cga} = -P_{cla,0} [(\bar{S}_a)^{-1/m} - 1]^{1/n} - P_{cgl,0} [(\bar{S}_l)^{-1/m} - 1]^{1/n}$$

where  $S_m = CP(1)$ ;  $n = CP(2)$ ;  $P_{cgl,0} = CP(3)$ ;  $P_{cla,0} = CP(4)$ .

and  $\bar{S}_a$  and  $\bar{S}_l$  are as given for  $ICP = 9$ .

Additional capillary pressure functions can be programmed into subroutine PCAP in a fashion completely analogous to that for relative permeabilities (see Appendix A).

## Appendix C. Notation for Mass Fractions

Presenting algorithms for phase compositions and phase changes requires careful notation. Here we summarize the parameters relevant to phase partitioning used in Sec. 2.

$X$	CO <sub>2</sub> mass fraction in aqueous phase
$X_{\text{aq}}$	CO <sub>2</sub> mass fraction in aqueous phase
$X_{\text{aq,l}}$	aqueous phase CO <sub>2</sub> mass fraction in equilibrium with a liquid CO <sub>2</sub> phase
$X_{\text{aq,g}}$	aqueous phase CO <sub>2</sub> mass fraction in equilibrium with a gaseous CO <sub>2</sub> phase
$X_{\text{aq,C}}$	aqueous phase CO <sub>2</sub> mass fraction in equilibrium with a CO <sub>2</sub> -rich phase C (= liquid, gas)
$X_{\text{l}}$	CO <sub>2</sub> mass fraction in liquid phase
$X_{\text{g}}$	CO <sub>2</sub> mass fraction in gas phase
$X_{\text{C}}$	CO <sub>2</sub> mass fraction in CO <sub>2</sub> -rich phase C (= liquid, gas)
$X_{\text{l,eq}}$	CO <sub>2</sub> mass fraction in liquid phase in equilibrium with an aqueous phase
$X_{\text{g,eq}}$	CO <sub>2</sub> mass fraction in gas phase in equilibrium with an aqueous phase
$X_{\text{C,eq}}$	CO <sub>2</sub> mass fraction in CO <sub>2</sub> -rich phase C (= liquid, gas) in equilibrium with an aqueous phase
$X_{\text{tot}}$	total CO <sub>2</sub> mass fraction in brine-CO <sub>2</sub> mixture
$Y$	total water mass fraction in two-phase liquid-gas mixture
$Y_{\text{l}}$	water mass fraction in liquid phase
$Y_{\text{g}}$	water mass fraction in gas phase
$Y_{\text{C}}$	water mass fraction in CO <sub>2</sub> -rich phase C (= liquid, gas)
$Y_{\text{l,eq}}$	water mass fraction in liquid phase in equilibrium with an aqueous phase
$Y_{\text{g,eq}}$	water mass fraction in gas phase in equilibrium with an aqueous phase

## DISCLAIMER

This document was prepared as an account of work sponsored by the United States Government. While this document is believed to contain correct information, neither the United States Government nor any agency thereof, nor The Regents of the University of California, nor any of their employees, makes any warranty, express or implied, or assumes any legal responsibility for the accuracy, completeness, or usefulness of any information, apparatus, product, or process disclosed, or represents that its use would not infringe privately owned rights. Reference herein to any specific commercial product, process, or service by its trade name, trademark, manufacturer, or otherwise, does not necessarily constitute or imply its endorsement, recommendation, or favoring by the United States Government or any agency thereof, or The Regents of the University of California. The views and opinions of authors expressed herein do not necessarily state or reflect those of the United States Government or any agency thereof or The Regents of the University of California.

Ernest Orlando Lawrence Berkeley National Laboratory is an equal opportunity employer.